

UNCLASSIFIED

AD NUMBER
AD859670
NEW LIMITATION CHANGE
TO Approved for public release, distribution unlimited
FROM Distribution authorized to U.S. Gov't. agencies and their contractors; Critical Technology; JUL 1969. Other requests shall be referred to Air Force Cambridge Research Laboratory, Attn: CRDG, Hanscom AFB, MA 01730.
AUTHORITY
AFCRL ltr, 31 Jul 1981

THIS PAGE IS UNCLASSIFIED

RADIATION AND SCATTERING FROM
BODIES OF REVOLUTION

by

Roger F. Harrington

Joseph R. Mautz

July 1969

Electrical Engineering Department
Syracuse University
Syracuse, New York 13210

Contract No. F-19628-67-C-0233

Project No. 8683

Task No. 868302

Work Unit No. 86830201

FINAL REPORT

for the period

1 June 1967 to 31 July 1969

Contract Monitor: John K. Schindler
Microwave Physics Laboratory

This document is subject to special export controls and each transmittal to foreign governments or foreign nationals may be made only with the prior approval of AFCRL (CRDG), L.G. Hanscom Field, Bedford, Massachusetts 01730

Prepared for

AIR FORCE CAMBRIDGE RESEARCH LABORATORIES

OFFICE OF AEROSPACE RESEARCH

UNITED STATES AIR FORCE

BEDFORD, MASSACHUSETTS

01730

This document has been approved
for public release and sale; its
distribution is unlimited.

ABSTRACT

The problem of electromagnetic radiation and scattering from conducting bodies of revolution, both loaded and unloaded, is considered. The solution is obtained by the method of moments applied to the integro-differential equation, and is expressed in terms of generalized network parameters. Computer programs are given for plane-wave scattering and for radiation from apertures. The programs are valid for solid bodies, zero thickness conductors, and bodies with points and edges. The solution for planar bodies is also a solution for diffraction through apertures in a conducting plane, according to Babinet's principle. Representative computations are given for scattering and radiation from disks, washers, toroids, hemispheres, and cone-spheres.

CONTENTS

	Page
ABSTRACT.	1
I. INTRODUCTION AND SUMMARY	1
II. METHOD OF SOLUTION	2
III. REPRESENTATIVE COMPUTATIONS.	8
IV. GENERALIZED NETWORK MATRICES	21
V. PLANE-WAVE SCATTERING, AXIAL INCIDENCE	30
VI. APERTURE RADIATION, ROTATIONAL SYMMETRY.	35
VII. BACKSCATTERING, OBLIQUE INCIDENCE.	41
REFERENCES.	43
APPENDIX A. PROGRAM AND SAMPLE INPUT-OUTPUT DATA FOR SECTION IV. .	44
APPENDIX B. PROGRAM AND SAMPLE INPUT-OUTPUT DATA FOR SECTION V. .	55
APPENDIX C. PROGRAM AND SAMPLE INPUT-OUTPUT DATA FOR SECTION VI. .	69
APPENDIX D. PROGRAM AND SAMPLE INPUT-OUTPUT DATA FOR SECTION VII..	83

I. INTRODUCTION AND SUMMARY

The objectives of this project were to develop practical methods for computing the generalized impedance matrix applicable to the study of electromagnetic radiation and scattering from highly conducting bodies of revolution. Specific topics considered were: (A) Development of a computer program to allow numerical evaluation of the generalized impedance matrix for a conducting cone-sphere of maximum dimension approximately six wavelengths. (B) Application of the impedance matrix to determine the scattering properties of a cone-sphere with and without loading elements on the body. (C) Application of the impedance matrix to determine the radiation and scattering properties of a cone-sphere with antenna slots on its surface.

The project work was performed during the period 1 June 1967 to 30 June 1969. The technical personnel working on the project were Dr. Roger F. Harrington and Dr. Joseph R. Mautz. During the contract period one previous scientific report was written entitled "Generalized Network Parameters for Bodies of Revolution," dated May 1968.^[1] Also, one paper entitled "Radiation and Scattering from Bodies of Revolution" has been published in Applied Scientific Research.^[2] The material in the above listed scientific report and paper also formed a part of Dr. Mautz's Ph.D. thesis, Syracuse University.^[3]

The following is a summary of the research performed during the project.

(A) A general program was developed for computing generalized network parameters for conducting bodies of revolution. The theory and original program is given in the previous report.^[1] An improved program is given in this report.

(B) Aperture antennas in conducting bodies of revolution were analyzed, and computations made for body currents and radiation patterns. The theory is given in the previous report,^[1] and the computer program is given in this report.

(C) Electromagnetic scattering by conducting bodies of revolution was considered. The theory is given in the previous report,^[1] and the computer programs for plane-wave scattering are given in this report.

(D) Radiation and scattering from loaded bodies of revolution was studied, and computations made for representative bodies. The theory and some computations for cone-spheres are given in this report.

(E) The problem of determining the eigencurrents for conducting bodies of revolution was considered, and representative computations were made. Details are not included in this report because only a preliminary study was made.

(F) The problem of synthesizing and optimizing radiation and scattering patterns from loaded bodies of revolution was considered, and representative computations were made. Details are not included in this report because only a preliminary study was made.

II. METHOD OF SOLUTION

The problem is formulated in terms of potential integrals, and the boundary conditions at the body are applied. This results in an integral equation, which is then solved by the method of moments. The matrices obtained thereby can be expressed in terms of generalized network parameters.^[4] A general exposition of the procedure is given in a recent monograph.^[5] The following is a summary of the theory as it applies to the present problem.

Let \mathbf{E}^i denote the known impressed field and \mathbf{E}^s the scattered field due to currents on the body. Then the total field \mathbf{E} is the sum of the impressed and scattered fields, that is,

$$\mathbf{E} = \mathbf{E}^i + \mathbf{E}^s \quad (1)$$

The scattered field can be expressed in terms of a vector potential \mathbf{A} and scalar potential Φ as

$$\mathbf{E}^s = -j\omega\mathbf{A} - \nabla\Phi \quad (2)$$

where

$$A = \mu \oint_S J \frac{e^{-jkR}}{4\pi R} ds \quad (3)$$

$$\Phi = \frac{1}{\epsilon} \oint_S \sigma \frac{e^{-jkR}}{4\pi R} ds \quad (4)$$

Here S is the surface of the conductor, R is the distance from a source point to the field point, J is the surface current on S , and σ is the surface charge on S . The current and charge are related by the equation of continuity

$$\nabla \cdot J = -j\omega\sigma \quad (5)$$

The boundary condition requires that the tangential component of total E vanish on S . Hence,

$$E_{\text{tan}}^i = -E_{\text{tan}}^s \quad (6)$$

where the subscript tan denotes tangential component on S . The problem can now be stated succinctly as

$$L(J) = E_{\text{tan}}^i \quad (7)$$

where L is the integro-differential operator

$$L(J) = [j\omega A + \nabla\Phi]_{\text{tan}} \quad (8)$$

A solution of (7) gives the current J on S . Usually we are interested in some functional of J which can be computed once J is known.

To effect a solution by the method of moments, let the inner product be defined as

$$\langle J, J' \rangle = \oint_S E \cdot J' ds \quad (9)$$

where \underline{W} and \underline{J} are tangential vectors on S . A set of expansion functions $\{\underline{J}_j\}$ is next defined, and the current on S approximated by

$$\underline{J} = \sum_j I_j \underline{J}_j \quad (10)$$

where I_j are constants to be determined. Equation (10) is substituted into (7), which, because of the linearity of L , reduces to

$$\sum_j I_j L \underline{J}_j = \underline{E}_{\text{tan}}^i \quad (11)$$

A set of testing functions $\{\underline{W}_i\}$ is defined, and the inner product of (11) with each \underline{W}_i is taken. The result is

$$\sum_j I_j \langle \underline{W}_i, L \underline{J}_j \rangle = \langle \underline{W}_i, \underline{E}^i \rangle \quad (12)$$

$i = 1, 2, 3, \dots$. The subscript tan has been dropped from \underline{E}^i because the inner product involves only tangential components. We now define the generalized network matrices

$$[Z] = [\langle \underline{W}_i, L \underline{J}_j \rangle] \quad (13)$$

$$[V] = [\langle \underline{W}_i, \underline{E}^i \rangle] \quad (14)$$

$$[I] = [I_i] \quad (15)$$

and rewrite the set (12) as

$$[Z] [I] = [V] \quad (16)$$

$[Z]$ is the generalized impedance matrix, and $[Y] = [Z]^{-1}$ is the generalized admittance matrix. The inverse of (16)

$$[I] = [Y] [V] \quad (17)$$

gives the coefficients I_j of the current expansion (10), and hence is an approximate solution to the problem.

The impedance elements of (13) are explicitly

$$Z_{ij} = \oint\oint_S \underline{W}_i \cdot (j\omega \underline{A}_j + \nabla \Phi_j) ds \quad (18)$$

where we have used (8) and (9). The subscript j denotes that \underline{A}_j and Φ_j are the potentials due to I_j and σ_j . If the two-dimensional divergence theorem is applied to the vector $\Phi \underline{W}_i$ on a closed surface, the following identity results:

$$\oint\oint_S \nabla \Phi \cdot \underline{W}_i ds = - \oint\oint_S \Phi \nabla \cdot \underline{W}_i ds \quad (19)$$

If \underline{W} is thought of as a current, the charge associated with it is

$$\sigma_i = \frac{-1}{j\omega} \nabla \cdot \underline{W}_i \quad (20)$$

Now (18) can be written as

$$Z_{ij} = j\omega \oint\oint_S (\underline{W}_i \cdot \underline{A}_j + \sigma_i \Phi_j) ds \quad (21)$$

Equation (21) is more convenient for computation than (18) because the gradient operation on Φ has been eliminated.

The above formulas have been specialized to bodies of revolution in the previous report.^[1] Also given there are representative computations for radiation and scattering from unloaded conducting bodies of revolution. Computer programs and further computations are given in this report. An alternative solution for the case of plane-wave scattering from unloaded conducting bodies of revolution has been given by Andreassen.^[6]

The general theory of loaded antennas and scatterers with lumped loads is available in the literature.^[5,7] An extension to continuously loaded surfaces will now be given. Lumped loads can be considered

as a special case of continuous loads localized to infinitesimal sections of the surface.

A continuously loaded surface S is defined as one for which the total tangential electric field is related to the current \underline{J} on S by an impedance function of position \underline{z} according to

$$\underline{E}_{\text{tan}} = \underline{E}_{\text{tan}}^i + \underline{E}_{\text{tan}}^s = \underline{Z} \underline{J} \quad (22)$$

Now $\underline{E}_{\text{tan}}^s$ is related to the current \underline{J} by

$$\underline{E}_{\text{tan}}^s = -\underline{L}(\underline{J}) \quad (23)$$

where \underline{L} is given by (8). Combining (22) and (23), and rearranging, we have

$$\underline{L}(\underline{J}) = \underline{E}_{\text{tan}}^i - \underline{Z} \underline{J} \quad (24)$$

This reduces to (7) when $\underline{Z} = 0$, that is, when S is covered by a perfect conductor. We can now reduce (24) to a matrix equation in the usual way by the method of moments, obtaining

$$[\underline{Z}][\underline{I}] = [\underline{V}] - [\underline{Z}_L][\underline{I}] \quad (25)$$

where $[\underline{Z}]$, $[\underline{V}]$, $[\underline{I}]$ are given by (13), (14), (15), and

$$[\underline{Z}_L] = [\langle \underline{A}_i, \underline{Z} \underline{J}_j \rangle] \quad (26)$$

The solution to (25) for the current coefficient matrix is

$$[\underline{I}] = [\underline{Z} + \underline{Z}_L]^{-1} [\underline{V}] \quad (27)$$

Note that this solution is analogous to that for two n -port networks connected in series with the voltage source $[\underline{V}]$.

The impedance function \underline{Z} is zero over those parts of S covered by a

perfect electric conductor. If subsectional expansion and testing functions are used, many of the elements of $[Z_L]$ may be zero when the surface S is partially covered by an electric conductor. In such cases the following alternative solution may be computationally faster. Suppose $[Z_L]$ has some zero rows and columns. Let $[Z_L^r]$ be the matrix obtained from $[Z_L]$ by deleting all zero rows, $[Z_L^c]$ by deleting all zero columns, and $[Z_L^{rc}]$ by deleting all zero rows and columns. Other matrices with the same rows and/or columns deleted will be identified by the same superscripts. Then, multiplying (25) by $[Y] = [Z^{-1}]$, and deleting the appropriate rows and columns, we have

$$[I^r] = [Y^r][V] - [Y^{rc}][Z_L^{rc}][I^r] \quad (28)$$

The solution of this for $[Z_L^{rc}][I^r]$ is

$$[Z_L^{rc}][I^r] = [Y^{rc} + Y_L^{rc}]^{-1} [Y^r][V] \quad (29)$$

where $[Y_L^{rc}] = [Z_L^{rc}]^{-1}$. The solution is now given by (17) with $[V]$ replaced by

$$[V'] = [V] + [V_L] \quad (30)$$

where $[V_L]$ is the matrix obtained by adding the appropriate zeros to

$$\begin{aligned} [V_L^r] &= - [Z_L^{rc}][I^r] \\ &= - [Y^{rc} + Y_L^{rc}]^{-1} [Y^r][V] \end{aligned} \quad (31)$$

The excitation is thus viewed as the superposition of the impressed voltage $[V]$ plus the load voltage $[V_L]$.

The computations of the next section for loaded antennas and scatterers were made using this second formulation. A problem arises in the case of an open circuit, since then elements of $[Z_L^{rc}]$ may become infinite.

However, $[Y_L^{rc}]$ is still well defined, and may be obtained from $[Z_L^{rc}]^{-1}$ by setting the "infinite" elements to some very large number.

III. REPRESENTATIVE COMPUTATIONS

The graphs of this section are intended to illustrate some of the types of computations that we have made during the project. Computer programs for the unloaded antenna and scatterer computations are described in the next section, and listed in the Appendix. Included in the programs are printer plot routines, so that rough graphs of the computations are available immediately.

All programs have been run on spherical bodies, and compared to the classical eigenfunction solutions for spheres. Far-zone quantities, such as radiation fields, agree very closely (usually within a fraction of one percent) with the classical solution. Near-zone quantities, such as currents on the body, also agree well (usually within a few percent) with the classical solution. Examples of such comparisons are given in the previous report.^[1]

The programs have been written to handle correctly the following types of bodies: (A) solid conductors, such as spheres, closed cylinders, (B) zero thickness conductors, such as disks, open cylinders, (C) bodies intersecting the axis, such as spheres, disks, (D) bodies not intersecting the axis, such as toroids, washers, (E) bodies with points, such as cone-spheres, (F) bodies with edges, such as disks and open cylinders, and (G) bodies with corners, such as closed cylinders. The programs have not been written to handle multi-body problems, but the modification required is simple. The accuracy of computations depends on the smoothness of the body and of the excitation. For example, solutions with bodies having points or edges converge more slowly than solutions for bodies with gently curved surfaces. Solutions for localized aperture excitation converge more slowly than solutions for plane-wave excitation.

Solutions involving zero-thickness conductors in the $z = 0$ plane are interesting because they are also solutions to the dual problem of apertures in an infinite conducting screen (Babinet's principle).^[8] In particular,

the duality relationship is

$$E_{\rho} = J_{\phi}/2 \qquad E_{\phi} = -J_{\rho}/2 \qquad (32)$$

where J_{ϕ} , J_{ρ} is the current on the conducting plate, and E_{ρ} , E_{ϕ} is the tangential E field in the complementary aperture. A number of computations for the circular disk and aperture were made, and compared to available measurements.^[9,10,11] The agreement was within the estimated experimental accuracy.

Figure 1 shows the current on a circular disk of diameter $D = 0.8\lambda$, excited by an axially incident plane wave, as computed by the program of Section V. Note that $J_{\rho} \rightarrow 0$ and $J_{\phi} \rightarrow \infty$ at the edge, as theory predicts. Figure 2 shows the computed bistatic radar cross section patterns for the same disk. The curve labeled $\sigma^{x\theta}/\lambda^2$ is the E-plane pattern, and that labeled $\sigma^{x\phi}/\lambda^2$ is the H-plane pattern. (See the previous report^[1] for a discussion of the notation.) By duality, the same patterns are also power patterns for the field diffracted through a circular aperture in an infinite conducting plane excited by a plane wave at normal incidence.

Figure 3 shows the computed current on a circular washer of outside diameter $D = 2.4\lambda$ and inside diameter $d = 0.8\lambda$, excited by an axially incident plane wave. Again J_{ρ} and J_{ϕ} have the expected behavior at the edges. Figure 4 shows the computed bistatic radar cross section patterns for the same disk. By duality, these patterns are also power patterns for the field diffracted through a circular annulus in an infinite conducting plane excited by a plane wave at normal incidence.

Figure 5 shows another example of a bistatic radar cross section pattern for a body of revolution excited by an axially incident plane wave. It is for a toroid of mean radius $R = 0.5\lambda$ and circular cross section of radius $r = 0.12\lambda$. The previous report^[1] showed bistatic radar cross sections of cone-spheres, as well as the currents on the bodies. These computations are repeated in the computer print-out of Appendix B.

Figures 6, 7, and 8 show some examples of radiation from rotationally symmetric apertures in bodies of revolution. Figure 6 is the power gain pattern for a circular disk of diameter $D = 1.6\lambda$ excited by a voltage across

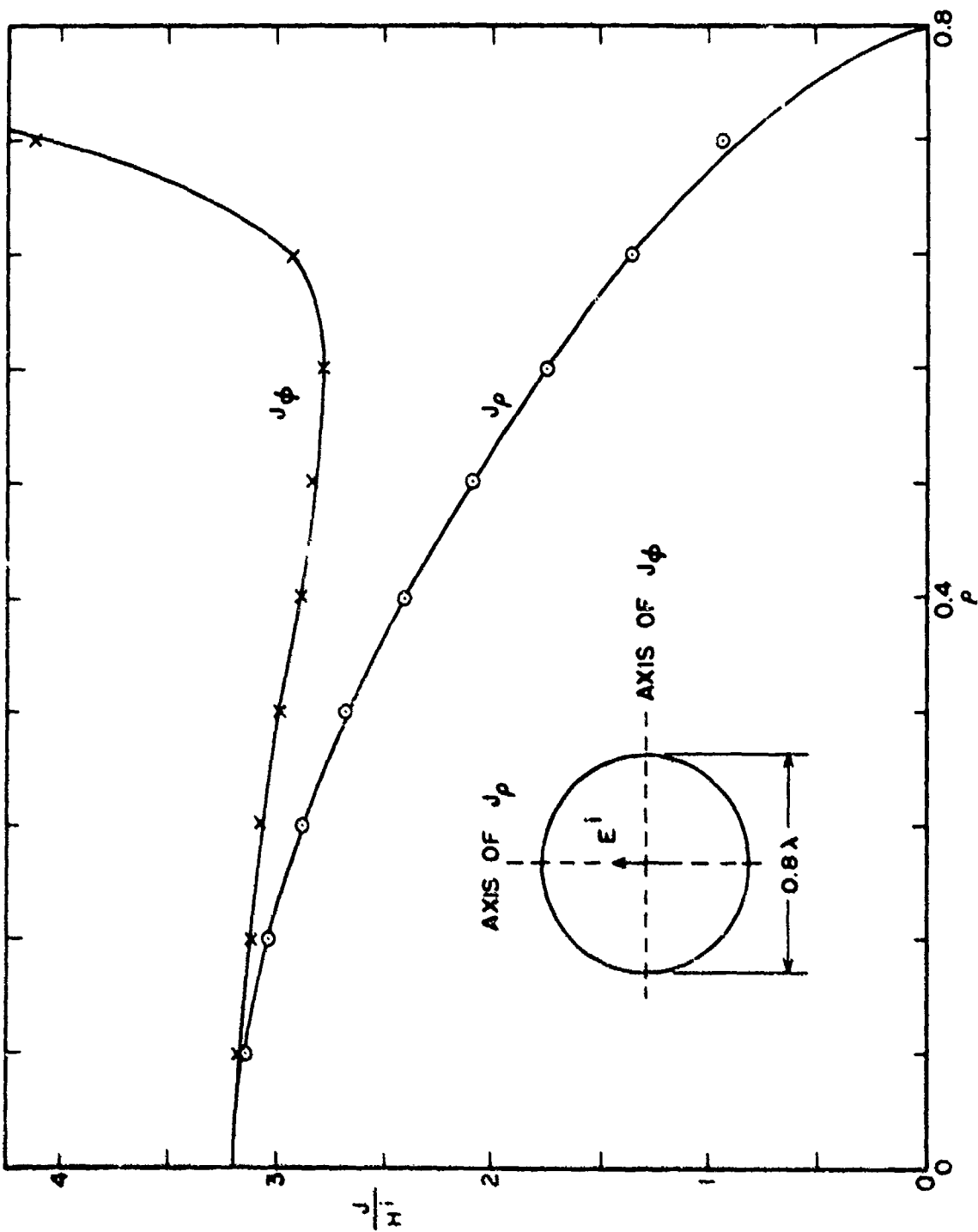


Figure 1. Current on a conducting circular disk of 0.8λ diameter excited by an axially incident plane wave.

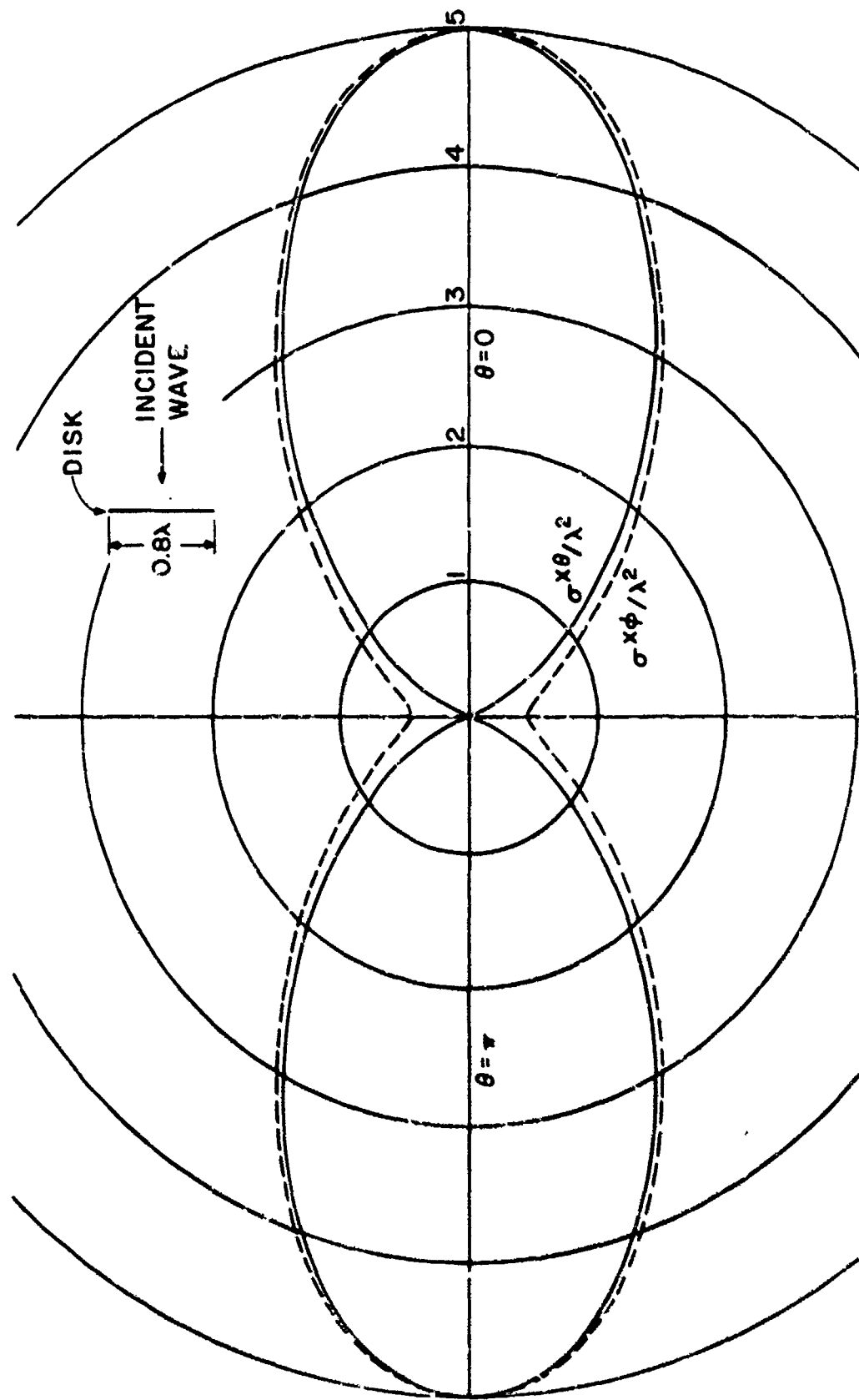


Figure 2. Bistatic radar cross section for a conducting circular disk of 0.8λ diameter excited by an axially incident plane wave. The E-plane pattern is labeled σ^{xe} and the H-plane pattern σ^{xp} .

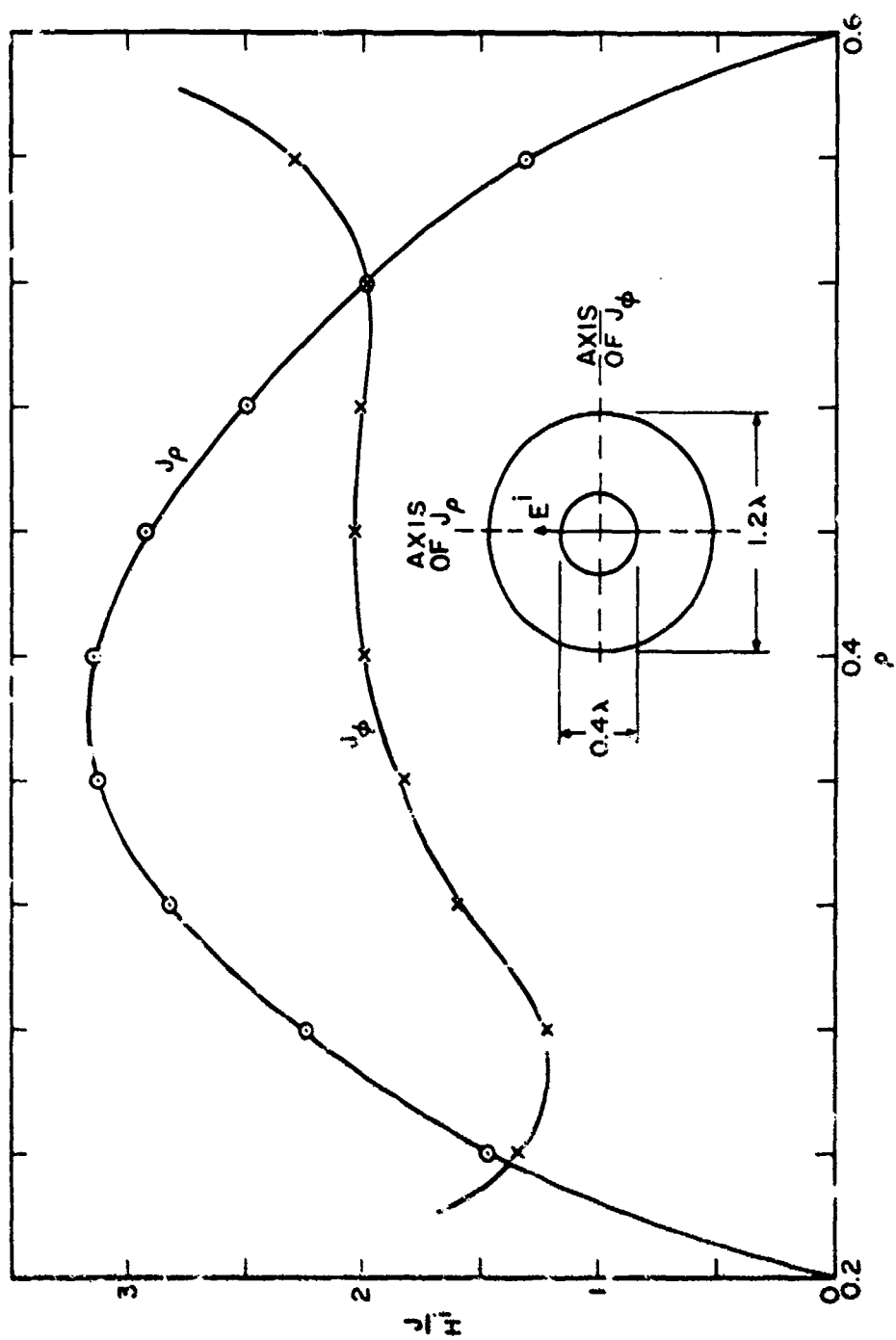


Figure 3. Current on a conducting circular washer of 1.2λ outside diameter and 0.4λ inside diameter, excited by an axially incident plane wave.

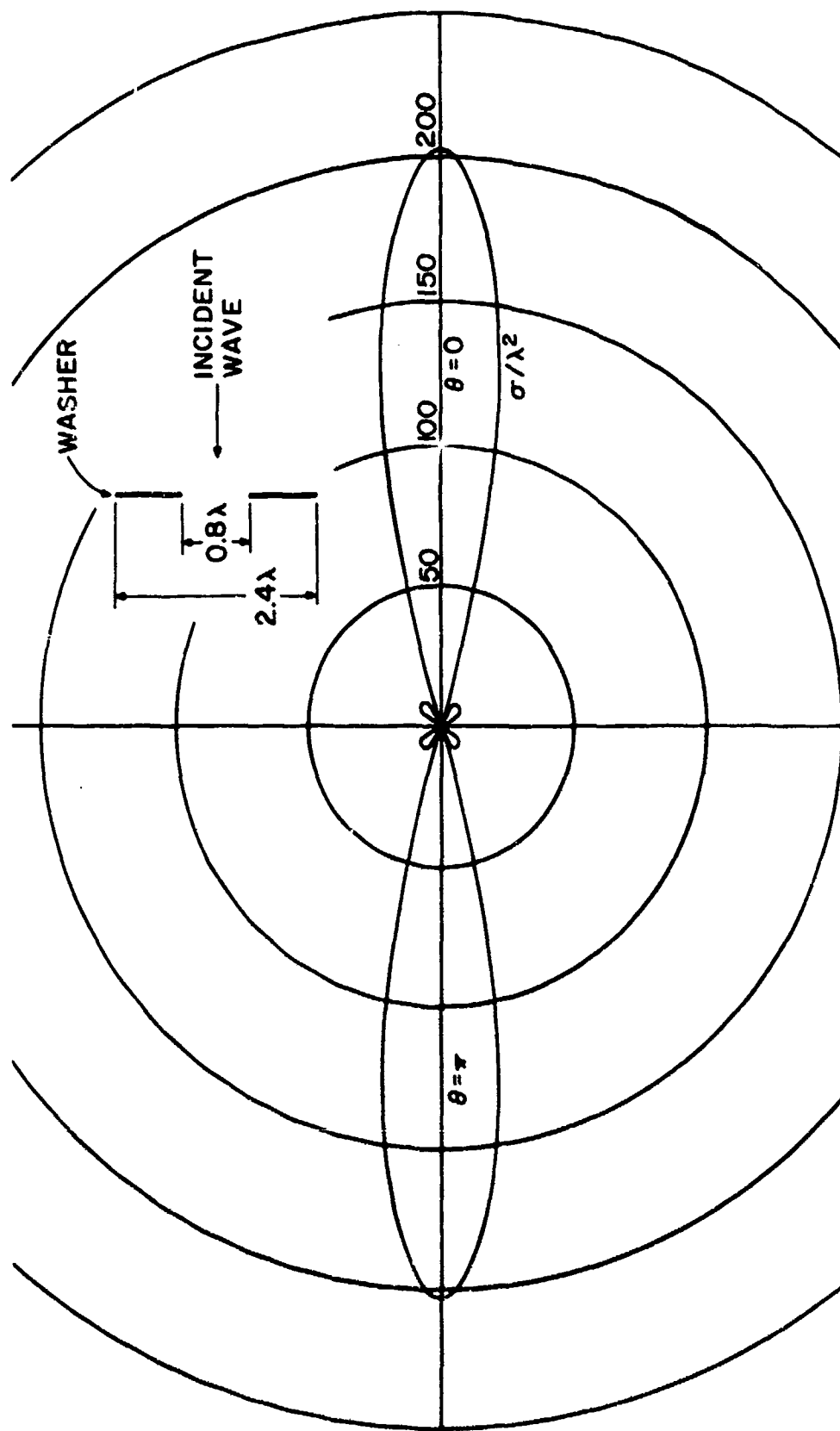


Figure 4. Bistatic radar cross section for a conducting circular washer of 2.4λ outside diameter and 0.8λ inside diameter, excited by an axially incident plane wave. E-plane and H-plane patterns are almost the same.

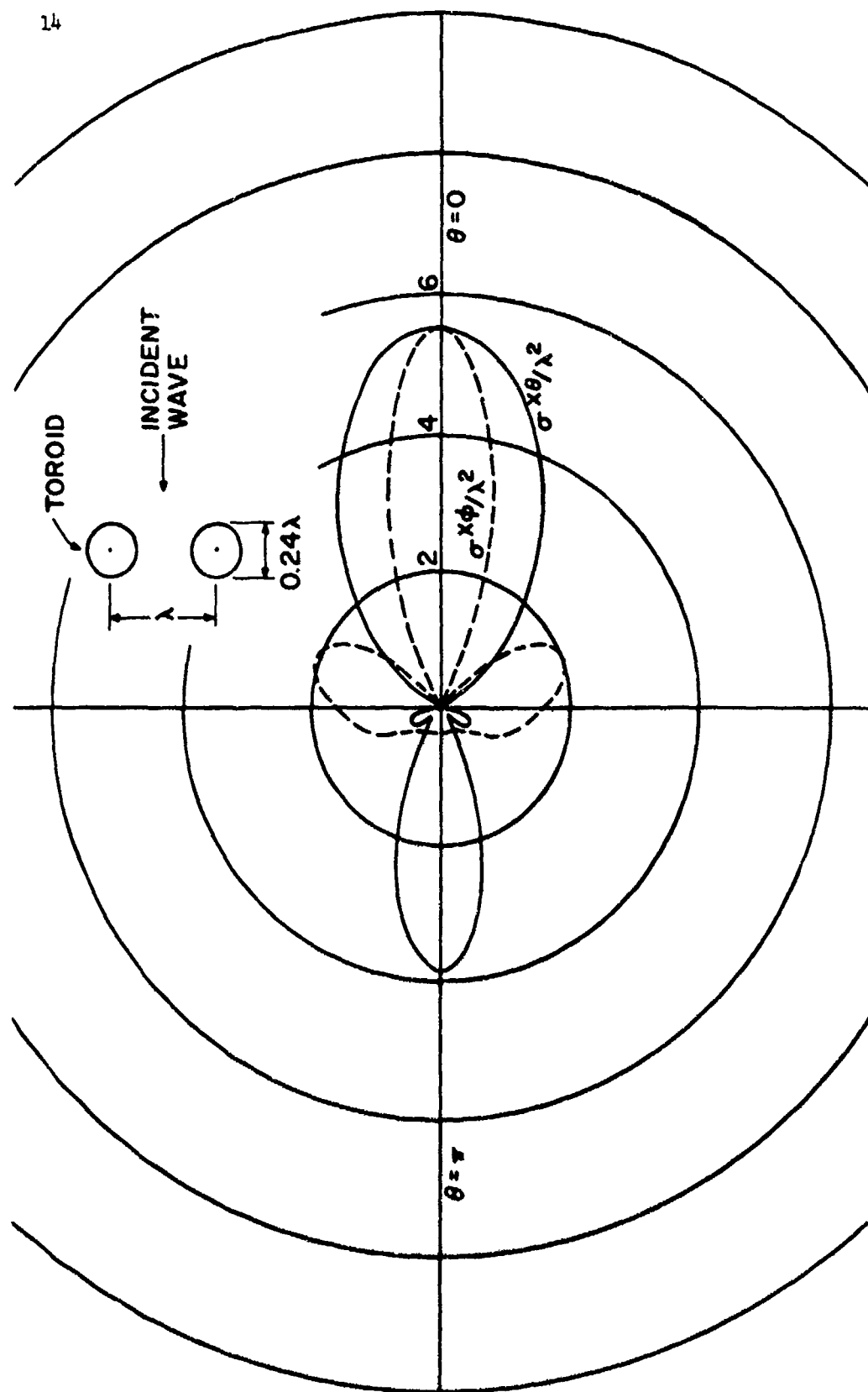


Figure 5. Bistatic radar cross section for a conducting toroid of 1λ mean diameter and 0.24λ cross-sectional diameter, excited by an axially incident plane wave. The E-plane pattern is labeled σ_H and the H-plane pattern σ_E .

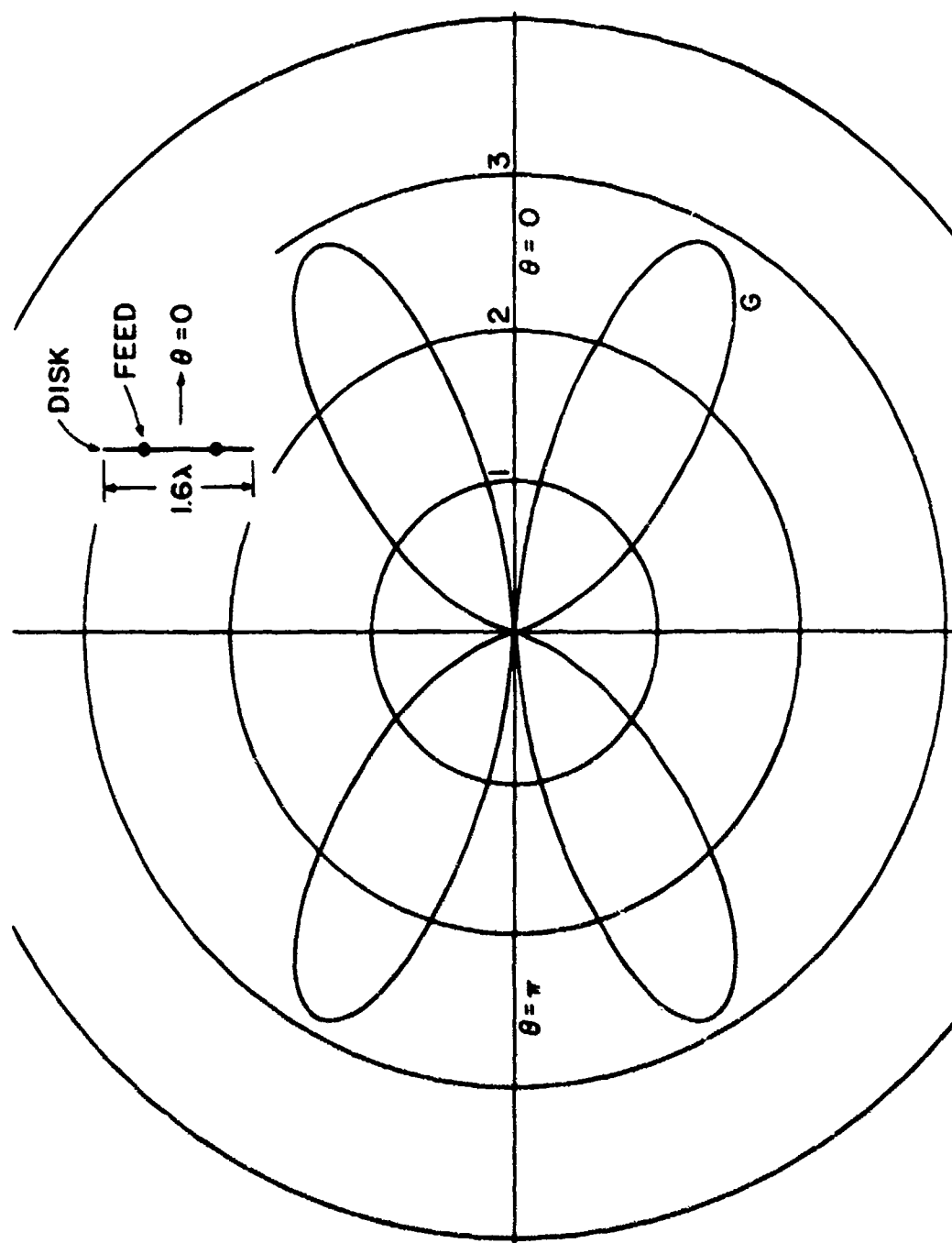


Figure 6. Power gain pattern for a conducting circular disk of 1.6λ diameter, excited by a voltage across a narrow slot of 0.8λ diameter.

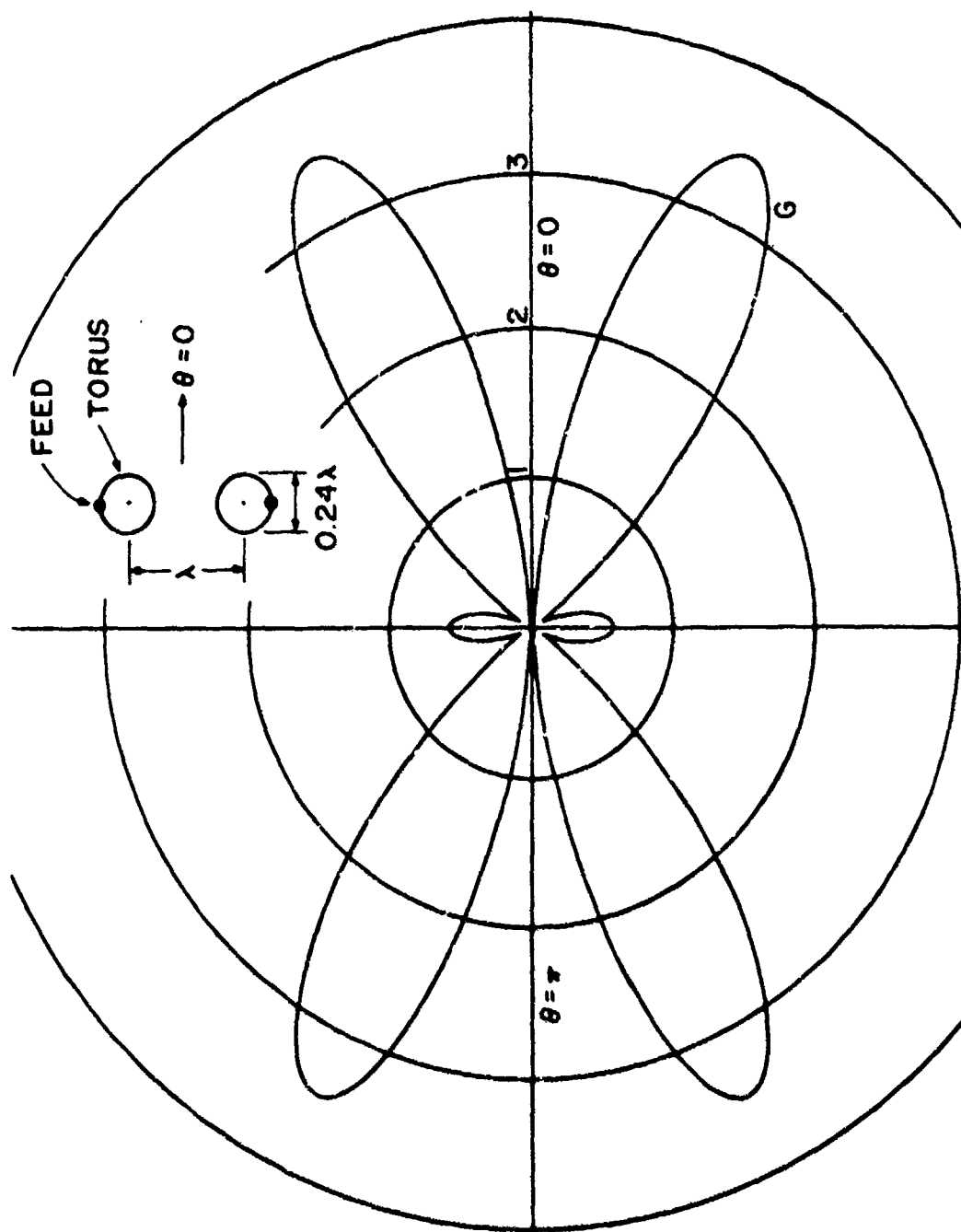


Figure 7. Power gain pattern for a conducting toroid of 1λ mean diameter and 0.24λ cross-sectional diameter, excited by a voltage across a narrow slot at the maximum diameter.

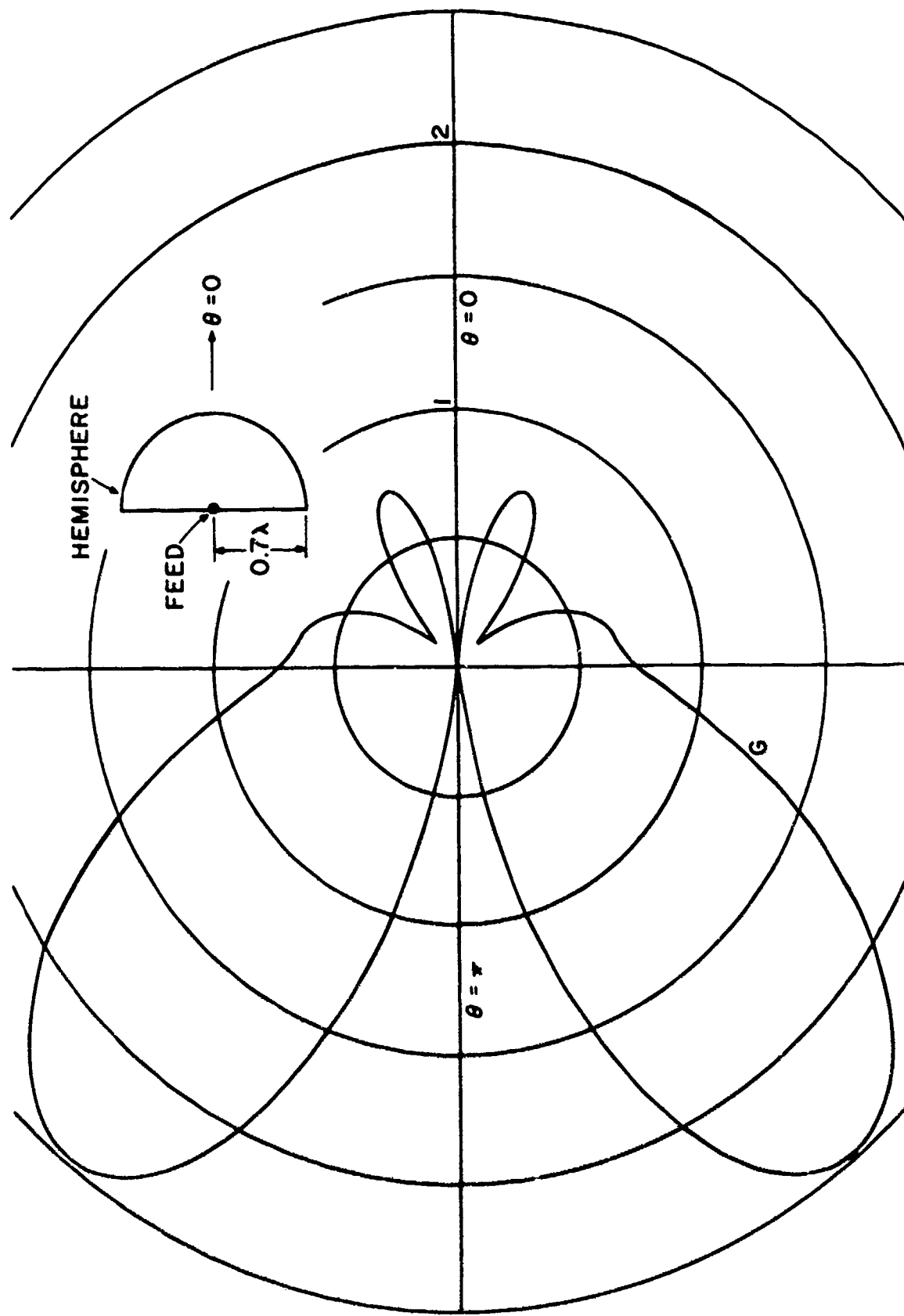


Figure 3. Power gain pattern for a conducting hemisphere of 1.4λ diameter, excited by a voltage across a small annular slot at the center of the flat face.

a narrow slot at a radius $R = 0.4\lambda$. Figure 7 is the power gain pattern for a toroid of mean radius 0.5λ and cross sectional radius $r = 0.12\lambda$, excited by a voltage across a narrow slot at the furthest point from the z axis. Figure 8 is the power gain pattern for a hemisphere of radius $R = 0.7\lambda$, excited by a voltage across a small annular slot at the center of the flat plate. This physically corresponds to excitation by an open-ended coaxial line. It is also equivalent to excitation by a small z -directed electric dipole at the center of the flat plate. Radiation from apertures in cone-spheres are shown in the previous report.^[1] These computations are repeated in the computer print-out of Appendix C.

Figures 9 and 10 are examples of monostatic radar cross sections for bodies of revolution excited by plane waves of arbitrary direction of incidence. The curves of $\sigma^{\theta\theta}/\lambda^2$ are for θ -polarized incident waves, and the curves of $\sigma^{\phi\phi}/\lambda^2$ are for ϕ -polarized incident waves. There are no cross-polarized components of backscattered fields from bodies of revolution. Figure 9 shows the monostatic radar cross section of a disk of diameter $D = 0.8\lambda$. Figure 10 shows the monostatic radar cross section for a hemisphere of radius $R = 0.7\lambda$. The computer print-out of Appendix D gives the monostatic radar cross section for a cone-sphere, half cone angle 10° , sphere radius 0.2λ .

The computer print-out of Appendix D also shows the convergence of the pattern as more modes are included in the solution. Calling the modes which vary as $e^{+jn\phi}$ the n -th modes, for accurate far-field patterns one should include all modes for which

$$n \leq C_{\max} + 1 \quad (33)$$

where C_{\max} = maximum body circumference in wavelengths. A justification of (33) can be made in terms of spherical mode theory. Those modes having n greater than C_{\max} are cut-off, that is, are highly reactive and do not contribute materially to far-zone fields.

Similar convergence problems arise in aperture problems for which the excitation is not rotationally symmetric. To illustrate this, we have computed the power gain pattern for a cone-sphere excited by a voltage across a

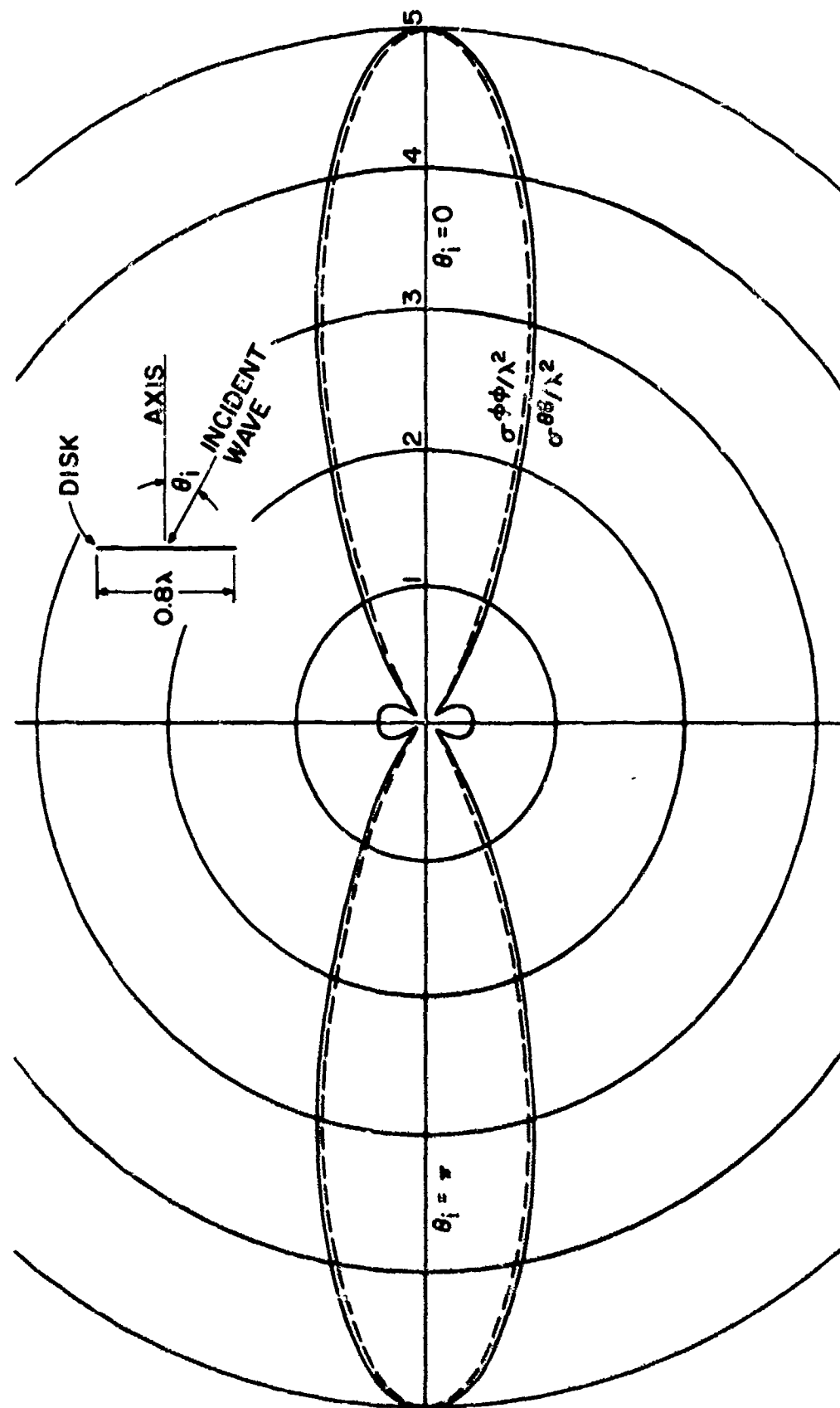


Figure 9. Monostatic radar cross section for a conducting disk of 0.8λ diameter, excited by a plane wave incident at an angle θ . The θ -polarized pattern is labeled $\sigma^{\theta\theta}$, and the ϕ -polarized pattern $\sigma^{\phi\phi}$.

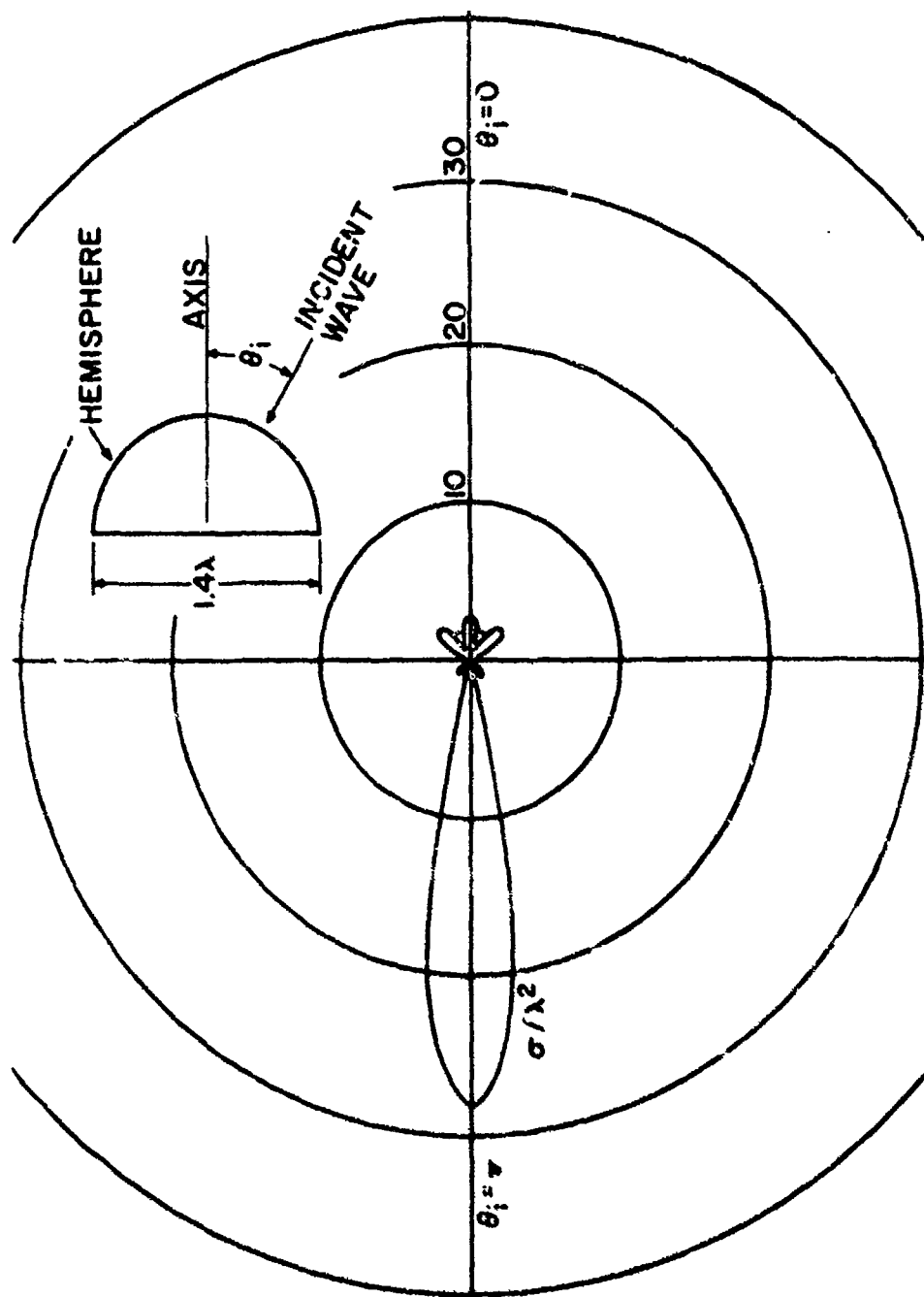


Figure 10. Monostatic radar cross section for a conducting hemisphere of 1.4λ diameter, excited by a plane wave incident at an angle θ . The θ -polarized and ϕ -polarized patterns are nearly the same.

slot at the cone-to-sphere junction, extending over a 90° angular sector of the body. Figure 11 shows how the power gain pattern converges as modes are added to the solution. All curves are normalized to the power radiated by the entire aperture, that is, to the sum of the modal powers. Note that criterion (33) is still a good indication of convergence.

Figure 12 illustrates a computation of monostatic radar cross section vs. frequency for a conical sector of a sphere. Our computations (x's) are compared to those by Schultz *et al.*,^[12] who used an eigenfunction expansion and nonfinal determination of coefficients. Also shown are an approximate solution of Keller and measurements by Keys. The accuracy of our computations is estimated to be better than can be read from the graph.

Computations for the cone-sphere, both as a loaded scatterer and as a loaded radiator, have been made. The dimensions of the cone-sphere and points of loading are pictured in Fig. 13. Computations were made for four types of loads as follows:

- (A) Short circuit
- (B) Open circuit
- (C) Resonant load
- (D) Matched load

For the scattering problem, these loads were applied one at a time to each of the four loading points. The plane-wave illumination was axially incident on either the point or the sphere. For the radiation problem, the excitation was taken at one of the four points, and one of the other points was loaded by one of the above loads. We have a complete set of these patterns for all permutations of the excitations and loads. Representative sets of scattering and radiation patterns are shown in Figs. 14 and 15 to illustrate the results.

IV. GENERALIZED NETWORK MATRICES

This program computes the $[Z]$ and $[Y]$ matrices for bodies of revolution. The theory is that of the previous report^[1] modified to allow unequal segments of contour. The input data consists primarily of NP points specifying the contour plus the mode number. The output consists primarily of the

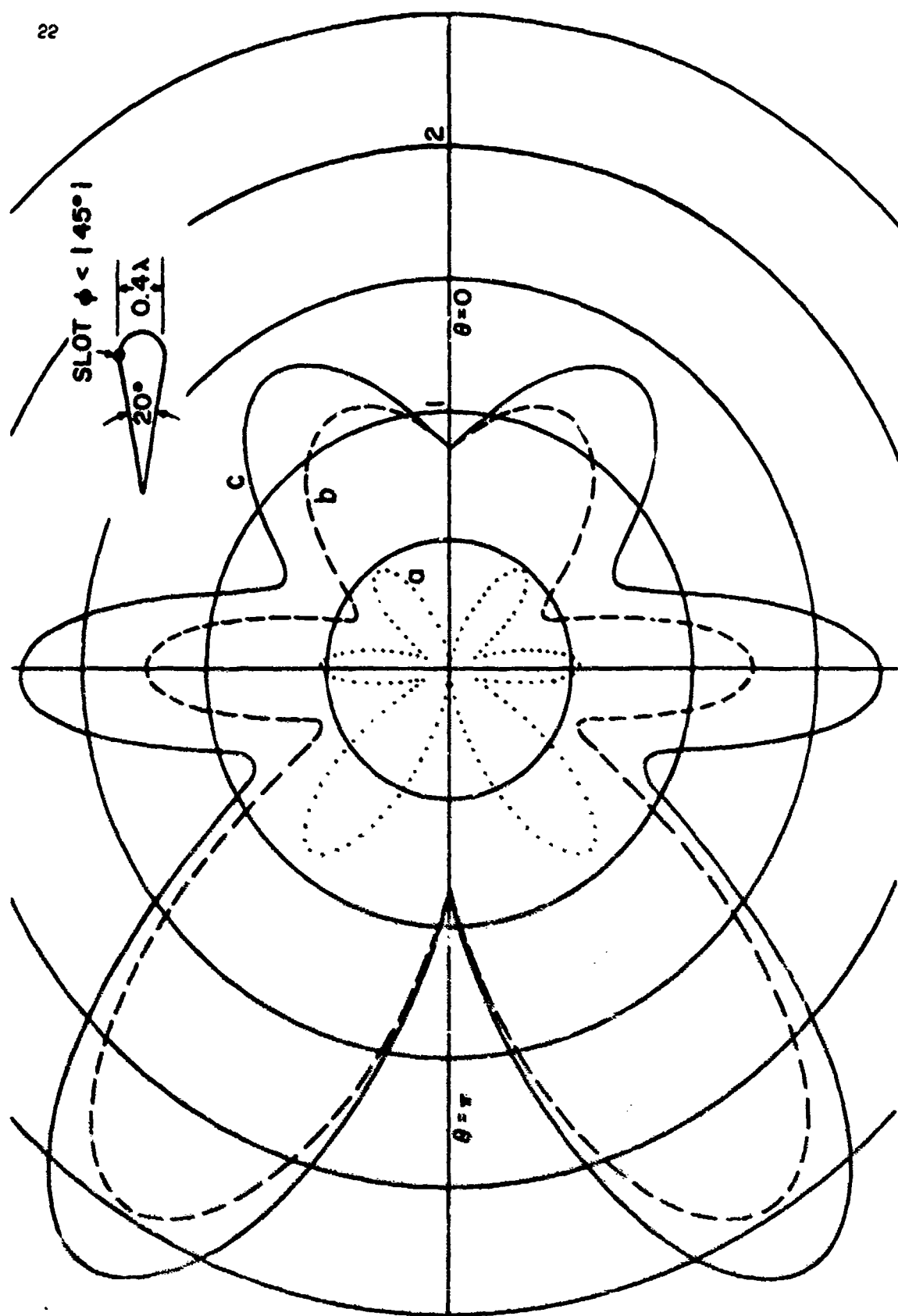


Figure 11. Convergence of the power gain pattern for radiation from a 90° slot in a conducting cone-sphere. Curve (a) is the $n = 0$ mode, curve (b) is the $n = 0, \pm 1$ modes, curve (c) is the $n = 0, \pm 1, \pm 2$ modes. Addition of more modes did not materially change the pattern.

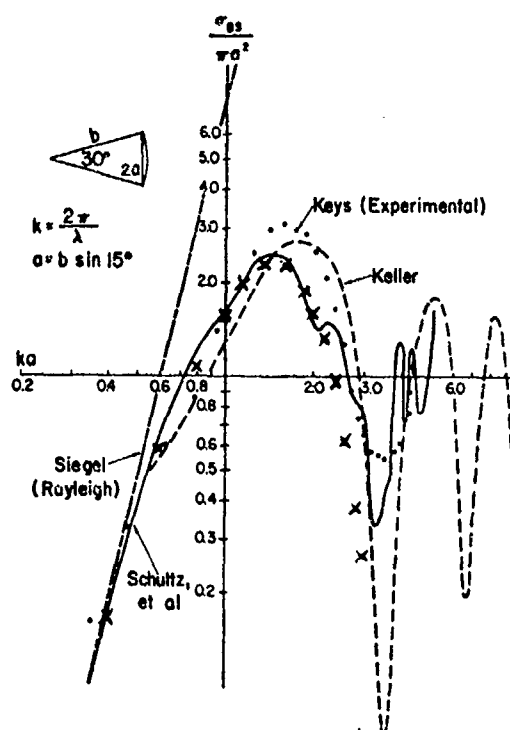


Figure 12. Monostatic radar cross section for a conical sector of a sphere, as computed and measured by various persons. Our computations are shown by x's.

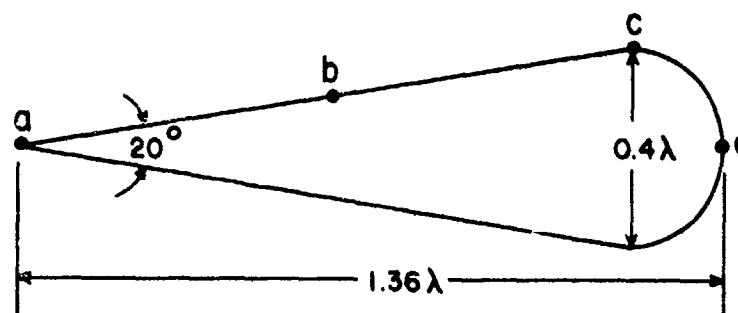


Figure 13. Conducting cone-sphere and points of loading.

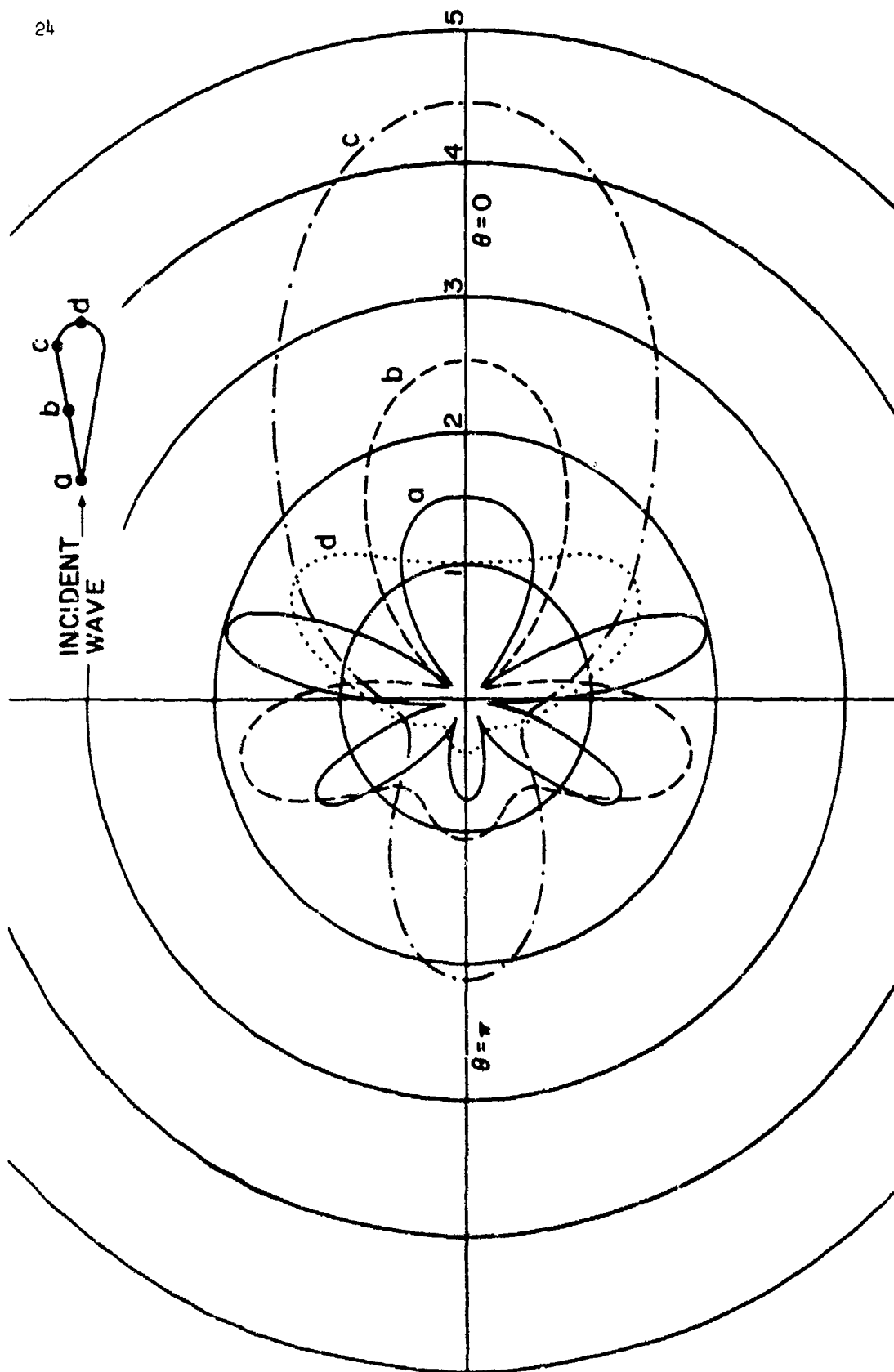


Figure 14. Bistatic scattering patterns (σ/λ^2 vs. θ) for a loaded cone-sphere. Loads are resonant bands at (a), (b), (c), or (d). The plane wave is axially incident on the tip, and the patterns are in the E plane. Cone angle is 20° , sphere diameter is 0.4λ . (Maximum σ/λ^2 for unloaded cone-sphere is 0.38 .)

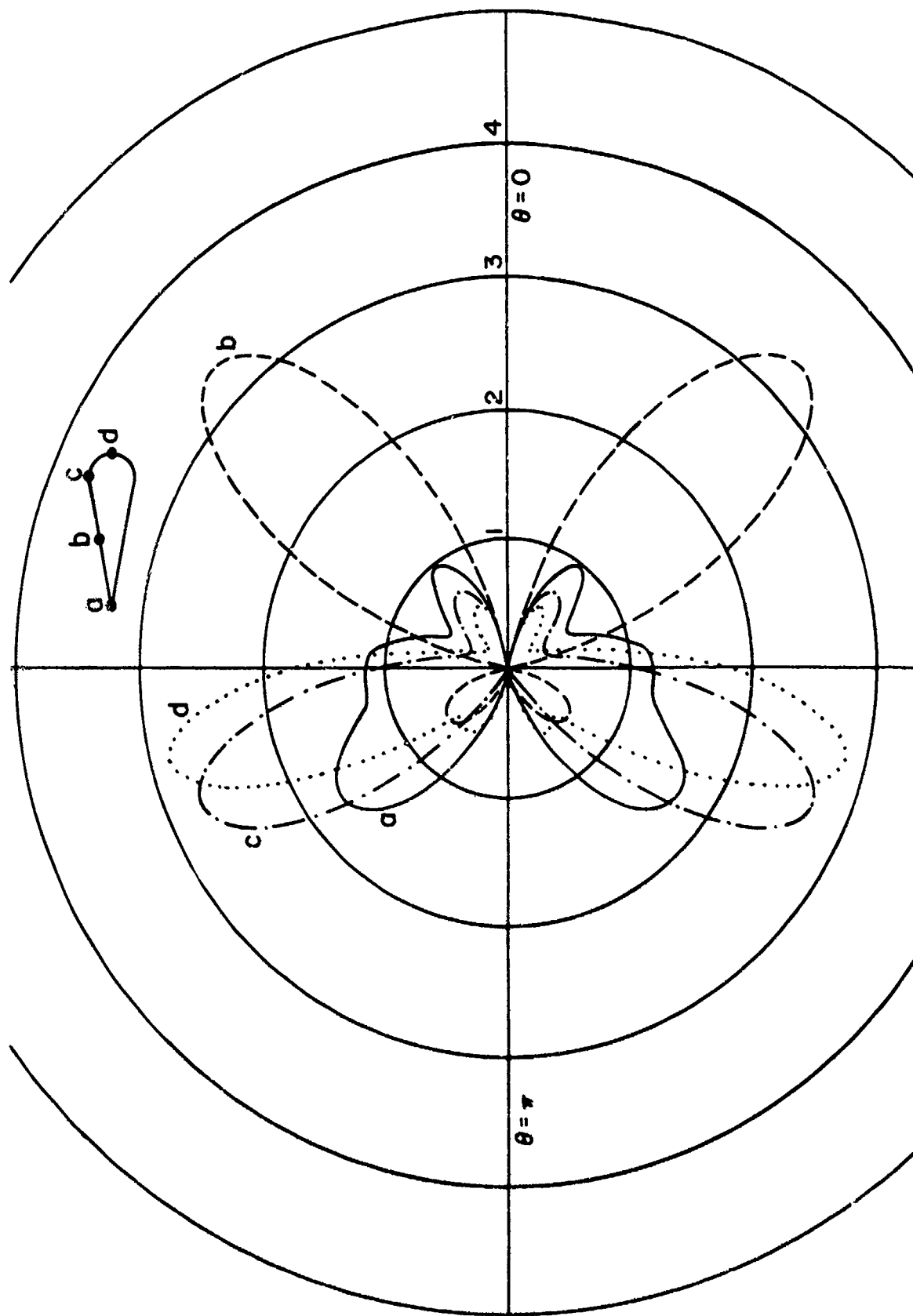


Figure 15. Power gain patterns (G vs. θ) for a loaded cone-sphere slot radiator. Feed is at (b). Loads are resonant bands at (a), (b), (c), or (d). Cone angle is 20° , sphere diameter is 0.4λ . There is no ϕ variation.

elements of the generalized admittance matrix for the particular mode. The program listing plus sample input-output data are given in Appendix A.

The subroutine LINEQ(LL,C) replaces the LL by LL matrix C by its inverse. C is a complex one-dimensional variable. The $(I,J)^{th}$ matrix element resides in $C(I + (J-1) * LL)$. If $LL > 58$, the dimension of the variable LR must be increased to at least LL.

Punched card data is read early in the main program according to

```
50 READ(1,51, END = 52) NN, NP, NPHI, BK
```

```
51 FORMAT(313, E14.7)
```

```
READ(1,53)(RH(I), I = 1, NP)
```

```
READ(1,53)(ZH(I), I = 1, NP)
```

```
53 FORMAT(10F8.4)
```

The excitation will have $e^{j(NN)\phi}$ dependence, NPHI has the same meaning as on page 55 of the previous report.^[1] BK is the propagation constant $k = \omega\sqrt{\mu\epsilon}$. An odd number NP of points are taken from the generating curve of the body of revolution. RH(I) and ZH(I) are respectively the distance ρ from the axis (z axis) of the body of revolution and the corresponding z coordinate. RH(I) may be zero only when $I = 1$ or $I = NP$. If the generating curve closes upon itself, care must be taken to make the coordinates at $I = 1$ identical to those at $I = NP$. The data is printed just after it is read.

If the first and NP^{th} data points are the same, the second and third data points are overlapped into the $NP + 1$ and $NP + 2$ position and NP is increased by two before going to do loop 57 which interpolates to find the distance DH(I) between the I^{th} and $(I + 1)^{th}$ data points, the radius ρ midway between the I^{th} and $(I + 1)^{th}$ data points, the corresponding z coordinate ZS(I), and the sine SV(I) and cosine CV(I) of the angle between the z axis and the straight line from the I^{th} to the $(I + 1)^{th}$ data points. Next, a few constants are entered among which PI is π and ETA is the intrinsic impedance $\eta = 376.707$ taken from the second edition of Smythe.^[13] The third edition of Smythe gives $\eta = 376.730$. DO loop 117 computes the t coordinate (arc length along the generating curve) TJ(I) of the peak of the I^{th} triangular expansion function. TJ is printed. DO loop 10 calculates

$$\text{CSM}(K+(I-\text{NN}+1)*\text{NPFI}) = \frac{\text{PI}}{\text{NPFI}} * \cos \left[I * \frac{\text{PI}*(K-.5)}{\text{NPFI}} \right] \text{ for } K = 1, 2, \dots, \text{NPFI}$$

and $I = \text{NN}-1, \text{NN}, \text{NN}+1$.

DO loop 16 calculates

$$\frac{1}{\text{DH}(J)} \int dt \int_0^\pi d\phi \frac{e^{-jkR}}{kR} \cos n\phi \quad (34)$$

The t integration is over the portion (assumed to be a straight line) of the generating curve between the J^{th} and $(J+1)^{\text{th}}$ data points. ϕ is the angle swept when the generating curve is revolved about the z axis. R is the distance between some field coordinate $(t', \phi' = 0)$ and the source coordinates (t, ϕ) . The expression (34) is proportional to the scalar potential at $(t', 0)$ coming from a $\frac{\cos n\phi}{\rho}$ charge density on the lateral surface of the frustum of a cone. The index J of do loop 16 indicates that the source coordinate t is between the J^{th} and $(J+1)^{\text{th}}$ data points. The index I of do loop 17 indicates that the field coordinate t' is midway between the I^{th} and $(I+1)^{\text{th}}$ data points. Except when the field point lies on the surface charge, the surface charge is approximated by line charges at $\phi = \frac{(K-.5)*\text{PI}}{\text{NPFI}}$, $K = 1, 2, \dots, \text{NPFI}$. When the field point lies on the surface charge, the surface charge $\frac{\cos n\phi}{\rho}$ is approximated by $\cos (.5*\text{PI}/\text{NPFI})/R(I)$ when $0 \leq \phi \leq \frac{\text{PI}}{\text{NPFI}}$, but for the region $\frac{\text{PI}}{\text{NPFI}} < \phi \leq \pi$ the line charges at $\phi = \frac{(K-.5)*\text{PI}}{\text{NPFI}}$, $K = 2, 3, \dots, \text{NPFI}$ are used. Do loop 5 stores the results of the t integrations at $\phi = \frac{(K-.5)*\text{PI}}{\text{NPFI}}$, $K = 1, 2, \dots, \text{NPFI}$ in GS. Do loop 13 multiplies the GS(K) by $\frac{\text{PI}}{\text{NPFI}} * \cos (n * \frac{(K-.5)*\text{PI}}{\text{NPFI}})$ and sums them over K to obtain expression (34) stored in G. Do loop 68 obtains $n = \text{NN}-1, \text{NN}$, and $\text{NN}+1$. The location $G(I + (J-1)*(\text{NP}-1) + (\text{NP}-1) * (\text{NP}-1) * (n-\text{NN}+1))$ corresponds to field point I , source region J and mode n . If the generating curve closes upon itself, the present NP is two more than the original NP of the input data.

The impedance matrix Z will be the same as that of equation (45) of the previous report^[1] except that the previously defined G_n 's will be used and the T_p and T'_p are modified. Also, since the new G_n 's are divided by k to make them insensitive to the absolute size of the body of revolution, the

new Z's must be multiplied by k. Because of possible unequal spacing of data points the 8 numbers T_p and T'_p were stored separately for each triangular expansion function. In do loop 74, the index J refers to the J^{th} triangular function while the numbers T_p and T'_p are stored in T and TP respectively. The J^{th} triangular function is approximated by 4 pulses of base lengths $DH(I + 2 * (J-1))$, $I = 1, 2, 3, 4$. The derivative of the J^{th} triangular function is just a pulse doublet. Denoting base lengths by Δ_1 , Δ_2 , Δ_3 , and Δ_4 ,

$$\begin{aligned} T(1 + 4*(J-1)) &= \frac{\Delta_1^2}{2*(\Delta_1 + \Delta_2)} \\ T(2 + 4*(J-1)) &= \frac{(\Delta_1 + .5*\Delta_2)*\Delta_2}{\Delta_1 + \Delta_2} \\ TP(1 + 4*(J-1)) &= \frac{\Delta_1}{\Delta_1 + \Delta_2} \\ TP(2 + 4*(J-1)) &= \frac{\Delta_2}{\Delta_1 + \Delta_2} \end{aligned} \quad (35)$$

Similar expressions involving Δ_3 and Δ_4 are used to treat the trailing edge of the triangular function. Expressions (35) are functional values (T for the triangle and TP for the derivative of the triangle) weighted by the base length in question. The base length weighting is necessary because the G_n 's have a factor $\frac{1}{DH(J)} = \frac{1}{\Delta_j}$ which must be offset. Also, the factor Δ_j is necessary for the field integration. For the field integral, the triangular function and its derivative are each approximated by four delta functions.

Unless the generating curve closes upon itself, there will be no peak of triangular function at the starting point and end point. The expansion function which is actually a triangular function over radius ρ will reduce to a constant at a starting point or end point on the z axis. However, if the starting point or end point is not on the z axis, the expansion functions reduce to zero there. In problems involving, perhaps, a conducting disk, the electric current normal to the rim goes to zero as the square root of the distance from the rim and the current parallel to the rim becomes large as one

over the square root of the distance from the rim, at least when an incident plane wave propagates perpendicular to the plane of the disk. The triangular functions used to expand the ϕ directed current were modified near the extremities of the generating curve where no overlapping occurs remote from the z axis. The triangular function (associated with the ϕ directed current) nearest such an extremity was modified by increasing its value at the extremity from zero to two. The logic from statements 115 to 116 performs this modification. Whereas the triangular functions associated with the t directed current were stored in T, the functions associated with the ϕ directed current are assigned TR.

Using G_n , T, TP, and TR the impedance matrix is calculated inside do loop 30. The calculation of the present impedance elements is very similar to a previous calculation using equation (45) of the previous report.^[1]

Statement 81 CALL LINEQ (NM2, Z) inverts the impedance matrix stored in Z to obtain the admittance matrix. The admittance matrix is printed inside do loop 93. If superscripts t ϕ are replaced by rs and if r = 0 denotes t, r = 1 denotes ϕ and similarly for s, then $(Z_n^{rs})_{i,j}$, $i = 1, 2, \dots, N-1$ is given by the $[J + r * (N-1) + s * 2 * (N-1)]^{\text{th}}$ execution of write statement 96. Here, N-1 is the number (either $\frac{NP-3}{2}$ or $\frac{NP-1}{2}$) of triangular functions. Immediately following statement 81, the admittance matrix of the array Z is recorded on a direct access device by

WRITE(6) (Z(I), I = 1, NZ)

If no direct access device is available, statements should be added to either punch the admittance matrix on cards or store it on tape. At the end of the program, execution is transferred back to read statement 50. If there is another set of data, it is processed. If not, execution terminates.

The dimension statements in the main program will not accommodate NPHI larger than 40 nor NP larger than 41 if the generating curve closes on itself. If the generating curve does not close on itself, NP may be as large as 43. Assuming that the generating curve might close on itself, minimum dimensions are:

COMPLEX Z((NP-1)*(NP-1)), GS(NPHI), G(3*(NP+1)*(NP+1))

DIMENSION RH(NP+2), ZH(NP+2), DH(NP+2), TJ($\frac{NP-1}{2}$)

DIMENSION SV(NP+1), CV(NP+1), ZS(NP+1), R(NP+1),

ANG(NPHI), AC(NPHI), CSM(3*NPHI)

DIMENSION TP(2*(NP-1)), T(2*(NP-1)), TR(2*(NP-1))

The NP referred to above is the original NP of the input data.

V. PLANE-WAVE SCATTERING, AXIAL INCIDENCE

This program computes the current on a conducting body of revolution and scattering patterns for excitation by a plane wave axially incident on the body. The input consists primarily of NP points defining the body contour, plus the [Y] matrix for the $n = 1$ mode. The output consists primarily of the current on the body, the scattered far-zone field, and the bistatic radar cross section. Printer plot routines are included to graph both the current and the radar cross sections. The program listing plus sample input-output data are given in Appendix B.

Subroutine PLANE(VVR, THR, NT) provides the measurement matrix elements of equations (77) and (81) of the report.^[1] NT angles θ_r (in radians) appear as input in THR. Other input appears in the common statement. U is the complex constant (0.,1.), R, ZS, SV and CV are respectively the radius ρ , the z coordinate, and the sine and cosine of the angle between the direction of the generating curve and the z axis. R(I), ZS(I), SV(I) and CV(I) are evaluated midway between the I^{th} and $(I+1)^{th}$ data points RH and ZH by drawing a straight line between them. BK is the propagation constant, there are (NP-1) R's, the excitation has $e^{j(NN)\phi}$ dependence, and T and TR are the previously computed weighted samples of the triangular functions for both the t and ϕ directed electric currents. When execution returns to the main program, the $(R_n)_i$ of equation (77) or (81) of the report^[1] will be stored in VVR($i + (K-1)*NM + (L-1)*4*NM$) where $K = 1, 2, 3, 4$ denotes respectively $(R_n^{t\theta})_i$, $(R_n^{\phi\theta})_i$, $(R_n^{t\phi})_i$ and $(R_n^{\phi\phi})_i$. As defined in the subprogram, NM is the number $\frac{NP-3}{2}$ of the triangular functions and L denotes the L^{th} of the angles θ_r .

In the subroutine PLANE, do loop 153 puts J! in FK(J+1). Do loop 156 sweeps the NT angles θ_r . Do loop 302 computes the required Bessel functions according to $J_n(x) = \sum_K \frac{(-1)^K \left(\frac{x}{2}\right)^{n+2K}}{K! (n+K)!}$. If the series for $J_n(x)$ does not converge readily, do loop 155 may be satisfied in which case error stop 155 is reached. When $\rho = R(J)$, $J_{NN+K} \left(k_\rho \sin \theta_r\right)$ will be stored in BJ(J + (K+1)*(NP-1)) for K = -1, 0, 1. To avoid direct computation of a Bessel function of negative order when NN = 0, $J_{-1}(x)$ is obtained from $J_1(x)$ in do loop 309. With ρf_i being represented by either T or TR, the t integration of equations (77) and (81) of the report^[1] is simulated in do loop 301. The ρf_i triangular function is approximated by four delta functions.

If NP (either the original NP of the data or 2 plus it if the generating curve overlaps) is larger than 43, the dimension of some of the variables in PLANE must be increased. These variables and their dimensions are:

```
COMMON R(NP-1), ZS(NP-1), SV(NP-1), CV(NP-1),
```

```
T(2*(NP-3)), TR(2*(NP-3))
```

```
DIMENSION BJ(3*(NP-1))
```

The common statement in the subroutine PLANE should be identical to that in the main program. In the unlikely case that the mode number NN is larger than 17, the dimension of FK must be increased to NN+3. Since the arguments VVR and THR are only dummy variables, their present dimension of 1 is always sufficient.

The subroutine REORD(K1, K3, L) rearranges the first L elements of K3 in descending order. Also, the first L elements of K1 are rearranged so as to maintain the original correspondence between the elements of K3 and those of K1.

Punched card data is read in early in the main program according to

```
50 READ(1,51, END = 52) NN, NP, NT, BK
```

```
51 FORMAT(3I3, E14.7)
```

```
READ(1,53)(RH(I), I = 1, NP)
```

```
READ(1,53)(ZH(I), I = 1, NP)
```

```
53 FORMAT(10F8.4)
```

All the input variables except NT are the same as the variables of the previous program. The receiver angles θ_r are given by

$$(\theta_r)_i = \frac{\pi(i-1)}{NT-1}, \quad i = 1, 2, \dots, NT$$

The punched card data is printed out immediately after it is read in.

Statement 126 checks to see whether the first and last points on the generating curve are identical. If they are identical, the variable KL is set equal to 0 and RH and ZH are expanded by overlapping the second and third points on the generating curve. In this way, an expansion function centered about the last original data point is obtained. If the first and last original data points are not identical, KL is 1 and execution proceeds to statement 58 in which case there are no expansion functions centered about the first and last data points. The logic between statements 58 and 78 prepares input data for the subroutine PLANE. Statement 85 inserts the receiver voltage matrices into VVR. Statement 127 inputs the admittance matrix appearing in (17) of the report.^[1] This admittance matrix will have been generated by the previous computer program.

Nearly all the statements following statement 127 are enclosed in do loop 108. When INC = 1, the electric field of the incident plane wave is $\mu_x e^{-jkz}$ and when INC = 2 it is $-\mu_x e^{jkz}$. The I column vector of equation (17) of the report is computed in do loop 2 and stored in TI. The inner do loop 3 uses transmitter voltage matrices obtained from the last $(\theta_r = \pi, \text{INC} = 1)$ and first $(\theta_r = 0, \text{INC} = 2)$ receiver voltage matrices. Equation (82) of the report^[1] and the fact that $R_n^{t\theta}$ is even in n and $R_n^{\phi\theta}$ is odd in n are used to relate the transmitter voltage matrices to the receiver voltage matrices. Do loops 7 and 8 compute TJ(J), the arc length which locates the center point of the J^{th} expansion function along the generating curve. The total length of the generating curve is normalized to 16. Do loop 9 performs the matrix multiplication indicated in equation (65) of the report.^[1] The measurement is stored in E1 and E2 corresponding to the θ and ϕ receiver polarizations. In do loop 11, E1 and E2 are normalized so that the quantity σ/λ^2 associated with each one is the square

of its magnitude. The phase of E_1 is set equal to zero in the backscattering direction which is $\theta_r = \pi$ for the e^{-jkz} incidence and $\theta_r = 0$ for the e^{+jkz} incidence.

Do loop 128 divides the expansion function coefficients by ρ to obtain the current. A multiplication by 2 or $2j$ converts from the exponential $e^{j\phi}$ to $\cos \phi$ or $\sin \phi$. The factor η is necessary to normalize the current to the incident magnetic intensity H^i . Do loop 129 averages the ϕ directed current J_ϕ according to

$$\frac{J_\phi(i-1) + 2J_\phi(i) + J_\phi(i+1)}{4}$$

The averaging was deemed necessary to attenuate extraneous oscillations in J_ϕ . If the generating curve does not close upon itself, the first and last J_ϕ are not averaged. Do loop 4 prints the arc length and real and imaginary parts and magnitude of the t and ϕ directed current. For an incident magnetic intensity $H^i = \underline{u}_y e^{-jkz}$ (INC = 1) or $H^i = \underline{u}_y e^{+jkz}$ (INC = 2), the current sinor \underline{J} is given in terms of the printed output JT and $J\phi$ by

$$\underline{J} = \underline{u}_t JT \cos \phi + \underline{u}_\phi J\phi \sin \phi$$

Do loop 12 prints the scattering patterns as functions of θ_r . $SIG X\theta$ is σ/λ^2 in the E plane and $SIG X\phi$ is σ/λ^2 in the H plane. $LSIG X\theta$ is $\log_{10} \sigma/\lambda^2$ in the E plane and $LSIG X\phi$ is $\log_{10} \sigma/\lambda^2$ in the H plane. $SIG X\theta$ and $SIG X\phi$ are respectively the magnitudes squared of $SX\theta$ and $SX\phi$. The phase of $SX\theta$ is taken to be zero in the backscattering direction. The magnitudes (MAG) and phase (ANG) of $SX\theta$ and $SX\phi$ are also tabulated. The scattered electric field will be proportional to

$$\underline{u}_\theta (SX\theta) \cos \phi + \underline{u}_\phi (SX\phi) \sin \phi$$

All the statements following do loop 12 are devoted to obtaining plots of the previously tabulated quantities MAG JT, MAG J ϕ , SIG X θ , and SIG X ϕ . Do loop 13 scales the current for plotting. K3 is the t directed current

and K_4 is the ϕ directed current. K_3 has been assigned the abscissa K_1 and K_4 the abscissa K_2 . After execution of statements 14 and 15, $K_3(J)$ will be the J^{th} largest K_3 and $K_1(J)$ its abscissa. The quantities K_3 and K_4 with abscissas K_1 and K_2 are plotted by do loop 20. Entering do loop 20, $K_5 = 1$. One line is printed for each J . If $K_3(K_5)$ is greater than or equal to $(51-J)$, an X is written after $K_1(K_5)$ blanks and K_5 is incremented by one. If $K_3(K_5)$ is still greater than or equal to $(51-J)$, another X is written after $K_1(K_5)$ blanks and K_5 is incremented. The process continues until $K_3(K_5)$ is less than $(51-J)$ in which case statement 20 is reached. Similar action is associated with K_4 and K_2 . If $K_3(NM)$ is larger than or equal to zero, $K_3(NM+1)$ will be observed, but $K_3(NM+1)$ has been set equal to -1 immediately after do loop 14.

The patterns SIG X_θ and SIG X_ϕ are plotted in a similar fashion. Actually, the logarithms of SIG X_θ and SIG X_ϕ are plotted but the scale is graduated in terms of SIG X_θ and SIG X_ϕ to simulate semi-log paper. Do loop 80 generates the abscissas K_1 and K_2 and ordinates K_3 and K_4 . Statements 16 and 17 arrange K_3 and K_4 in descending order. Do loop 87 plots SIG X_θ and SIG X_ϕ as X's and O's respectively. After do loop 108 is satisfied, execution goes back to the read statement 50. If another set of input data is encountered, execution traverses the program again. If not, execution stops.

Let NP be either the original NP of the data if the generating curve does not close upon itself or 2 plus the original NP of the data if the generating curve closes upon itself. When $NP > 43$ or $NT > 73$, some variables require larger dimensions. These variables are listed along with their minimum dimensions.

COMPLEX Y(4*NM*NM), VVR(4*NT*NM), TI(2*NM),

E3(NM), E1(NT), E2(NT)

COMMON R(NP-1), ZS(NP-1), SV(NP-1), CV(NP-1), T(4*NM), TR(4*NM)

DIMENSION RH(NP), ZH(NP), DH(NP-1), TJ(NM), THR(NT)

DIMENSION K1(NM), K1(NT), K2(NM), K2(NT), K3(NM), K3(NT), K4(NM), K4(NT)

The variables K1, K2, K3 and K4 must be dimensioned at least as large as the larger of NM and NT. Here, as in the main program, $NM = \frac{NP-3}{2}$.

VI. APERTURE RADIATION, ROTATIONAL SYMMETRY

This program computes the current on a conducting body of revolution excited by one or more rotationally symmetric apertures. It is assumed that the tangential electric field is known over the apertures. The input consists primarily of NP points defining the body contour, the [Y] matrix for the $n = 0$ mode, plus tangential E at the NP points on S. The output consists primarily of the current on the body, the radiation field, and the normalized power gain patterns. Printer plot routines are included to graph both the current and the power gain patterns. The program listing plus sample input-output data are given in Appendix C.

The program is similar to the one concerning scattering for axially incident plane waves except that the excitation voltage matrix is determined by input data instead of by an incident plane wave. Also, a gain instead of a scattering cross section is obtained from the measurement. (Equation (69) of the report.^[1])

The subroutine PLANE provides the measurement matrix elements of equations (77) and (81) of the report^[1] for the special case $n = 0$. This subroutine PLANE is similar to the subroutine of the same name used in the program concerning scattering for axially incident plane waves. For the case $n = 0$, R^{00} and R^{t0} may be dispensed with since they are zero.

The subroutine REORD is exactly the same as the one of the same name appearing in the program concerning scattering for axially incident plane waves.

Punched card data is read early in the main program according to

```
50 READ(1,51,END = 52) KK, NP, NT, BK
```

```
51 FORMAT(3I3, E14.7)
```

```
READ(1,53)(RM(I), I = 1, NP)
```

```
READ(1,53)(ZH(I), I = 1, NP)
```

```

53  FORMAT(10F8.4)
      IF(KK.EQ.2) GO TO 40
      READ(1,68)(E1(I), I = 1,NP)
168  FORMAT(7E11.4)
      IF(KK.EQ.1) GO TO 41
40  READ(1,168)(E2(I), I = 1, NP)
41  KL = 1

```

KK = 1 if the aperture electric field has only a t component.

KK = 2 if the aperture electric field has only a ϕ component.

KK = 3 if the aperture electric field has both t and ϕ components. NP points define the generating curve of the body of revolution. The first point and the NP^{th} point mark the extremities of the generating curve. NP must be odd. The gain pattern will be observed at NT angles θ_r . In degrees,

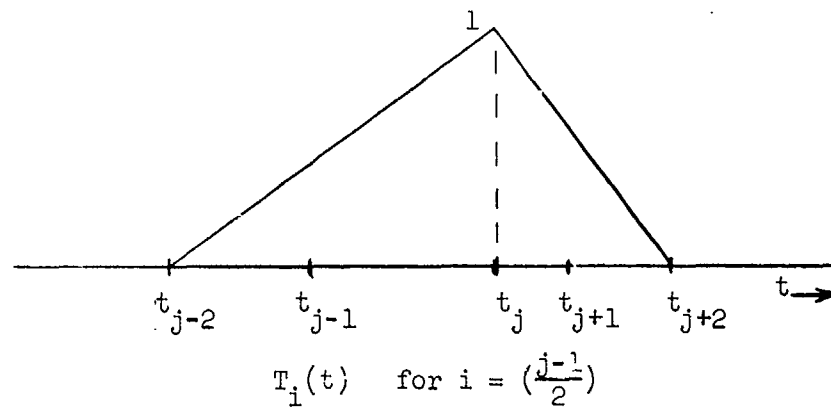
$$\theta_r = \frac{180(I-1)}{NT-1}, \quad I = 1, 2, \dots, NT.$$

BK is the propagation constant $k = \omega\sqrt{\mu\epsilon}$. RH(I) and ZH(I) are respectively the cylindrical coordinate radius ρ and axial distance z at data point I of the generating curve. E1 and E2 are complex. If $KK \neq 2$, E1(I) is the t component of the axially symmetric aperture electric field at point I on the generating curve. All the E1's except E1(J) being zero represents an aperture field $\frac{E1(J)}{2}$ between the $(J-1)^{th}$ and $(J+1)^{th}$ points or between the J^{th} and $(J+1)^{th}$ points if $J = 1$ or between the $(J-1)^{th}$ and J^{th} points if $J = NP$. If $RH(1) = RH(NP) \neq 0$ and $ZH(1) = ZH(NP)$, an E1(1) must be accompanied by an identical E1(NP). If $KK \neq 1$, E2(I) represents a ϕ directed aperture field in exactly the same way as E1(I) represented a t directed aperture field. If $KK = 3$, both E1 and E2 occur simultaneously. The punched card data is printed out soon after it is read.

Statement 126 sets KL = 0, overlaps two of the data points and adds 2 to NP if the generating curve closes upon itself. Do loop 57 draws a straight line between the $(I+1)^{th}$ and I^{th} data points to obtain BH(I), R(I), ZS(I),

SV(I), and CV(I), the increment of arc length, the cylindrical coordinate radius, the axial distance, and the sine and cosine of the angle between \underline{t} and the z axis, all evaluated midway between the $(I+1)^{\text{th}}$ and I^{th} data points. Do loop 1 stores the NT angles θ_r in THR.

The triangle functions (equation 31 of the report^[1]) are modified slightly if the data points on the generating curve are not exactly equally spaced.



For J odd, the $\left(\frac{J-1}{2}\right)^{\text{th}}$ modified function is given by

$$T_i(t) = \begin{cases} 1 + \frac{t-t_j}{t_j-t_{j-2}} & t_{j-2} \leq t \leq t_j \\ 1 - \frac{t-t_j}{t_{j+2}-t_j} & t_j \leq t \leq t_{j+2} \\ 0 & \text{all other } t. \end{cases}$$

where $i = \frac{(j-1)}{2}$.

The subscript j on t indicates the J^{th} data point. For J odd, this $\left(\frac{J-1}{2}\right)^{\text{th}}$ function is characterized by 4 numbers $T(2*J-6+I)$, $I = 1, 2, 3, 4$. Coming out of do loop 74, $T(2*J-6+I)$ is $T_i(t)$ midway between the $(J-3+I)^{\text{th}}$ and $(J-2+I)^{\text{th}}$ data points multiplied by the arc length included between the $(J-3+I)^{\text{th}}$ and $(J-2+I)^{\text{th}}$ data points. The multiplication by the increment of arc length factor facilitates integrations over the source and field regions.

If $KL \neq 0$ and if $RH(1)$ is not zero, the body of revolution has a rim. The previously defined $T(t)$ nearest the rim will be zero at the rim. Since the ϕ directed current is not expected to be zero at the rim, the $T(t)$ associated with the ϕ directed current nearest the rim was changed to 2 at the rim. This amplitude 2 makes the function linear in t when the points t_j in question are equally spaced. The logic between statements 74 and 78 represents the functions associated with the ϕ directed current by TR.

Do loop 7 computes the arc length TJ at every other data point along the generating curve. Do loop 8 normalizes TJ for a generating curve of length 10.

Using T and TR to invoke a pulse approximation to the $T(t)$ functions, do loop 44 uses the aperture electric field data to calculate and store in E3 the excitation voltage matrices, (equation (27) of the report^[1]). If $E3(J)$ represents excitation in the t direction, $E3(J+NM)$ represents a corresponding excitation in the ϕ direction. Actually if $KK \neq 5$, there is only one type of excitation and either $E3(J)$ or $E3(J+NM)$ is automatically set equal to zero.

Statement 185 reads the admittance matrix Y from, in this case, direct access data set 6. Do loop 134 calculates the coefficients TI of the current expansion functions by multiplying the admittance matrix Y by the excitation voltage matrix E3. If $TI(J)$ represents a t directed current, then $TI(J+NM)$ represents the corresponding ϕ directed current. Since the admittance submatrices $Y^{\phi t}$ and $Y^{t\phi}$ are zero, the t directed aperture field will excite only a t directed electric current and the ϕ directed aperture field only a ϕ directed current. Still in do loop 134, the power required to maintain the aperture field is obtained by summing the products of the complex conjugate of a coefficient of a current expansion function with the corresponding excitation voltage matrix element. The power associated with the t directed aperture electric field is put in P1 and the power associated with the ϕ directed aperture electric field in P2. Since only the real part of the complex power is required to normalize the gain, neither P1 nor P2 are defined to be complex variables. P1 and P2 are written just after do loop 134. The sample printer output for the cone sphere data came from an

earlier version of the program which printed P1 and P2 according to

```
WRITE(3,169) P1, P2, P3
169 FORMAT(1X,7E11.4)
```

where P3 was just the constant $4\pi/k^2\eta$. If $KK \neq 3$, either P1 or P2 is zero. For some problems with aperture excitation very near the poles of the body of revolution, P2 was negative. This apparent error is due not to the method of moments itself, but to the approximations made in obtaining the source and field integrals.

Do loop 9 calculates complex numbers E1 and E2 whose magnitude is the square root of the gain by pre-multiplying the matrix of current coefficients TI by the measurement voltage matrices VVR previously supplied by the subroutine PLANE. The proper normalization is obtained in statements 190 and 191. E1 and E2 at 1 and NT are expected to be zero. Just to be definite, the 4 statements before do loop 139 assign the phase 0 to E1 and E2 at 1 and NT. The magnitude of E1 squared is the gain associated with the t directed aperture electric field and the magnitude of E2 squared is the gain associated with the ϕ directed aperture electric field. Since the measurement voltage submatrices $R^{\phi\theta}$ and $R^{t\phi}$ are zero, the t directed electric current will excite only a θ directed far field and the ϕ directed current only a ϕ directed far field. Do loop 139 converts the coefficients TI of the current expansion functions to actual currents per unit length by dividing by the cylindrical coordinate radius RH.

After do loop 139, the remainder of the program is devoted to printing and plotting the electric currents and gains. The currents are printed in either do loop 140 or do loop 143. These currents in amperes per unit length are independent of ϕ and possess real and imaginary parts. The gains are printed in either do loop 156, 159 or 167. In the heading, $G\theta$ is the gain associated with the t directed current and $G\phi$ is the gain associated with the ϕ directed current. $E\theta$ and $E\phi$ are the square roots of the respective gains. ANG $E\theta$ and ANG $E\phi$ are indicative of the phases of the θ and ϕ directed electric fields in the far zone.

In do loop 171, $M = 1$ obtains plots of the t directed current JT and

gain $G\theta$ while $M = 2$ obtains plots of the ϕ directed current $J\phi$ and gain $G\phi$. Do loop 172 finds $X1$ and $X2$, the maximum magnitudes of the real and imaginary parts of the current. Do loop 13 normalizes $X1$ and $X2$ to full scale. $K3$ and $K4$ represent the real and imaginary parts of the currents and $K1$ and $K2$ their corresponding abscissas. $\text{CALL REORD}(K1, K3, NM)$ arranges $K3$ in descending order. The abscissas $K1$ are arranged accordingly to maintain the original correspondence between $K3$ and $K1$. $\text{CALL REORD}(K2, K4, NM)$ operates similarly upon $K2$ and $K4$. The current is plotted in do loop 20. One line is printed for each J . Data is plotted on a given line only if the ordinate of the data is greater than or equal to the ordinate of the line. If some data is out of range, that which is too large accumulates at the top of the plot while that which is too small is ignored. Do loop 80 prepares the gain to be plotted on a logarithm scale via $K3$ and $K1$. $\text{CALL REORD}(K1, K3, NT)$ arranges $K3$ in descending order while still keeping track of $K1$. The gain is plotted by do loop 87. At the end of the program execution is transferred back to read statement 50. If there is another set of punched card data, the program recycles. If not, execution stops.

Let NP be either the original NP of the data if the generating curve does not close upon itself or 2 plus the original NP of the data if the generating curve closes upon itself. When $NP > 43$ or $NT > 73$, some variables require larger dimensions. These variables are listed along with their minimum dimensions.

```
COMPLEX Y(4*NM*NM), VVR(2*NT*NM), TI(2*NM),
      E3(2*NM), E1(NP), E1(NT), E2(NP), E2(NT)
COMMON R(NP-1), ZS(NP-1), SV(NP-1), CV(NP-1),
      T(4*NM), TR(4*NM)
DIMENSION RH(NP), ZH(NP), DH(NP-1), TJ(NM), THR(NT)
DIMENSION K1(NM), K1(NT), K2(NM), K3(NM), K3(NT), K4(NM)
```

Here, as in the main program, $NM = \frac{NP-3}{2}$. The variables $E1, E2, K1$, and $K3$ serve a dual purpose. The common statement in the subroutine PLANE should be exactly as it is in the main program.

VII. BACKSCATTERING, OBLIQUE INCIDENCE

This program computes the backscattered field and monostatic radar cross section for a conducting body of revolution excited by a plane wave from an arbitrary direction of incidence. The current is also found but not printed out. The input consists primarily of NP points defining the body contour plus the [Y] matrices for all modes n satisfying (33). The output consists primarily of the backscattered field and monostatic radar cross section patterns. The cross section patterns are graphed by a printer plot routine. The program listing plus sample input-output data are given in Appendix D.

The subroutines PLANE and REORD are exactly the same as the ones in the program concerning scattering for axially incident plane waves.

Punched card data is read early in the main program according to

```
50 READ(1,51, END = 52) KK, NP, NT, BK
51 FORMAT(3I3, E14.7)
   READ(1,53)(RH(I), I = 1, NP)
   READ(1,53)(ZH(I), I = 1, NP)
53 FORMAT(10F8.4)
```

The punched card data for the backscattering program is the same as that for the program concerning scattering for axially incident plane waves except that NN is replaced by KK. For oblique incidence, the R_n 's of equations (77) and (81) of the report^[1] are considered for only $n = 0, 1, 2, \dots, KK-1$. Up to and including do loop 8, the programs for backscattering and for axial incidence are essentially the same.

Do loop 42 initializes E1, the measurement for a θ directed transmitter and a θ directed receiver, and E2, the measurement for a ϕ directed transmitter and a ϕ directed receiver. When both transmitter and receiver are located at $\phi = 0$, there are no $\theta\phi$ or $\phi\theta$ polarization components. For the $\theta\theta$ and $\phi\phi$ polarizations, $\tilde{R}_{-n} Y_{-n} V_{-n} = \tilde{R}_n Y_n V_n$ so that the measurement must be multiplied by an extra factor 2 if $n \neq 0$. Inside do loop 40, the subroutine

PLANE is called upon to provide VVR, the receiver voltage corresponding to R_n for $n = KK-1$. From the KK^{th} record of data set 6, statement 127 reads the admittance matrix Y_n for the same $(M-1)^{th}$ mode. Each L of do loop 41 denotes a different polar angle θ . For transmitters in the direction θ from an origin near the body of revolution, do loop 3 puts the currents in E3 and E4. The transmitter voltage matrices necessary for computation of the currents have been abstracted from the receiver voltage matrices VVR by merely changing the sign of the elements corresponding to $R^{\phi\theta}$ and $R^{t\phi}$. Do loop 43 adds the measurements $\tilde{R}_n Y_n V_n$ to E1 and E2. Toward the end of do loop 41, SIG $\theta\theta$ and SIG $\phi\phi$ along with their square roots MAG S $\theta\theta$ and MAG S $\phi\phi$ are printed. SIG $\theta\theta$ and SIG $\phi\phi$ are echo areas per square wavelength (σ/λ^2) obtained by squaring the product of E1 or E2 with P1. P1 is the constant $k^2 \eta/2\pi^{3/2}$ defined earlier in the program just after do loop 1.

The fixed point ordinates K3 and K4 and abscissas K1 and K2 appearing in do loop 80 facilitate plotting the echo areas per square wavelength on a logarithm scale. Do loop 80 also repeats the final printing of the echo areas per square wavelength. Statements 14 and 15 arrange K3 and K4 in descending order and do loop 87 plots the echo areas per square wavelength in the same way that the bistatic scattering cross sections were plotted in the program for axially incident plane waves.

If $NP > 43$ or $NT > 73$, most variables require larger dimensions. The affected variables are the same as those of the same name appearing in the program for axially incident plane waves except E3 and E4 which must be dimensioned at least as large as TI was in the program for axially incident plane waves.

VIII. REFERENCES

- [1] J. R. Mautz and R. F. Harrington, "Generalized Network Parameters for Bodies of Revolution," Scientific Report No. 1, Contract No. F-19628-67-C-0233, Air Force Cambridge Research Laboratories, Bedford, Massachusetts, with Syracuse University, Syracuse, New York, May 1968.
- [2] J. R. Mautz and R. F. Harrington, "Radiation and Scattering from Bodies of Revolution," Applied Scientific Research, vol. 20, 1969.
- [3] J. R. Mautz, "Radiation and Scattering from Bodies of Revolution," Ph.D. Thesis, Syracuse University, June 1968.
- [4] R. F. Harrington, "Generalized Network Parameters in Field Theory," Proc. Symposium on Generalized Networks, MRIS Series, vol. XVI, Polytechnic Press, Brooklyn, N. Y., 1966.
- [5] R. F. Harrington, Field Computation by Moment Methods, Macmillan Co., New York, 1968.
- [6] M. G. Andreasen, "Scattering from Bodies of Revolution," IEEE Trans., vol AP-13, No. 2, March 1965.
- [7] R. F. Harrington, "Theory of Loaded Scatterers," Proc. IEE (London), vol. 111, No. 4, April 1964.
- [8] R. F. Harrington, Time-Harmonic Electromagnetic Fields, McGraw-Hill Book Co., 1961, pp. 365-380.
- [9] C. L. Andrews, "Diffraction Pattern in a Circular Aperture Measured in the Microwave Region," Journ. Appl. Phys., vol. 21, No. 8, August 1950.
- [10] H. L. Robinson, "Diffraction Patterns in Circular Apertures Less Than One Wavelength in Diameter," Journ. Appl. Phys., vol. 24, No. 1, Jan. 1953.
- [11] M. J. Ehrlich, S. Silver, G. Held, "Studies of the Diffraction of Electromagnetic Waves by Circular Apertures and Complementary Obstacles: The Near-zone Field," Journ. Appl. Phys., vol. 26, No. 3, March 1955.
- [12] F. V. Schultz, G. M. Ruckgaber, J. K. Schindler, C. C. Rogers, "The Theoretical and Numerical Determination of the Radar Cross Section of a Finite Cone," Proc. IEEE, vol. 53, No. 8, August 1965.
- [13] W. R. Smythe, Static and Dynamic Electricity, McGraw-Hill Book Co., Second Edition 1950, Third Edition, 1968, Appendix.

APPENDIX A. PROGRAM AND SAMPLE INPUT-OUTPUT DATA FOR SECTION IV.

```

//          (0034,EE,6,2),'MAUTZ,JOE',MSGLEVEL=1
// EXEC FORTGCLG,PARM.FORT='MAP'
//FORT.SYSIN DD *
      SUBROUTINE LINEQ(LL,C)
      COMPLEX C(1),STOR,STO,ST,S
      DIMENSION LR(58)
      DO 20 I=1,LL
      LR(I)=I
20  CONTINUE
      M1=0
      DO 18 M=1,LL
      K=M
      DO 2 I=M,LL
      K1=M1+I
      K2=M1+K
      IF(CABS(C(K1))-CABS(C(K2))) 2,2,6
6  K=I
2  CONTINUE
      LS=LR(M)
      LR(M)=LR(K)
      LR(K)=LS
      K2=M1+K
      STOR=C(K2)
      J1=0
      DO 7 J=1,LL
      K1=J1+K
      K2=J1+M
      STO=C(K1)
      C(K1)=C(K2)
      C(K2)=STO/STOR
      J1=J1+LL
7  CONTINUE
      K1=M1+M
      C(K1)=1./STOR
      DO 11 I=1,LL
      IF(I-M) 12,11,12
12  K1=M1+I
      ST=C(K1)
      C(K1)=0.
      J1=0
      DO 10 J=1,LL
      K1=J1+I
      K2=J1+M
      C(K1)=C(K1)-C(K2)*ST
      J1=J1+LL
10  CONTINUE
11  CONTINUE
      M1=M1+LL
18  CONTINUE
      J1=0
      DO 9 J=1,LL
      IF(J-LR(J)) 14,8,14
14  LRJ=LR(J)
      J2=(LRJ-1)*LL
21  DO 13 I=1,LL
      K2=J2+I
      K1=J1+I
      S=C(K2)
      C(K2)=C(K1)
      C(K1)=S

```



```

13 CONTINUE
  LR(J)=LR(LRJ)
  LR(LRJ)=LRJ
  IF(J-LR(J)) 14,8,14
8 J1=J1+LL
9 CONTINUE
  RETURN
  END
  COMPLEX A3,A4,Z(1600),GS(40),G(5292),U
  DIMENSION RH(43),ZH(43),DH(43),TJ(20)
  DIMENSION SV(42),CV(42),ZS(42),R(42),ANG(40),AC(40),CSM(120)
  DIMENSION TP(80),T(80),TR(80),JK(4)
  REWIND 6
  U=(0.,1.)
50 READ(1,51,END=52) NN,NP,NPHI,BK
51 FORMAT(3I3,E14.7)
  READ(1,53)(RH(I),I=1,NP)
  READ(1,53)(ZH(I),I=1,NP)
53 FORMAT(10F8.4)
76 WRITE(3,54) NN,NP,NPHI,BK
54 FORMAT(1X// ' NN=' ,I3, ' NP=' ,I3, ' NPHI=' ,I3, ' BK=' ,E14.7)
55 FORMAT(1X/ ' RH' )
  WRITE(3,55)
  WRITE(3,46)(RH(I),I=1,NP)
46 FORMAT(1X,10F8.4)
  WRITE(3,56)
56 FORMAT(1X/ ' ZH' )
  WRITE(3,46)(ZH(I),I=1,NP)
  IF((RH(1)-RH(NP)).NE.0..OR.(ZH(1)-ZH(NP)).NE.0.) GO TO 58
  RH(NP+1)=RH(2)
  ZH(NP+1)=ZH(2)
  RH(NP+2)=RH(3)
  ZH(NP+2)=ZH(3)
  NP=NP+2
58 DO 57 I=2,NP
  I2=I-1
  RR1=RH(I)-RH(I2)
  RR2=ZH(I)-ZH(I2)
  DH(I2)=SQRT(RR1*RR1+RR2*RR2)
  ZS(I2)=.5*(7H(I)+ZH(I2))
  R(I2)=.5*(RH(I)+RH(I2))
  SV(I2)=RR1/DH(I2)
  CV(I2)=RR2/DH(I2)
57 CONTINUE
  KG=NP-1
  N=KG/2
  NM=N-1
  NM2=NM*2
  NM4=NM*4
  NZ=NM2*NM2
  NG=KG*KG
  M5=NN+2
  M6=NN+4
  FM=NN
  FM2=NN*NN
  PI=3.141593
  ETA=376.707
  DP=PI/NPHI
  CA=BK*BK*ETA

```

```

      CQ=ETA
      SS=0.
      DO 117 I=1,NM
        I1=2*(I-1)+1
        I2=I1+1
        SS=SS+DH(I1)+DH(I2)
        TJ(I)=SS
117  CONTINUE
      WRITE(3,118)
118  FORMAT(1X/' TJ')
      WRITE(3,46) (TJ(I),I=1,NM)
      DO 2 J=1,NPHI
        ANG(J)=(J-.5)*DP
        AC(J)=COS(ANG(J))
      2  CONTINUE
      M3=0
      DO 10 MM=M5,M6
        M1=MM-3
        M2=M3*NPHI
        DO 11 K=1,NPHI
          K1=M2+K
          CSM(K1)=DP*COS(M1*ANG(K))
11  CONTINUE
        M3=M3+1
10  CONTINUE
      DO 16 J=1,KG
        DEL=.5*DH(J)
        DEL1=DH(J)*BK
        AA=DP*R(J)*DEL*BK
        DO 17 I=1,KG
          Z3=ZS(J)-ZS(I)
          RR1=SV(J)*R(J)+CV(J)*Z3
          RR2=-SV(J)*R(I)
          RR3=R(J)*R(J)+R(I)*R(I)+Z3*Z3
          RR4=-2.*R(J)*R(I)
          X1=ABS(R(J)-R(I))+ABS(Z3)
          DO 5 K=1,NPHI
            IF(K.NE.1.OR.X1.NE.0.) GO TO 7
            X=R(J)*DP
            XX=SQRT(DEL*DEL+X*X)
            W1=(X*ALOG((DEL+XX)/X)+DEL*ALOG((X+XX)/DEL))/AA
            W2=-1.
            GS(1)=W1+U*W2
            GO TO 5
          7  Y=ABS(RR1+AC(K)*RR2)
            RD=RR3+RR4*AC(K)
            RK=BK*SQRT(RD)
            D2=RD-Y*Y
            Y1=Y-DEL
            Y2=Y+DEL
            R1=SQRT(Y1*Y1+D2)
            R2=SQRT(Y2*Y2+D2)
            IF(Y1) 72,73,73
          72  TIN=ALOG((1-Y1+R1)*(Y2+R2)/D2)
            GO TO 25
          73  TIN=ALOG((Y2+R2)/(Y1+R1))
25  SN=SIN(RK)
      CS=COS(RK)
      GS(K)=(CS-U*SN)*(TIN-U*(BK*DH(J)-RK*TIN))/DEL1
      5  CONTINUE

```

```

M3=(J-1)*KG+I
DO 68 MM=1,3
M1=MM-1
M4=M1*NPHI
M2=M1*NG+M3
G(M2)=0.
DO 13 K=1,NPHI
K2=K+M4
G(M2)=G(M2)+GS(K)*CSM(K2)
13 CONTINUE
68 CONTINUE
17 CONTINUE
16 CONTINUE
DO 74 J=1,NM
J2=2*(J-1)+1
J3=J2+1
J4=J3+1
J5=J4+1
J6=4*(J-1)+1
J7=J6+1
J8=J7+1
J9=J8+1
DEL1=DH(J2)+DH(J3)
DEL2=DH(J4)+DH(J5)
TP(J6)=DH(J2)/DEL1
TP(J7)=DH(J3)/DEL1
TP(J8)=-DH(J4)/DEL2
TP(J9)=-DH(J5)/DEL2
T(J6)=DH(J2)*DH(J2)/2./DEL1
T(J7)=DH(J3)*(DH(J2)+DH(J3)/2.)/DEL1
T(J8)=DH(J4)*(DH(J5)+DH(J4)/2.)/DEL2
T(J9)=DH(J5)*DH(J5)/2./DEL2
74 CONTINUE
DO 75 J=1,NM4
TR(J)=T(J)
75 CONTINUE
115 IF((ZH(1)-ZH(NP-2)).EQ.0..AND.(RH(1)-RH(NP-2)).EQ.0.) GO TO 78
IF(RH(1)) 77,23,77
77 DEL1=DH(1)+DH(2)
TR(1)=DH(1)*(1.+(DH(2)+DH(1)/2.)/DEL1)
TR(2)=DH(2)*(1.+(DH(2)/2.)/DEL1)
23 IF(RH(NP)) 79,78,79
79 J1=(N-2)*4+3
J2=J1+1
DEL2=DH(NP-2)+DH(KG)
TR(J1)=DH(NP-2)*(1.+(DH(NP-2)/2.)/DEL2)
116 TR(J2)=DH(KG)*(1.+(DH(NP-2)+DH(KG)/2.)/DEL2)
78 DO 30 J=1,NM
JL=(J-1)*NM2
J3=(J-1)*4
J1=2*(J-1)
DO 31 I=1,NM
L1=JL+I
L2=L1+NM
L3=NM*NM2+L1
L4=L3+NM
Z(L1)=0.
Z(L2)=0.
Z(L3)=0.

```

```

Z(L4)=0.
I1=2*(I-1)
I3=(I-1)*4
DO 70 JJ=1,4
J2=J1+JJ
J7=J3+JJ
DO 71 I1=1,4
I2=I1+I1
I7=I3+I1
J4=(J2-1)*KG+I2
J5=J4+NG
J6=J5+NG
SS=SV(I2)*SV(J2)
CC=CV(I2)*CV(J2)
A3=.5*(G(J6)+G(J4))
A4=.5*(G(J6)-G(J4))
Z(L1)=Z(L1)+(CA*TP(I7)*T(J7)*(SS*A3+CC*G(J5))-CW*TP(I7)*TP(J7)*G(J5
1))*U
Z(L2)=Z(L2)+CA*SV(J2)*TR(I7)*T(J7)*A4-FM*CO*G(J5)*TR(I7)*TP(J7)/R(
1I2)
Z(L3)=Z(L3)-CA*SV(I2)*T(I7)*TR(J7)*A4+FM*CO*G(J5)*TP(I7)*TR(J7)/R(
1J2)
Z(L4)=Z(L4)+(CA*A3-FM2*CO/R(I2)/R(J2)*G(J5))*TR(I7)*TR(J7)*U
71 CONTINUE
70 CONTINUE
31 CONTINUE
30 CONTINUE
81 CALL LINEO(NM2,Z)
WRITE(6)(Z(I),I=1,NZ)
JK(1)=1
JK(2)=N
JK(3)=NM2*N+1
JK(4)=JK(3)+NM
DO 93 J=1,4
K1=JK(J)
WRITE(3,24) J
24 FORMAT(1X,'Y',I1)
DO 92 I=1,NM
K2=K1+NM-1
9A WRITE(3,88)(Z(K),K=K1,K2)
88 FORMAT(1X,10G11.4)
K1=K1+NM2
92 CONTINUE
93 CONTINUE
GO TO 50
52 STOP
END

```

```

/*
//GO.FTOAF001 DD DSNAME=EE0034.REV1,DISP=OLD,UNIT=2314,
// VOLUME=SER=SU0004,DCR=(RECFM=V,BLKSIZE=1800,LRECL=1796)
//GO.SYSIN DD *
001041 20 0.4A59995E+00
0.0 0.0868 0.1736 0.2605 0.3473 0.4341 0.5209 0.6078 0.6946 0.7814
0.8682 0.9551 1.0419 1.1287 1.2155 1.3024 1.3892 1.4760 1.5628 1.6497
1.7365 1.8233 1.9101 1.9970 2.0838 2.1706 2.2574 2.3442 2.4311 2.5179
2.6047 2.6837 2.6863 2.5969 2.4184 2.1570 1.8216 1.4238 0.9772 0.4971
-0.0000
0.0 0.4924 0.9848 1.4772 1.9696 2.4620 2.9544 3.4468 3.9392 4.4316
4.9240 5.4164 5.9088 6.4013 6.8937 7.3861 7.8785 8.3709 8.8633 9.3557
9.8481 10.3405 10.8329 11.3253 11.8177 12.3101 12.8025 13.2949 13.7873 14.2797
14.7721 15.2657 15.7650 16.2562 16.7225 17.1478 17.5177 17.8195 18.0427 18.1798
18.2260
/*

```

[illegible]

0.2949E-03	0.2949E-02	0.4193E-05	0.7113E-02	0.4945E-05	0.1775E-02	0.3165E-05	0.1626E-02	0.1437E-05	0.2234E-03
0.4118E-04	0.1197E-04	0.3191E-05	0.1629E-02	0.5941E-05	0.1811E-02	0.6520E-05	0.1005E-02	0.6319E-05	0.1979E-03
0.4044E-04	0.1194E-04	0.2459E-05	0.4646E-03	0.7607E-06	0.3084E-03	0.2779E-05	0.4893E-03	0.4631E-05	0.2703E-03
0.4045E-05	0.2464E-05	0.3463E-05	0.0404E-03	0.1101E-05	0.9675E-04	0.2494E-07	0.1372E-03		
0.6143E-05	0.2187E-07	0.7994E-05	0.4245E-02	0.1059E-05	0.5166E-03	0.1115E-04	0.5611E-03	0.4773E-05	0.8043E-04
0.6507E-05	0.1034E-04	0.1767E-05	0.3671E-05	0.3671E-05	0.6666E-03	0.6640E-05	0.3676E-03	0.1178E-04	0.7613E-04
0.1500E-04	0.1197E-05	0.1186E-05	0.1902E-03	0.6567E-05	0.1705E-03	0.4131E-05	0.1501E-03	0.6932E-06	0.6405E-04
0.4045E-04	0.6462E-04	0.4177E-05	0.4001E-05	0.3727E-04	0.1559E-05	0.5119E-04			
0.6711E-05	0.1754E-07	0.1047E-06	0.5111E-05	0.1796E-05	0.2490E-02	0.2321E-04	0.1746E-02	0.2389E-04	0.2207E-02
0.3143E-04	0.1660E-03	0.1465E-05	0.6645E-03	0.6741E-05	0.1875E-02	0.2680E-05	0.1001E-02	0.1394E-04	0.1949E-03
0.2716E-04	0.1991E-03	0.2698E-04	0.5966E-03	0.2476E-05	0.5265E-03	0.2181E-04	0.3600E-03	0.1397E-04	0.2909E-03
0.4045E-04	0.1451E-05	0.4643E-05	0.1415E-05	0.6816E-05	0.9538E-04	0.5006E-05	0.1331E-03		
0.2968E-05	0.1410E-07	0.1032E-06	0.5405E-03	0.2316E-06	0.1741E-02	0.1835E-04	0.1047E-02	0.3424E-04	0.2804E-03
0.3676E-04	0.4814E-06	0.3373E-06	0.1901E-03	0.2011E-06	0.2888E-03	0.8227E-05	0.2267E-03	0.8727E-05	0.1032E-03
0.3941E-04	0.1197E-06	0.3441E-06	0.1946E-04	0.4077E-06	0.6061E-04	0.3831E-06	0.2864E-04	0.3025E-04	0.7042E-04
0.1491E-04	0.5610E-04	0.0806E-05	0.1295E-04	0.1077E-06	0.1295E-04	0.6154E-05	0.2331E-04		
0.1496E-04	0.2764E-07	0.6746E-06	0.8111E-05	0.2399E-06	0.2222E-02	0.3425E-04	0.2830E-03	0.3964E-04	0.2894E-02
0.4765E-04	0.1197E-06	0.4193E-06	0.1415E-05	0.6935E-06	0.1970E-02	0.2511E-04	0.9853E-03	0.3766E-05	0.2355E-03
0.4765E-04	0.1197E-06	0.4193E-06	0.1415E-05	0.6935E-06	0.1970E-02	0.2511E-04	0.9853E-03	0.3766E-05	0.2355E-03

[illegible]

-0.6414E-02 0.7840E-06 0.4153E-02 0.6501E-07 0.2861E-07 0.5708E-06 0.9863E-02 0.2898E-06 0.1375E-01 0.3429E-06
 -0.1416E-01 0.1031E-05 0.1225E-01 0.8510E-06 0.9412E-07 0.1511E-05 0.6435E-02 0.1031E-05 0.4390E-02 0.1203E-05
 0.7745E-02 0.0607E-07 0.1608E-02 0.1161E-05 0.7612E-03 0.2719E-07 0.1146E-03 0.1436E-06
 0.3323E-03 0.6062E-06 0.4050E-03 0.1307E-05 0.8745E-03 0.1881E-05 0.2289E-03 0.8288E-03 0.2878E-05
 -0.2287E-02 0.2024E-05 0.1478E-02 0.7519E-05 0.2472E-05 0.3512E-02 0.1987E-05 0.4889E-02 0.1438E-05
 -0.5742E-03 0.0655E-06 0.4362E-06 0.6403E-06 0.3357E-02 0.4666E-06 0.2363E-02 0.1759E-06 0.1513E-05
 0.7444E-03 0.2109E-03 0.3872E-05 0.2682E-03 0.3425E-05 0.4293E-04 0.1444E-05
 -0.2433E-03 0.6408E-06 0.0755E-03 0.2105E-05 0.1417E-02 0.4151E-05 0.2763E-02 0.4251E-05 0.2392E-02 0.4549E-05
 0.6439E-02 0.7900E-05 0.4174E-02 0.6387E-05 0.2873E-02 0.5799E-05 0.9894E-02 0.4866E-05 0.1380E-01 0.1448E-05
 0.1429E-03 0.7838E-06 0.1228E-01 0.1664E-05 0.6441E-02 0.7757E-05 0.6654E-02 0.3710E-05 0.4401E-02 0.1637E-05
 -0.7555E-02 0.6062E-05 0.1609E-02 0.8663E-05 0.7486E-03 0.2434E-05 0.1086E-03 0.5086E-05
 -0.2501E-03 0.4041E-06 0.8690E-03 0.7705E-05 0.8433E-03 0.5649E-05 0.1437E-02 0.4103E-05 0.6403E-03 0.5609E-05
 0.1931E-02 0.1453E-03 0.7237E-05 0.7237E-05 0.5180E-03 0.8066E-05 0.1741E-02 0.1858E-04 0.2436E-02 0.2331E-05
 0.7507E-02 0.1865E-06 0.2165E-02 0.5345E-05 0.1668E-02 0.4681E-05 0.1171E-02 0.4623E-05 0.7780E-04 0.2674E-05
 -0.4822E-03 0.1021E-04 0.2884E-03 0.1207E-04 0.1331E-03 0.1384E-04 0.1850E-04 0.8556E-05
 0.3429E-03 0.1046E-06 0.1170E-02 0.7747E-05 0.9897E-03 0.5423E-05 0.3363E-02 0.2882E-05
 -0.6660E-03 0.1772E-04 0.3035E-02 0.7081E-05 0.7737E-03 0.1032E-04 0.9543E-02 0.2357E-04 0.1327E-01 0.1134E-05
 -0.1340E-01 0.2377E-04 0.1193E-01 0.7277E-05 0.9087E-02 0.1112E-04 0.6412E-02 0.4163E-05 0.4733E-02 0.3118E-05
 0.7667E-02 0.9147E-05 0.1561E-02 0.1362E-04 0.7464E-03 0.1372E-04 0.1066E-03 0.9844E-05
 -0.1557E-06 0.2670E-04 0.7706E-04 0.1778E-05 0.6070E-04 0.5072E-05 0.1481E-03 0.3854E-05 0.2089E-03 0.6265E-05
 0.1719E-03 0.1674E-06 0.2286E-02 0.1253E-04 0.1253E-02 0.1418E-04 0.4856E-02 0.2483E-04 0.0859E-02 0.7534E-05
 0.7726E-02 0.2511E-04 0.6090E-02 0.4080E-05 0.4680E-02 0.1475E-04 0.3922E-02 0.1695E-07 0.2193E-02 0.2929E-06
 -0.1340E-02 0.5792E-05 0.8184E-03 0.1093E-04 0.3622E-03 0.1158E-04 0.6416E-04 0.9855E-05
 -0.2553E-03 0.7425E-04 0.9726E-03 0.7734E-04 0.7572E-03 0.3971E-05 0.2355E-02 0.2815E-05
 0.4026E-02 0.1672E-06 0.3020E-02 0.1272E-04 0.1293E-02 0.1512E-04 0.3081E-02 0.2931E-04 0.4538E-02 0.8279E-05
 0.4589E-02 0.3714E-06 0.4000E-02 0.6767E-05 0.3064E-02 0.2131E-04 0.2155E-02 0.4270E-05 0.1445E-02 0.6040E-05
 0.7729E-03 0.8164E-06 0.4523E-03 0.3464E-05 0.2234E-03 0.1136E-05 0.5096E-04 0.7271E-05
 0.2061E-03 0.1100E-06 0.9698E-03 0.1379E-06 0.8794E-03 0.1136E-05 0.2672E-02 0.1214E-05 0.9578E-04 0.2979E-05
 -0.1270E-02 0.1270E-02 0.6747E-03 0.6747E-03 0.2072E-03 0.6088E-05 0.1272E-03 0.9117E-03 0.1783E-04 0.1888E-04
 -0.1021E-01 0.7731E-04 0.5483E-02 0.6734E-06 0.2072E-03 0.1334E-04 0.7457E-02 0.2776E-04 0.9693E-02 0.9566E-05
 0.1008E-02 0.1401E-06 0.1115E-02 0.1022E-04 0.5764E-03 0.7864E-05 0.6053E-04 0.3153E-07
 -0.1444E-03 0.1290E-06 0.5716E-03 0.1817E-05 0.4975E-03 0.1498E-05 0.1543E-02 0.1733E-05 0.9149E-04 0.7289E-06
 0.7745E-02 0.7138E-04 0.4863E-02 0.7711E-04 0.3306E-02 0.3154E-04 0.7423E-02 0.3386E-04 0.0924E-02 0.1888E-04
 0.1734E-02 0.6581E-06 0.5774E-03 0.1631E-03 0.3026E-03 0.3765E-04 0.2474E-04 0.1929E-04
 0.5232E-06 0.8319E-04 0.1820E-03 0.3472E-05 0.1536E-03 0.7018E-05 0.5030E-03 0.6665E-05 0.1373E-04 0.7288E-05
 -0.7439E-03 0.1245E-06 0.1012E-02 0.6435E-05 0.2144E-03 0.1312E-05 0.6075E-03 0.5226E-05 0.2077E-07 0.1639E-04
 -0.1747E-03 0.0004E-06 0.2184E-02 0.2268E-04 0.3270E-04 0.1176E-02 0.5066E-04 0.1065E-02 0.4301E-04 0.5763E-03 0.5276E-04
 -0.4705E-03 0.6004E-06 0.2784E-02 0.7904E-04 0.9481E-05 0.5667E-04 0.1272E-03 0.3469E-04
 0.4000E-04 0.1781E-06 0.8045E-03 0.3158E-05 0.2618E-03 0.6697E-04 0.7580E-03 0.7944E-05 0.3290E-04 0.1111E-04
 -0.1137E-02 0.2600E-06 0.1605E-03 0.2747E-05 0.4061E-04 0.1435E-04 0.1124E-02 0.2901E-04 0.2747E-02 0.6552E-05
 -0.3331E-03 0.1285E-06 0.4387E-02 0.7490E-04 0.2000E-02 0.1254E-04 0.1720E-02 0.3613E-04 0.8422E-04 0.6240E-04
 -0.2509E-03 0.6024E-06 0.3068E-04 0.7188E-04 0.1015E-03 0.5227E-04 0.7655E-04 0.3520E-04
 -0.4509E-06 0.6637E-04 0.2160E-03 0.2287E-05 0.1807E-03 0.7807E-05 0.5970E-03 0.6516E-05 0.2824E-04 0.1101E-04
 0.4747E-03 0.2712E-06 0.1164E-02 0.1935E-04 0.3769E-02 0.1972E-04 0.9757E-03 0.3530E-04 0.1975E-02 0.6126E-04
 0.3004E-03 0.2777E-06 0.7802E-03 0.1685E-04 0.3773E-04 0.1685E-04 0.1254E-04 0.1422E-02 0.1837E-04 0.2554E-02 0.1449E-04
 0.1555E-03 0.5645E-06 0.4377E-03 0.5495E-04 0.3758E-04 0.3552E-04 0.1722E-04 0.2695E-04
 -0.4739E-04 0.0687E-06 0.1537E-03 0.9616E-04 0.1356E-03 0.5064E-05 0.4054E-03 0.5075E-05 0.2217E-04 0.8998E-05
 -0.4537E-03 0.2345E-06 0.8088E-03 0.1988E-04 0.7085E-03 0.7114E-04 0.6179E-03 0.3568E-04 0.1483E-02 0.1030E-04
 -0.1481E-03 0.2480E-06 0.7316E-02 0.7455E-04 0.7538E-05 0.7538E-05 0.3042E-02 0.1927E-04 0.8775E-03 0.3653E-04
 -0.1445E-04 0.0640E-06 0.8654E-04 0.4714E-05 0.7107E-04 0.1474E-05 0.2481E-03 0.1912E-05 0.7320E-05 0.5135E-05
 -0.1789E-03 0.1187E-06 0.4747E-04 0.1464E-06 0.1408E-03 0.1812E-04 0.3887E-03 0.2770E-04 0.8065E-03 0.1773E-04


```

//          (0034,EE,6,2),'MAUTZ,JOE',MSGLEVEL=1
// EXEC FORTGCLG,PARM.FORT='MAP'
//FORT.SYSIN DD *
SUBROUTINE PLANE(VVR,THR,NT)
COMPLEX VVR(1),A5,A6,U
COMMON U,R(42),ZS(42),SV(42),CV(42),BK,NP,NN,T(80),TR(80)
DIMENSION BJ(126),THR(1),FK(20)
KG=NP-1
NM=KG/2-1
M2=NN+2
A5=2.*3.141593*U**(NN+1)
NV=NM*4
FK(1)=1.
DO 153 J=1,M2
J1=J+1
FK(J1)=FK(J)*J
153 CONTINUE
DO 156 L=1,NT
L1=(L-1)*NV
CS=COS(THR(L))
SN=SIN(THR(L))
BCS=BK*CS
DO 302 J=1,KG
X=R(J)*BK*SN
J1=J
I1=NN
IF(I1) 303,304,303
304 I1=I1+1
J1=J1+KG
303 DO 305 JJ=I1,M2
IF(X-1.E-5) 1,1,2
1 IF(JJ-1) 3,3,4
3 BJ(J1)=1.
GO TO 306
4 BJ(J1)=0.
GO TO 306
2 RH=X/2.
RH2=RH*RH
RH3=RH**(JJ-1)
BJ(J1)=RH3/FK(JJ)
SS=BJ(J1)
8 SST=SS*1.E-7
DO 155 K=1,20
SS=-SS*RH2/K/(K+JJ-1)
BJ(J1)=BJ(J1)+SS
IF(ABS(SS)-SST) 306,306,155
155 CONTINUE
STOP 155
306 J1=J1+KG
305 CONTINUE
302 CONTINUE
IF(NN) 307,308,307
308 DO 309 J=1,KG
J1=J+2*KG
BJ(J)=-BJ(J1)
309 CONTINUE
307 DO 300 J=1,NM
J1=J+1
J2=J1+NM

```

```

J3=J2+NM
J4=J3+NM
VVR(J1)=0.
VVR(J2)=0.
VVR(J3)=0.
VVR(J4)=0.
DO 301 I=1,4
I1=2*(J-1)+I
I4=4*(J-1)+I
I2=I1+K6
I3=I2+K6
A6=(COS(ZS(I1)*BCS)+U*SIN(ZS(I1)*BCS))*A5
BJ1=(BJ(I3)+BJ(I1))*0.5
BJ2=(BJ(I3)-BJ(I1))*0.5
VVR(J1)=VVR(J1)+A6*(CS*SV(I1)*BJ2+SN*CV(I1)*BJ(I2)*U)*T(I4)
VVR(J2)=VVR(J2)+A6*CS*BJ1*U*TR(I4)
VVR(J3)=VVR(J3)-A6*SV(I1)*BJ1*U*TR(I4)
VVR(J4)=VVR(J4)+A6*BJ2*TR(I4)
301 CONTINUE
300 CONTINUE
156 CONTINUE
RETURN
END
SUBROUTINE REORD(K1,K3,L)
DIMENSION K1(1),K3(1)
DO 81 J=1,L
K8=K3(J)
K6=J
DO 82 I=J,L
IF(K3(I)-K8) 82,82,84
84 K8=K3(I)
K6=I
82 CONTINUE
K3(K6)=K3(J)
K3(J)=K8
K8=K1(K6)
K1(K6)=K1(J)
K1(J)=K8
81 CONTINUE
K3(L+1)=-1
RETURN
END
COMPLEX A3,Y(1600),VVR(5840),TI(40),E3(20),E1(73),E2(73),U
COMMON U,R(42),ZS(42),SV(42),CV(42),BK,NP,NN,T(80),TR(80)
DIMENSION RH(43),ZH(43),DH(42),TJ(20),INT(11),THR(73)
DIMENSION AA(105),K1(73),K2(73),K3(73),K4(73)
DATA AA(1),AA(104),AA(105)/' ','X','0'/
DO 107 I=1,102
107 AA(I+1)=AA(I)
U=(0.,1.)
ETA=376.707
ETA2=ETA*2.
PI=3.141593
PR=180./PI
REWIND 6
50 READ(1,51,END=52) NN,NP,NT,BK
51 FORMAT(3I3,E14.7)
READ(1,53)(RH(I),I=1,NP)
READ(1,53)(ZH(I),I=1,NP)
53 FORMAT(10F8.4)

```

```

76 WRITE(3,54) NN,NP,NT,BK
54 FORMAT(1X// ' NN=',I3,' NP=',I3,' NT=',I3,' BK=',E14.7)
WRITE(3,55)
55 FORMAT(1X// ' RH' )
WRITE(3,46)(RH(I),I=1,NP)
46 FORMAT(1X,10F8.4)
WRITE(3,56)
56 FORMAT(1X// ' ZH' )
WRITE(3,46)(ZH(I),I=1,NP)
KL=1
126 IF((RH(1)-RH(NP)).NE.0..OR.(ZH(1)-ZH(NP)).NE.0.) GO TO 58
KL=0
RH(NP+1)=RH(2)
ZH(NP+1)=ZH(2)
RH(NP+2)=RH(3)
ZH(NP+2)=ZH(3)
NP=NP+2
58 DO 57 I=2,NP
I2=I-1
RR1=RH(I)-RH(I2)
RR2=ZH(I)-ZH(I2)
DH(I2)=SQRT(RR1*RR1+RR2*RR2)
ZS(I2)=.5*(ZH(I)+ZH(I2))
R(I2)=.5*(RH(I)+RH(I2))
SV(I2)=RR1/DH(I2)
CV(I2)=RR2/DH(I2)
57 CONTINUE
DT=PI/(NT-1)
DO 1 J=1,NT
THR(J)=DT*(J-1)
1 CONTINUE
NM=(NP-3)/2
NM4=NM*4
NM2=NM*2
NZ=NM2*NM2
DO 74 J=1,NM
J2=2*(J-1)+1
J3=J2+1
J4=J3+1
J5=J4+1
J6=4*(J-1)+1
J7=J6+1
J8=J7+1
J9=J8+1
DEL1=DH(J2)+DH(J3)
DEL2=DH(J4)+DH(J5)
T(J6)=DH(J2)*DH(J3)/2./DEL1
T(J7)=DH(J3)*(DH(J2)+DH(J3)/2.)/DEL1
T(J8)=DH(J4)*(DH(J5)+DH(J4)/2.)/DEL2
T(J9)=DH(J5)*DH(J5)/2./DEL2
74 CONTINUE
DO 75 J=1,NM4
TR(J)=T(J)
75 CONTINUE
115 IF(KL.EQ.0) GO TO 78
IF(RH(1)) 77,23,77
77 DEL1=DH(1)+DH(2)
TR(1)=DH(1)*(1.+(DH(2)+DH(1)/2.)/DEL1)
TR(2)=DH(2)*(1.+(DH(2)/2.)/DEL1)

```

```

23 IF(RH(NP)) 79,78,79
79 J1=(NM-1)*4+3
   J2=J1+1
   DEL2=DH(NP-2)+DH(NP-1)
   TR(J1)=DH(NP-2)*(1.+DH(NP-2)/2./DEL2)
   TR(J2)=DH(NP-1)*(1.+(DH(NP-2)+DH(NP-1)/2.)/DEL2)
78 SS=0.
   DO 7 I=1,NM
   I1=2*(I-1)+1
   I2=I1+1
   SS=SS+DH(I1)+DH(I2)
   TJ(I)=SS
7 CONTINUE
   DEL=TJ(NM)
   IF(KL.NE.0) DEL=DEL+DH(NP-2)+DH(NP-1)
   DEL=DEL/10.
   DO 8 J=1,NM
   TJ(J)=TJ(J)/DEL
8 CONTINUE
85 CALL PLANE(VVR,THR,NT)
127 READ(6)(Y(I),I=1,NZ)
   DO 108 INC=1,2
   J3=0
   IF(INC.EQ.1) J3=NM4*(NT-1)
   DO 2 J=1,NM2
   TI(J)=0.
   DO 3 I=1,NM
   J1=J+(I-1)*NM2
   J2=J1+NM*NM2
   I1=I+J3
   I2=I1+NM
   TI(J)=TI(J)-Y(J1)*VVR(I1)+Y(J2)*VVR(I2)
3 CONTINUE
2 CONTINUE
   DO 9 J=1,NT
   E1(J)=0.
   E2(J)=0.
   J1=(J-1)*NM4
   DO 10 I=1,NM2
   I1=J1+I
   I2=I1+NM2
   E1(J)=E1(J)+VVR(I1)*TI(I)
   E2(J)=E2(J)+VVR(I2)*TI(I)
10 CONTINUE
9 CONTINUE
   J5=(2-INC)*(NT-1)+1
   A3=CABS(E1(J5))/E1(J5)*(BK*BK*ETA/2./PI/SORT(P1))
   DO 11 J=1,NT
   E1(J)=E1(J)*A3
   E2(J)=E2(J)*U*A3
11 CONTINUE
   WRITE(3,110)
110 FORMAT('1',2X,'T',4X,'REAL JT',1X,'IMAG JT',2X,'MAG JT',1X,'REAL J
10',1X,'IMAG JO',2X,'MAG JO')
   WRITE(3,109)
109 FORMAT('1',37X,'/',7X,'/',7X,'/')
   DO 128 J=1,NM
   J1=J+NM
   J2=2*(J-1)+3
   TI(J)=TI(J)*ETA2/RH(J2)

```

```

      E3(J)=TI(J1)*U*ETA2/RH(J2)
128 CONTINUE
      DO 129 J=1,NM
        J1=J+NM
        J3=J-1
        J5=J+1
        IF(J.NE.1.AND.J.NE.NM) GO TO 125
        J3=J
        J5=J
        IF(KL.EQ.1) GO TO 125
        J3=NM
        J5=J+1
        IF(J.EQ.1) GO TO 125
        J3=J-1
        J5=1
125 TI(J1)=.25*(E3(J3)+2.*E3(J)+E3(J5))
129 CONTINUE
      DO 4 J=1,NM
        J1=J+NM
        X2=REAL(TI(J))
        X3=AIMAG(TI(J))
        X4=CABS(TI(J))
        X5=REAL(TI(J1))
        X6=AIMAG(TI(J1))
        X7=CABS(TI(J1))
        WRITE(3,124) TJ(J),X2,X3,X4,X5,X6,X7
124 FORMAT(1X,F5.2,6F8.3)
      4 CONTINUE
      WRITE(3,112)
112 FORMAT('1', '  0',4X,'SIG X0',2X,'SIG X0',2X,'MAG SX0',1X,'ANG SX0',
1,1X,'MAG SX0',1X,'ANG SX0',1X,'LSIG X0',1X,'LSIG X0')
      WRITE(3,113)
113 FORMAT('1',2X,'-1',9X,'-1',7X,'/1',8X,'-1',7X,'-1',7X,'/1',7X,'/1',7X,'-1',
1,7X,'/1')
      DO 12 J=1,NT
        X1=THR(J)*PR
        X4=CABS(E1(J))
        X6=CABS(E2(J))
        X2=X4*X4
        X3=X6*X6
        X5=PR*ATAN2(AIMAG(E1(J)),REAL(E1(J)))
        X7=PR*ATAN2(AIMAG(E2(J)),REAL(E2(J)))
        X8=ALOG10(X2)
        X9=ALOG10(X3)
        WRITE(3,111) X1,X2,X3,X4,X5,X6,X7,X8,X9
111 FORMAT(1X,F5.1,3F8.3,F8.1,F8.3,F8.1,2F8.3)
      12 CONTINUE
      DO 13 J=1,NM
        K1(J)=TJ(J)*10.+3.5
        K2(J)=K1(J)
        K3(J)=CABS(TI(J))*10.+5
        J1=J+NM
        K4(J)=CABS(TI(J1))*10.+5
      13 CONTINUE
      14 CALL REORD(K1,K3,NM)
      15 CALL REORD(K2,K4,NM)
      DO 104 J=1,11
        INT(J)=J-1
104 CONTINUE

```

```

      K=5
      K5=1
      K6=1
      WRITE(3,106)
106  FORMAT('1')
      DO 20 J=1,51
      J1=51-J
      WRITE(3,25)
      25  FORMAT('1',99X,'1')
      IF((J-1)/5*5-(J-1))21,22,21
      22  WRITE(3,123)
123  FORMAT('+',3X,'--',97X,'--')
      IF((J-1)/10*10-(J-1)) 21,122,21
122  WRITE(3,24) K
      24  FORMAT('+',12)
      K=K-1
      IF(J.NE.1) GO TO 21
      WRITE(3,116)
116  FORMAT('+',4X,50('--'))
      WRITE(3,47)
      47  FORMAT('+',8X,19('1',4X))
      21  IF(K3(K5).LT.J1) GO TO 26
      60  K8=K1(K5)
      WRITE(3,48)(AA(I),I=1,K8),AA(104)
      48  FORMAT('+',105A1)
      K5=K5+1
      IF(K3(K5).GE.J1) GO TO 60
      26  IF(K4(K6).LT.J1) GO TO 20
      61  K8=K2(K6)
      WRITE(3,48)(AA(I),I=1,K8),AA(105)
      K6=K6+1
      IF(K4(K6).GE.J1) GO TO 61
      20  CONTINUE
      WRITE(3,47)
      WRITE(3,116)
      WRITE(3,63)(INT(J),J=1,11)
      63  FORMAT(3X,11(12,8X))
      WRITE(3,64)
      64  FORMAT('0',20X,'X X X  PLOT OF MAGNITUDE OF I DIRECTED CURRENT VER
      1SUS LENGTH T')
      WRITE(3,65)
      65  FORMAT(21X,'0 0 0  PLOT OF MAGNITUDE OF 0 DIRECTED CURRENT VERSUS
      1LENGTH T')
      WRITE(3,66)
      66  FORMAT('+',48X,'/')
      DO 80 J=1,NT
      K1(J)=THR(J)*77./PI+.5
      K2(J)=K1(J)
      K3(J)=20.*ALOG10(CABS(F1(J)))+20.5
      K4(J)=20.*ALOG10(CABS(E2(J)))+20.5
      80  CONTINUE
      16  CALL REORD(K1,K3,NT)
      17  CALL REORD(K2,K4,NT)
      DO 105 J=1,5
      INT(J)=(J-1)*45
105  CONTINUE
      X1=1000.
      K5=1
      K6=1
      WRITE(3,106)

```



```

      DO 87 J=1,51
      J1=51-J
      WRITE(3,88)
88  FORMAT(9X,'I',71X,'I')
      IF((J-1)/10*10-(J-1))92,90,92
89  WRITE(3,91) X1
91  FORMAT('+',F7.2,' --',69X,'--')
      X1=X1/10.
      IF(J.NE.1) GO TO 92
      WRITE(3,93)
93  FORMAT('+',17X,7('I',8X))
      WRITE(3,97)
97  FORMAT('+',8X,73('-'))
92  IF(K3(K5).LT.J1) GO TO 94
95  K8=K1(K5)
      WRITE(3,48)(AA(I),I=1,K8),AA(104)
      K5=K5+1
      IF(K3(K5).GE.J1) GO TO 95
94  IF(K4(K6).LT.J1) GO TO 87
96  K8=K2(K6)
      WRITE(3,48)(AA(I),I=1,K8),AA(105)
      K6=K6+1
      IF(K4(K6).GE.J1) GO TO 96
87  CONTINUE
      WRITE(3,93)
      WRITE(3,97)
      WRITE(3,98)(INT(J),J=1,5)
98  FORMAT(7X,3(13,15X),14,15X,13)
      WRITE(3,99)
99  FORMAT('0',15X,'X X X  PLOT OF SIGMA XO OVER LAMBDA SQUARED VERSUS
1 THETA')
      WRITE(3,101)
101  FORMAT('+',37X,'-')
      WRITE(3,100)
100  FORMAT(16X,'0 0 0  PLOT OF SIGMA XO OVER LAMBDA SQUARED VERSUS THE
1TA')
      WRITE(3,102)
102  FORMAT('+',37X,'/')
      WRITE(3,106)
108  CONTINUE
      GO TO 50
52  STOP
      END
/*
//GO,FT06F001 DD DSN=EE0034.REV1,DISP=OLD,UNIT=2314,
//          VOLUME=SER=SU0004,DCB=(RECFM=V,RLKS17F=1H00,LRFL=179A)
//GO,SYSLN DD *
001041037 0.4659945E+00
0.0      0.0868  0.1736  0.2605  0.3473  0.4341  0.5209  0.6078  0.6946  0.7814
0.8682  0.9551  1.0419  1.1287  1.2155  1.3024  1.3892  1.4760  1.5628  1.6497
1.7365  1.8233  1.9101  1.9970  2.0838  2.1706  2.2574  2.3442  2.4311  2.5179
2.6047  2.6915  2.7783  2.8651  2.9519  3.0387  3.1255  3.2123  3.2991  3.3859
-0.0000
0.0      0.4924  0.9848  1.4772  1.9696  2.4620  2.9544  3.4468  3.9392  4.4316
4.9240  5.4164  5.9088  6.4013  6.8937  7.3861  7.8785  8.3709  8.8633  9.3557
9.8481  10.3405  10.8329  11.3253  11.8177  12.3101  12.8025  13.2949  13.7873  14.2797
14.7721  15.2645  15.7569  16.2493  16.7417  17.2341  17.7265  18.2189  18.7113  19.2037
18.2260
/*

```

NOT REPRODUCIBLE

62

NN= 1 NP= 41 NT= 37 PK= 1.4659595E 00

KF

0.0	0.0868	0.1736	0.2605	0.3473	0.4341	0.5209	0.6078	0.6946	0.7814
0.8682	0.9551	1.0419	1.1287	1.2155	1.3024	1.3892	1.4760	1.5628	1.6497
1.7365	1.8233	1.9101	1.9970	2.0838	2.1706	2.2574	2.3442	2.4311	2.5179
2.6047	2.6915	2.7783	2.8651	2.9519	3.0387	3.1255	3.2123	3.2991	3.3859

ZF

0.0	0.4924	0.9848	1.4772	1.9696	2.4620	2.9544	3.4468	3.9392	4.4316
4.9240	5.4164	5.9088	6.4012	6.8936	7.3860	7.8784	8.3708	8.8632	9.3556
9.8480	10.3404	10.8328	11.3252	11.8176	12.3100	12.8024	13.2948	13.7872	14.2796
14.7720	15.2644	15.7568	16.2492	16.7416	17.2340	17.7264	18.2188	18.7112	19.2036

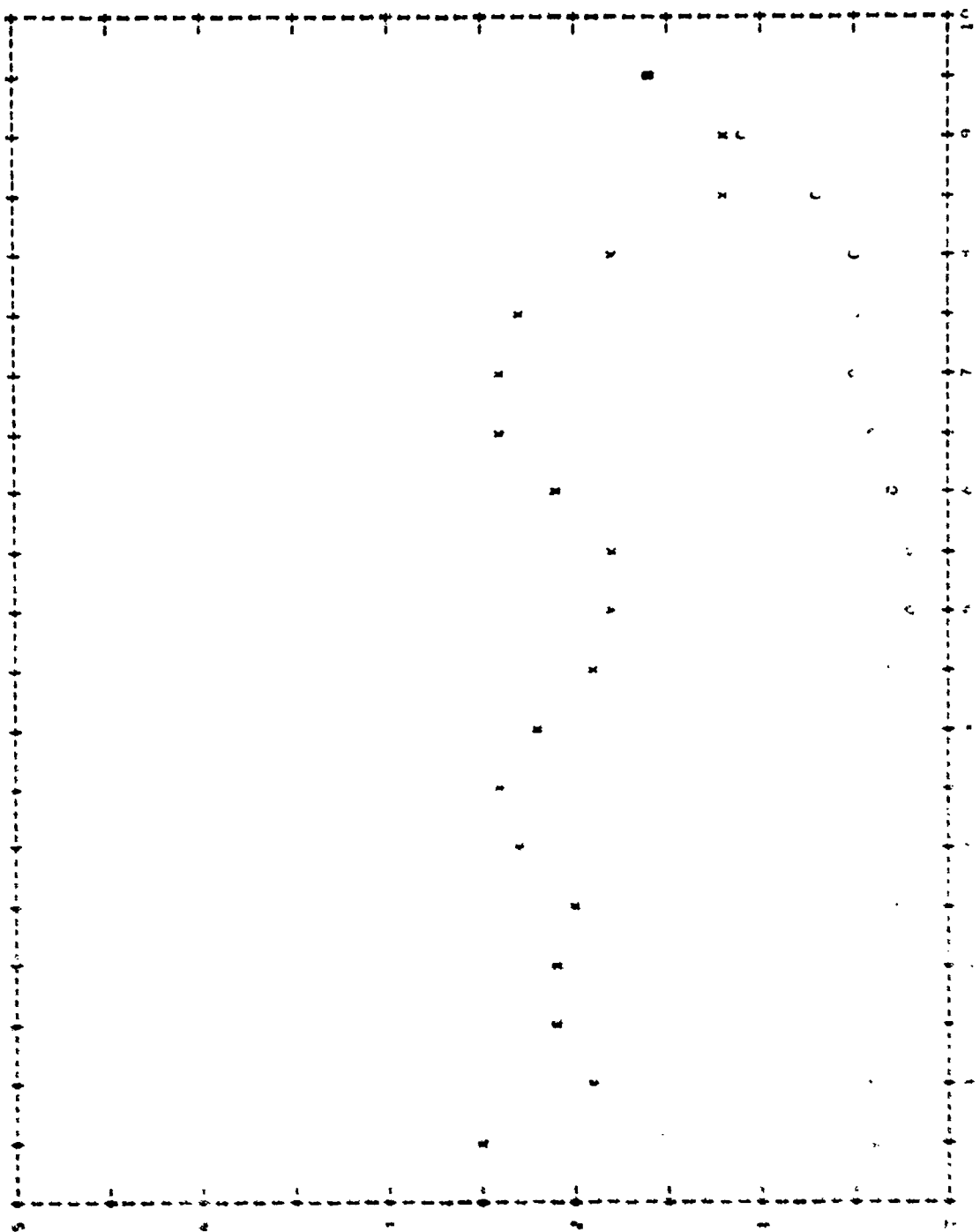
T	REAL JT	IMAG JT	MAG JT	REAL JF	IMAG JF	MAG JF
0.5	2.474	0.212	2.484	-0.437	-0.081	0.445
1.0	1.816	-1.053	1.929	-0.186	0.337	0.385
1.5	0.940	-2.000	2.140	0.010	0.396	0.396
2.0	-0.789	-1.944	2.111	0.110	0.145	0.186
2.5	-1.494	-1.093	1.650	0.250	0.130	0.240
3.0	-2.157	-0.773	2.273	0.406	0.177	0.443
3.5	-2.350	-0.632	2.350	0.384	-0.106	0.398
4.0	-1.983	-0.947	2.197	0.323	-0.173	0.366
4.5	-1.000	-1.000	1.414	0.230	-0.162	0.285
5.0	-0.507	-1.741	1.769	0.150	-0.244	0.249
5.5	0.000	-1.651	1.651	0.100	-0.127	0.163
6.0	0.673	-1.206	2.062	-0.257	-0.044	0.261
6.5	2.291	0.575	2.362	-0.368	0.091	0.377
7.0	2.424	-0.200	2.446	-0.431	0.210	0.479
7.5	2.005	-0.843	2.075	-0.497	0.264	0.539
8.0	1.000	-1.274	1.251	-0.490	0.183	0.520
8.5	0.000	-1.000	1.000	-0.000	0.000	0.000
9.0	-0.540	-0.735	1.103	-1.112	-0.237	1.137
9.50	-1.966	-0.130	1.972	-1.646	-0.234	1.647

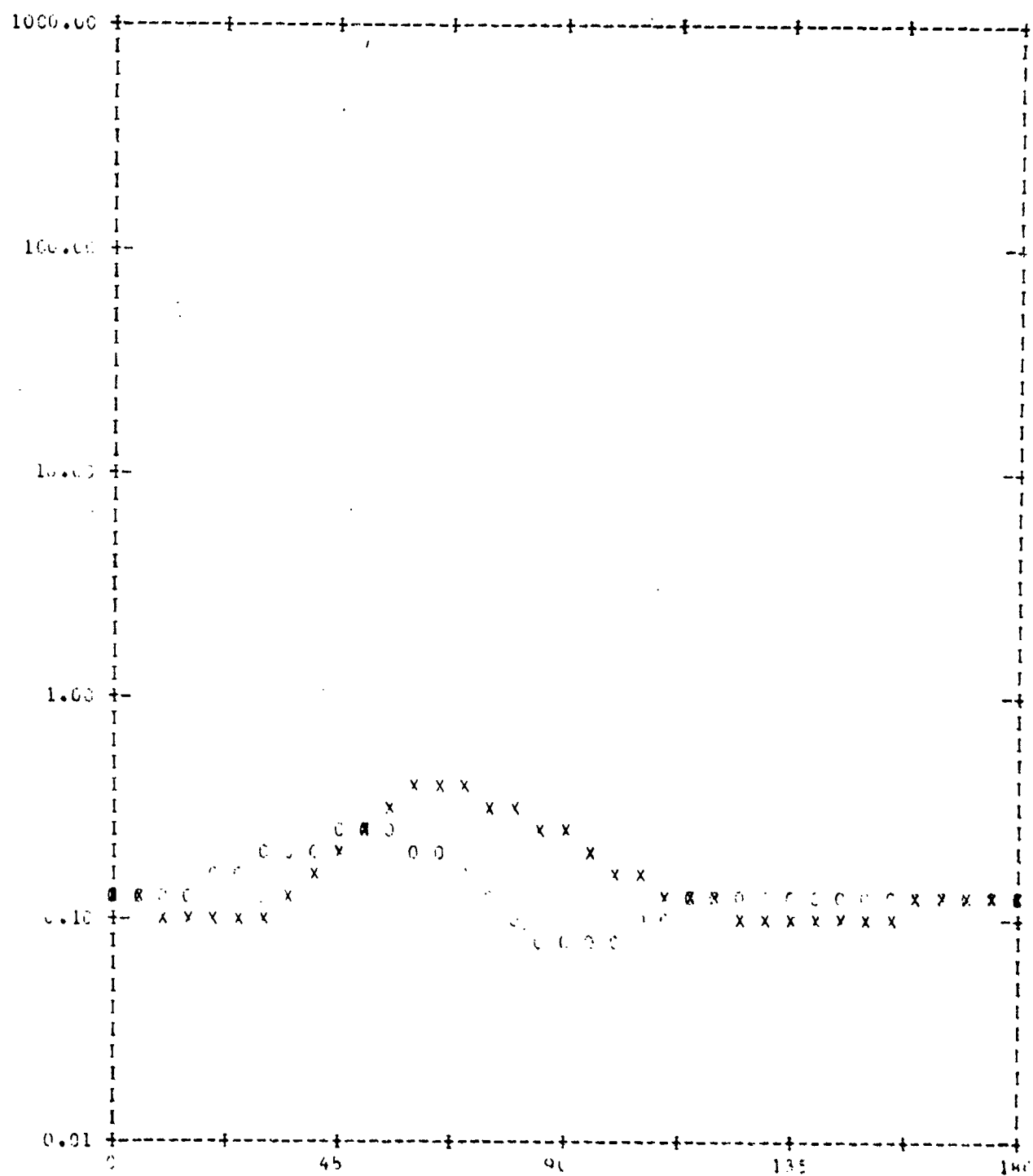
NOT REPRODUCIBLE

63

θ	SIG Xθ	SIG XZ	MAG SXθ	ANG SXθ	MAG SXθ	ANG SXθ	LSIG Xθ	LSIG Xθ
0.0	0.121	0.121	0.348	-89.8	0.348	90.2	-0.917	-0.917
5.0	0.119	0.123	0.345	-92.3	0.351	89.2	-0.926	-0.910
10.0	0.117	0.128	0.335	-105.0	0.358	86.2	-0.950	-0.892
15.0	0.104	0.137	0.322	-114.1	0.370	81.2	-0.985	-0.863
20.0	0.097	0.146	0.311	-131.8	0.386	74.1	-1.014	-0.826
25.0	0.096	0.164	0.310	-155.7	0.405	64.7	-1.018	-0.784
30.0	0.105	0.181	0.324	176.5	0.426	53.1	-0.978	-0.741
35.0	0.128	0.195	0.357	147.2	0.446	39.2	-0.894	-0.701
40.0	0.165	0.215	0.406	117.7	0.464	23.0	-0.784	-0.667
45.0	0.213	0.227	0.462	88.5	0.476	4.6	-0.671	-0.644
50.0	0.268	0.231	0.519	59.4	0.481	-16.2	-0.572	-0.636
55.0	0.320	0.226	0.565	30.0	0.476	-39.2	-0.495	-0.646
60.0	0.359	0.211	0.599	-0.3	0.460	-64.6	-0.445	-0.675
65.0	0.374	0.187	0.615	-31.7	0.433	-92.5	-0.427	-0.727
70.0	0.374	0.158	0.611	-64.4	0.398	-123.2	-0.427	-0.801
75.0	0.34	0.128	0.57	-94.8	0.358	-157.0	-0.454	-0.992
80.0	0.28	0.103	0.536	-114.5	0.320	165.5	-0.517	-0.989
85.0	0.265	0.085	0.515	-112.9	0.291	124.7	-0.576	-1.072
90.0	0.226	0.076	0.475	147.3	0.276	81.3	-0.647	-1.118
95.0	0.194	0.076	0.440	136.1	0.276	37.7	-0.712	-1.117
100.0	0.171	0.084	0.414	86.6	0.286	-4.3	-0.767	-1.081
105.0	0.155	0.093	0.395	24.4	0.305	-41.8	-0.811	-1.031
110.0	0.141	0.104	0.376	-15.4	0.323	-80.6	-0.857	-0.982
115.0	0.128	0.114	0.358	-55.9	0.338	-115.5	-0.892	-0.942
120.0	0.115	0.123	0.340	-53.7	0.350	-146.9	-0.939	-0.911
125.0	0.104	0.125	0.327	-131.1	0.359	180.0	-0.986	-0.889
130.0	0.095	0.135	0.318	-167.3	0.366	150.8	-1.029	-0.874
135.0	0.08	0.147	0.3	157.5	0.370	123.7	-1.047	-0.864
140.0	0.06	0.155	0.28	125.3	0.372	71.9	-1.047	-0.854
145.0	0.053	0.159	0.275	85.8	0.373	76.5	-1.031	-0.855
150.0	0.104	0.142	0.318	75.1	0.374	46.7	-1.001	-0.856
155.0	0.153	0.135	0.364	48.4	0.373	19.7	-0.965	-0.855
160.0	0.197	0.135	0.402	15.3	0.373	25.6	-0.931	-0.857
165.0	0.235	0.138	0.434	17.3	0.372	10.5	-0.903	-0.853
170.0	0.262	0.135	0.453	7.7	0.371	0.0	-0.881	-0.851
175.0	0.281	0.139	0.465	1.8	0.371	0.0	-0.867	-0.862
180.0	0.287	0.137	0.471	0.0	0.371	0.0	-0.862	-0.862

1. 1964-1965
 2. 1966-1967
 3. 1968-1969
 4. 1970-1971
 5. 1972-1973
 6. 1974-1975
 7. 1976-1977
 8. 1978-1979
 9. 1980-1981
 10. 1982-1983
 11. 1984-1985
 12. 1986-1987
 13. 1988-1989
 14. 1990-1991
 15. 1992-1993
 16. 1994-1995
 17. 1996-1997
 18. 1998-1999
 19. 2000-2001
 20. 2002-2003
 21. 2004-2005
 22. 2006-2007
 23. 2008-2009
 24. 2010-2011
 25. 2012-2013
 26. 2014-2015
 27. 2016-2017
 28. 2018-2019
 29. 2020-2021
 30. 2022-2023





X X X PLOT OF SIGMA X² OVER LAMBDA SQUARED VERSUS THETA
 O O O PLOT OF SIGMA X₀² OVER LAMBDA SQUARED VERSUS THETA

NOT REPRODUCIBLE

66

I	REAL JI	IMAG JI	MAG JI	REAL JZ	IMAG JZ	MAG JZ
0.5	2.453	-1.362	2.478	-0.43	0.111	2.444
1.0	1.783	1.367	2.078	-0.255	-0.377	0.455
1.5	0.775	2.211	2.437	-0.190	-0.490	0.500
2.0	-0.229	2.323	2.390	0.310	-0.265	0.265
2.5	-1.069	1.070	1.930	0.145	-0.287	0.321
3.0	-1.740	1.131	2.075	0.287	-0.379	0.475
3.5	-2.055	2.341	2.080	0.321	-0.195	0.334
4.0	-1.892	-1.772	2.043	0.324	-0.008	0.324
4.5	-1.400	-1.802	1.650	0.310	0.213	0.310
5.0	-0.720	-1.701	1.903	0.237	0.171	0.292
5.5	0.202	-1.912	1.800	0.186	0.141	0.234
6.0	1.040	-1.532	1.856	0.140	0.172	0.222
6.5	1.611	-0.600	1.850	0.128	0.178	0.210
7.0	1.780	-0.142	1.750	0.152	0.223	0.254
7.5	1.575	0.779	1.737	0.215	0.344	0.440
8.0	0.977	1.134	1.702	0.235	0.777	0.611
8.5	-0.007	1.047	1.840	-0.250	1.336	1.336
9.0	-0.718	1.915	2.082	-0.645	1.681	1.802
9.5	-1.211	1.601	2.131	-1.352	1.651	2.134

NOT REPRODUCIBLE

I	SIG X-	SIG XZ	MAG SX-	ANG SX-	MAG SXZ	ANG SXZ	LSIG X-	LSIG XZ
0.5	0.172	0.172	0.414	0.0	0.414	-130.7	-0.765	-0.765
5.0	0.171	0.172	0.414	-1.7	0.414	173.5	-0.766	-0.765
1.0	0.170	0.171	0.414	-3.0	0.414	173.1	-0.771	-0.767
1.5	0.169	0.170	0.414	-15.5	0.413	169.5	-0.770	-0.769
2.0	0.168	0.169	0.412	-27.0	0.412	160.0	-0.767	-0.771
2.5	0.158	0.168	0.399	-42.0	0.411	137.4	-0.760	-0.773
3.0	0.155	0.165	0.395	-60.2	0.410	119.1	-0.811	-0.774
3.5	0.150	0.160	0.387	-81.2	0.410	87.7	-0.824	-0.774
4.0	0.140	0.150	0.381	-100.1	0.411	78.0	-0.837	-0.772
4.5	0.141	0.147	0.370	-131.4	0.413	67.0	-0.851	-0.769
5.0	0.130	0.130	0.360	-154.0	0.415	10.1	-0.800	-0.765
5.5	0.131	0.173	0.352	169.0	0.415	-12.8	-0.880	-0.763
6.0	0.124	0.172	0.352	137.3	0.414	-46.7	-0.806	-0.765
6.5	0.115	0.163	0.339	103.0	0.410	-80.5	-0.940	-0.774
7.0	0.110	0.150	0.330	57.0	0.409	-117.0	-0.981	-0.784
7.5	0.090	0.130	0.300	20.0	0.390	-150.0	-1.000	-0.700
8.0	0.070	0.100	0.270	-10.0	0.387	160.0	-1.000	-0.700
8.5	0.070	0.100	0.270	-51.0	0.380	119.0	-1.000	-0.770
9.0	0.070	0.100	0.270	-93.0	0.355	77.0	-1.000	-0.720
9.5	0.060	0.227	0.280	-130.1	0.477	0.0	-1.000	-0.640
10.0	0.050	0.200	0.250	-170.0	0.300	-0.0	-1.000	-0.600
10.5	0.040	0.180	0.220	-165.0	0.277	-0.0	-1.000	-0.577
11.0	0.030	0.160	0.200	-120.0	0.260	-0.0	-1.000	-0.500
11.5	0.020	0.140	0.180	57.4	0.240	-100.0	-1.000	-0.477
12.0	0.010	0.120	0.200	73.0	0.200	-130.0	-1.000	-0.461
12.5	0.000	0.090	0.250	54.0	0.050	-160.0	-1.000	-0.469
13.0	0.000	0.070	0.100	0.0	0.000	171.0	-1.000	-0.000
13.5	0.000	0.050	0.050	38.0	0.000	160.0	-1.000	-0.000
14.0	0.000	0.030	0.030	0.0	0.000	100.0	-1.000	-0.000
14.5	0.000	0.010	0.010	0.0	0.000	0.0	-1.000	-0.000
15.0	0.000	0.000	0.000	0.0	0.000	0.0	-1.000	-0.000
15.5	0.000	0.000	0.000	0.0	0.000	0.0	-1.000	-0.000
16.0	0.000	0.000	0.000	0.0	0.000	0.0	-1.000	-0.000
16.5	0.000	0.000	0.000	0.0	0.000	0.0	-1.000	-0.000
17.0	0.000	0.000	0.000	0.0	0.000	0.0	-1.000	-0.000
17.5	0.000	0.000	0.000	0.0	0.000	0.0	-1.000	-0.000
18.0	0.000	0.000	0.000	0.0	0.000	0.0	-1.000	-0.000

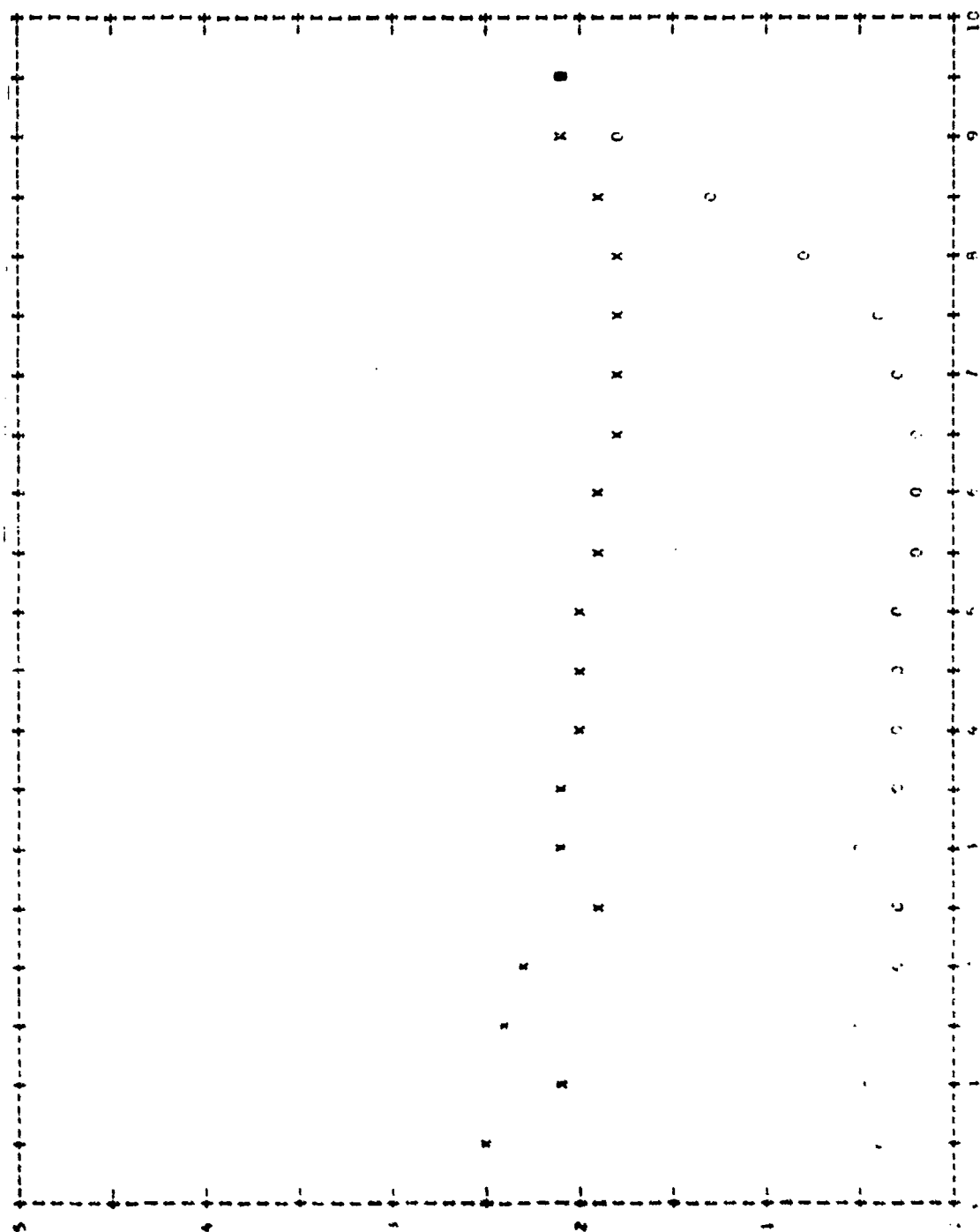
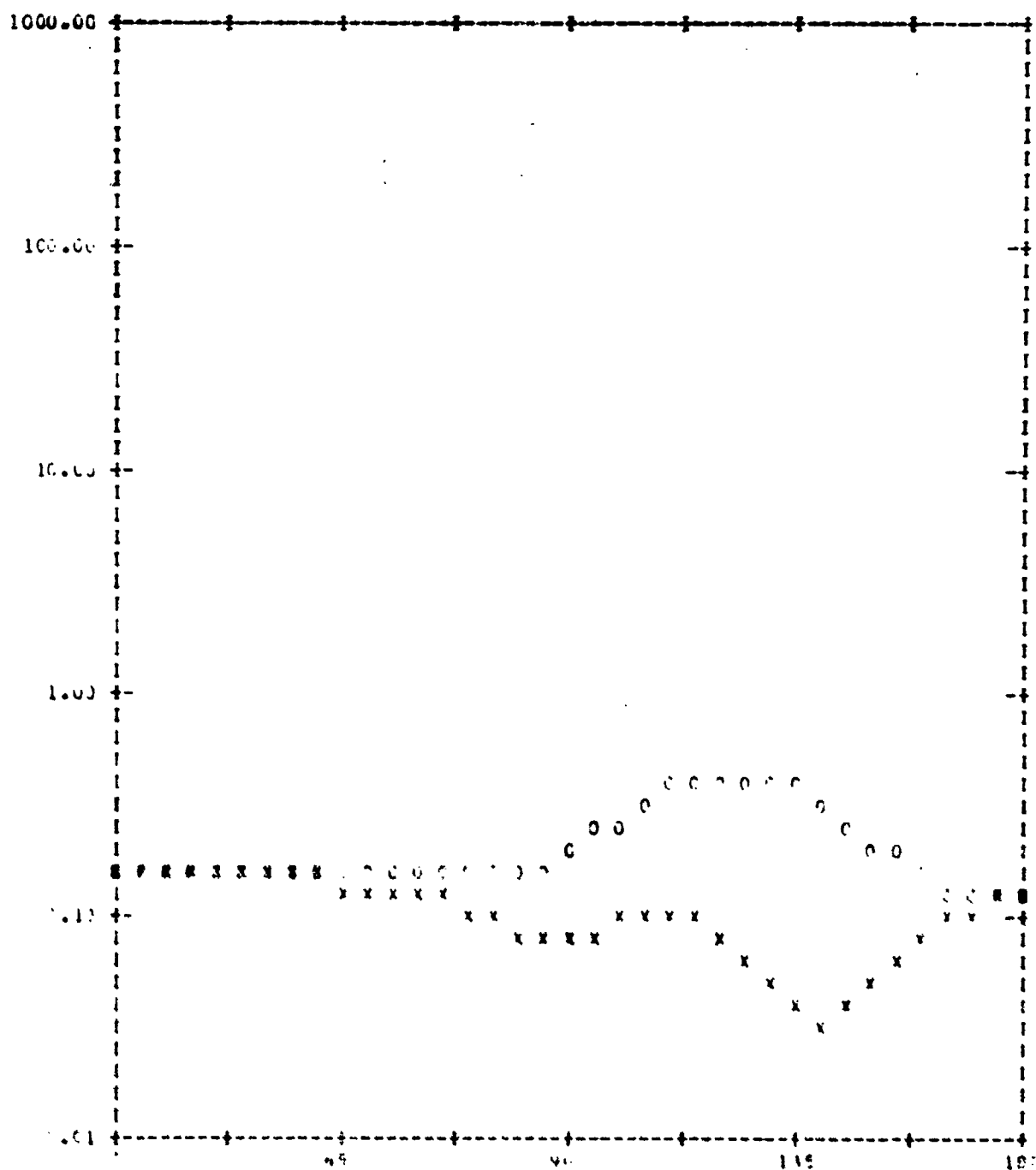


FIG. 1. PLOT OF MAGNITUDE OF Y (DIRECT OR INDIRECT) VERSUS LENGTH Y
 (X = DIRECT MAGNITUDE OF Y, O = INDIRECT MAGNITUDE OF Y)



X X X PLOT OF SIGMA X₂ OVER LAMBDA SQUARED VERSUS THETA
 O O O PLOT OF SIGMA X₁ OVER LAMBDA SQUARED VERSUS THETA


```

//      (0034,EE,6,2),'MAUTZ,JOE',MSGLEVEL=1
// EXEC FORTGCLG,PARM.FORT='MAP'
//FORT.SYSIN DD *
      SUBROUTINE PLANE(VVR,THR,NT)
      COMPLEX VVR(1),A5,A6,U
      COMMON U,R(42),ZS(42),SV(42),CV(42),BK,NP,T(80),TR(80)
      DIMENSION BJ(84),THR(1)
      KG=NP-1
      NM=KG/2-1
      A5=2.*3.141593*U
      NV=NM*2
      DO 156 L=1,NT
      L1=(L-1)*NV
      CS=COS(THR(L))
      SN=SIN(THR(L))
      BCS=BK*CS
      DO 302 J=1,KG
      J1=J
      X=R(J)*BK*SN
      DO 305 JJ=1,2
      IF(X-1.E-5) 1,1,2
1 IF(JJ-1) 3,3,4
3 BJ(J1)=1.
  GO TO 306
4 BJ(J1)=0.
  GO TO 306
2 RH=X/2
  RH2=RH*RH
  RH3=RH*(JJ-1)
  BJ(J1)=RH3
  SS=BJ(J1)
  A SST=SS*1.E-7
  DO 155 K=1,20
  SS=-SS*RH2/K/(K+JJ-1)
  BJ(J1)=BJ(J1)+SS
  IF(ABS(SS)-SST) 306,306,155
155 CONTINUE
  STOP 155
306 J1=J1+KG
305 CONTINUE
302 CONTINUE
  DO 300 J=1,NM
  J1=J+L1
  J2=J1+NM
  VVR(J1)=0.
  VVR(J2)=0.
  DO 301 I=1,4
  I1=2*(J-1)+1
  I4=4*(J-1)+1
  I2=I1+KG
  A6=(COS(ZS(I1)*BCS)+U*SIN(ZS(I1)*BCS))*A5
  VVR(J1)=VVR(J1)+A6*(CS*SV(I1)*BJ(I2)+SN*CV(I1)*BJ(I1)*U)*T(I4)
  VVR(J2)=VVR(J2)+A6*BJ(I2)*TR(I4)
301 CONTINUE
300 CONTINUE
156 CONTINUE
      RETURN
      END
      SUBROUTINE REORD(K1,K3,L)
      DIMENSION K1(1),K3(1)

```

```

      DO 81 J=1,L
      K8=K3(J)
      K6=J
      DO 82 I=J,L
      IF(K3(I)-K8) 82,82,84
84    K8=K3(I)
      K6=I
82    CONTINUE
      K3(K6)=K3(J)
      K3(J)=K8
      K8=K1(K6)
      K1(K6)=K1(J)
      K1(J)=K8
81    CONTINUE
      K3(L+1)=-1
      RETURN
      END
      COMPLEX A3,Y(1600),VVR(2920),TI(40),E3(40),E1(73),E2(73),U
      COMMON U,R(42),ZS(42),SV(42),CV(42),BK,NP,T(80),TR(80)
      DIMENSION RH(43),ZH(43),DH(42),TJ(20),INT(11),THR(73)
      DIMENSION AA(110),K1(73),K2(20),K3(73),K4(20)
      DATA AA(1),AA(109),AA(110)/' ','X','0'/
      DO 107 I=1,107
107    AA(I+1)=AA(I)
      U=(0.,1.)
      ETA=376.707
      PI=3.141593
      PR=180./PI
      RFWIND 6
50    READ(1,51,END=52) KK,NP,NT,BK
51    FORMAT(3I3,E14.7)
      READ(1,53)(RH(I),I=1,NP)
      READ(1,53)(ZH(I),I=1,NP)
53    FORMAT(10F8.4)
      WRITE(3,54) KK,NP,NT,BK
54    FORMAT(1X//' KK=',I3,' NP=',I3,' NT=',I3,' BK=',E14.7)
      WRITE(3,55)
55    FORMAT(1X/' RH')
      WRITE(3,46)(RH(I),I=1,NP)
46    FORMAT(1X,10F8.4)
      WRITE(3,56)
56    FORMAT(1X/' ZH')
      WRITE(3,46)(ZH(I),I=1,NP)
      DO 144 J=1,NP
      E1(J)=0.
      E2(J)=0.
144    CONTINUE
      IF(KK.EQ.2) GO TO 40
      READ(1,168)(E1(I),I=1,NP)
168    FORMAT(7G11.4)
      WRITE(3,131)
131    FORMAT(1X/' E0')
      WRITE(3,132)
132    FORMAT(' + - ')
      WRITE(3,169)(E1(I),I=1,NP)
169    FORMAT(1X,7E11.4)
      IF(KK.EQ.1) GO TO 41
40    READ(1,168)(E2(I),I=1,NP)
      WRITE(3,131)

```

```

WRITE(3,133)
133 FORMAT(' + /')
WRITE(3,169)(E2(I),I=1,NP)
41 KL=1
126 IF((RH(1)-RH(NP)).NE.0..OR.(ZH(1)-ZH(NP)).NE.0.) GO TO 58
KL=0
RH(NP+1)=RH(2)
ZH(NP+1)=ZH(2)
E1(NP+1)=E1(2)
E2(NP+1)=E2(2)
RH(NP+2)=RH(3)
ZH(NP+2)=ZH(3)
E1(NP+2)=E1(3)
E2(NP+2)=E2(3)
NP=NP+2
58 DO 57 I=2,NP
I2=I-1
RR1=RH(I)-RH(I2)
RR2=ZH(I)-ZH(I2)
DH(I2)=SQRT(RR1*RR1+RR2*RR2)
ZS(I2)=.5*(ZH(I)+ZH(I2))
R(I2)=.5*(RH(I)+RH(I2))
SV(I2)=RR1/DH(I2)
CV(I2)=RR2/DH(I2)
57 CONTINUE
DT=PI/(NT-1)
DO 1 J=1,NT
THR(J)=DT*(J-1)
1 CONTINUE
NM=(NP-3)/2
NM4=NM*4
NM2=NM*2
NZ=NM2*NM2
DO 74 J=1,NM
J2=2*(J-1)+1
J3=J2+1
J4=J3+1
J5=J4+1
J6=4*(J-1)+1
J7=J6+1
J8=J7+1
J9=J8+1
DEL1=DH(J2)+DH(J3)
DEL2=DH(J4)+DH(J5)
T(J6)=DH(J2)*DH(J2)/2./DEL1
T(J7)=DH(J3)*(DH(J2)+DH(J3)/2.)/DEL1
T(J8)=DH(J4)*(DH(J5)+DH(J4)/2.)/DEL2
T(J9)=DH(J5)*DH(J5)/2./DEL2
74 CONTINUE
DO 75 J=1,NM4
TR(J)=T(J)
75 CONTINUE
115 IF(KL.EQ.0.) GO TO 78
IF(RH(1))77,23,77
77 DEL1=DH(1)+DH(2)
TR(1)=DH(1)*(1.+(DH(2)+DH(1)/2.)/DEL1)
TR(2)=DH(2)*(1.+(DH(2)/2.)/DEL1)
23 IF(RH(NP))79,78,79
79 J1=(NM-1)*4+3
J2=J1+1

```

```

      DEL2=DH(NP-2)+DH(NP-1)
      TR(J1)=DH(NP-2)*(1.+DH(NP-2)/2./DEL2)
      TR(J2)=DH(NP-1)*(1.+(DH(NP-2)+DH(NP-1))/2.)/DEL2)
78  SS=0.
      DO 7 I=1,NM
        I1=2*(I-1)+1
        I2=I1+1
        SS=SS+DH(I1)+DH(I2)
        TJ(I)=SS
7  CONTINUE
      DEL=TJ(NM)
      IF(KL.NE.0.) DEL=DEL+DH(NP-2)+DH(NP-1)
      DEL=DEL/10.
      DO 8 J=1,NM
        TJ(J)=TJ(J)/DEL
8  CONTINUE
      DO 44 J=1,NM
        J1=J+NM
        J2=2*(J-1)
        J3=4*(J-1)
        E3(J)=0.
        E3(J1)=0.
      DO 45 I=1,4
        I1=J2+I
        I2=I1+1
        I3=J3+I
        E3(J)=E3(J)-(E1(I1)+E1(I2))*T(I3)
        E3(J1)=E3(J1)-(E2(I1)+E2(I2))*TR(I3)
45  CONTINUE
        E3(J)=E3(J)*PI
        E3(J1)=E3(J1)*PI
44  CONTINUE
185  READ(6)((Y(I),I=1,N7)
      P1=0.
      P2=0.
      P3=4.*PI/BK/BK/ETA
      DO 134 J=1,NM
        J1=J+NM
        T1(J)=0.
        T1(J1)=0.
      DO 135 I=1,NM
        I2=(I-1)*NM2+J
        I3=I2+(NM2+1)*NM
        I4=I+NM
        T1(J)=T1(J)+Y(I2)*E3(I)
        T1(J1)=T1(J1)+Y(I3)*E3(I4)
135  CONTINUE
        P1=P1+CONJG(T1(J))*E3(J)
        P2=P2+CONJG(T1(J1))*E3(J1)
134  CONTINUE
      WRITE(3,184) P1,P2
184  FORMAT(//1X,7E11.4)
      P1=SQRT(ABS(P1)*P3)
      P2=SQRT(ABS(P2)*P3)
      IF(P1.NE.0.) P1=1./P1
      IF(P2.NE.0.) P2=1./P2
      CALL PLANE(VVR,THR,NT)
      DO 9 J=1,NT
        E1(J)=0.

```

```

      E2(J)=0.
      J1=(J-1)*NM2
      DO 10 I=1,NM
        I1=J1+I
        I2=I1+NM
        I3=I+NM
        E1(J)=E1(J)+VVR(I1)*TI(I)
        E2(J)=E2(J)+VVR(I2)*TI(I3)
      10 CONTINUE
      190 E1(J)=E1(J)*P1
      191 E2(J)=E2(J)*P2
      9 CONTINUE
      E1(1)=1.E-10
      E2(1)=1.E-10
      E1(NT)=1.E-10
      E2(NT)=1.E-10
      DO 139 J=1,NM
        J2=2*(J-1)+3
        J1=J+NM
        TI(J)=TI(J)/RH(J2)
        TI(J1)=TI(J1)/RH(J2)
      139 CONTINUE
      GO TO(145,146,137),KK
      145 J1=0
      WRITE(3,138)
      138 FORMAT('1',2X,'T',5X,'REAL JT',4X,'IMAG JT')
      GO TO 147
      146 J1=NM
      WRITE(3,148)
      148 FORMAT('1',2X,'T',5X,'REAL JO',4X,'IMAG JO')
      WRITE(3,149)
      149 FORMAT('++',14X,'/',10X,'/')
      147 DO 140 J=1,NM
        J2=J1+J
        WRITE(3,124) TJ(J),TI(J2)
      124 FORMAT(1X,F5.2,4E11.3)
      140 CONTINUE
      GO TO 150
      137 WRITE(3,110)
      110 FORMAT('1',2X,'T',5X,'REAL JT',4X,'IMAG JT',4X,'REAL JO',4X,'IMAG JO')
      WRITE(3,109)
      109 FORMAT('++',36X,'/',10X,'/')
      DO 143 J=1,NM
        J1=J+NM
        WRITE(3,124) TJ(J),TI(J),TI(J1)
      143 CONTINUE
      150 GO TO (151,152,153),KK
      151 WRITE(3,155)
      155 FORMAT('1 0',6X,'GO',4X,'EO',4X,'ANG EO')
      WRITE(3,154)
      154 FORMAT('+-',7X,'-',7X,'-',9X,'-')
      DO 156 J=1,NT
        X3=CAHS(E1(J))
        X1=THR(J)*PR
        X2=X3*X3
        X4=PR*ATAN2(AIMAG(E1(J)),REAL(E1(J)))
        WRITE(3,111) X1,X2,X3,X4
      111 FORMAT(1X,F5.1,2F8.3,F8.1,2F8.3,F8.1)
      156 CONTINUE

```

```

      GO TO 157
152 WRITE(3,155)
      WRITE(3,158)
158 FORMAT('+' /',7X,'/',7X,'/',9X,'/')
      DO 159 J=1,NT
      X3=CABS(E2(J))
      X1=THR(J)*PR
      X2=X3*X3
      X4=PR*ATAN2(AIMAG(E2(J)),REAL(E2(J)))
      WRITE(3,111) X1,X2,X3,X4
159 CONTINUE
      GO TO 157
153 WRITE(3,160)
160 FORMAT('1 0',6X,'GO',6X,'EO',4X,'ANG EO',4X,'GO',6X,'EO',4X,'ANG
      EO')
      WRITE(3,161)
161 FORMAT('+' -',7X,'-',7X,'-',9X,'-',5X,'/',7X,'/',9X,'/')
      DO 167 J=1,NT
      X3=CABS(E1(J))
      X1=THR(J)*PR
      X2=X3*X3
      X4=PR*ATAN2(AIMAG(E1(J)),REAL(E1(J)))
      X6=CABS(E2(J))
      X5=X6*X6
      X7=PR*ATAN2(AIMAG(E2(J)),REAL(E2(J)))
      WRITE(3,111) X1,X2,X3,X4,X5,X6,X7
167 CONTINUE
157 M1=1
      M2=2
      IF(KK.EQ.1) M2=1
      IF(KK.EQ.2) M1=2
      DO 171 M=M1,M2
      M3=(M-1)*NM
      X1=ABS(REAL(TI(M3+1)))
      X2=ABS(AIMAG(TI(M3+1)))
      DO 172 J=1,NM
      J1=J+M3
      X3=ABS(REAL(TI(J1)))
      X4=ABS(AIMAG(TI(J1)))
      IF((X3-X1).GT.0.) X1=X3
      IF((X4-X2).GT.0.) X2=X4
172 CONTINUE
      DO 13 J=1,NM
      J1=J+M3
      K1(J)=TJ(J)*10.+R.5
      K2(J)=K1(J)
      K3(J)=25.*REAL(TI(J1))/X1+25.5
      K4(J)=25.*AIMAG(TI(J1))/X2+25.5
13 CONTINUE
      CALL REORD(K1,K3,NM)
      CALL REORD(K2,K4,NM)
      DO 104 J=1,11
      INT(J)=J-1
104 CONTINUE
      X1=1.
      K5=1
      K6=1
      WRITE(3,106)
106 FORMAT('1')

```

```

      DO 20 J=1,51
      J1=51-J
      WRITE(3,25)
25  FORMAT(9X,'I',99X,'I')
      IF((J-1)/5*5-(J-1)) 21,22,21
22  WRITE(3,123)
23  FORMAT('+',8X,'---',97X,'---')
22  WRITE(3,24) X1
24  FORMAT('+',F7.1)
      X1=X1-.2
      IF(J.NE.1) GO TO 173
      WRITE(3,116)
116 FORMAT('+',9X,50('---'))
      WRITE(3,47)
47  FORMAT('+',13X,19('I',4X))
173 IF(J.NE.26) GO TO 21
      WRITE(3,116)
21  IF(K3(K5).LT.J1) GO TO 26
60  K8=K1(K5)
      WRITE(3,48)(AA(I),I=1,K8),AA(109)
48  FORMAT('+',110A1)
      K5=K5+1
      IF(K3(K5).GE.J1) GO TO 60
26  IF(K4(K6).LT.J1) GO TO 20
61  K8=K2(K6)
      WRITE(3,48)(AA(I),I=1,K8),AA(110)
      K6=K6+1
      IF(K4(K6).GE.J1) GO TO 61
20  CONTINUE
      WRITE(3,47)
      WRITE(3,116)
      WRITE(3,63)(INT(J),J=1,11)
63  FORMAT(8X,11(12,8X)/,1X)
      WRITE(3,174)
174 FORMAT(32X,'X X X PLOT OF (REAL J )/MAX''REAL J '' VERSUS LENG
      TH T')
      IF(M.EQ.1) WRITE(3,175)
175 FORMAT('+',54X,'I',12X,'T')
      IF(M.EQ.2) WRITE(3,176)
176 FORMAT('+',54X,'O',12X,'O','+',54X,'I',12X,'I')
      WRITE(3,180)
180 FORMAT(32X,'O O O PLOT OF (IMAG J )/MAX''IMAG J '' VERSUS LENG
      TH T')
      IF(M.EQ.1) WRITE(3,175)
      IF(M.EQ.2) WRITE(3,176)
163 DO 80 J=1,NT
      K1(J)=THR(J)*72./PI+R.5
      IF(M.EQ.1) K3(J)=20.*ALOG10(CABS(F1(J)))+30.5
      IF(M.EQ.2) K3(J)=20.*ALOG10(CABS(F2(J)))+30.5
80  CONTINUE
      CALL REORD(K1,K3,NT)
      DO 105 J=1,5
      INT(J)=(J-1)*45
105  CONTINUE
      X1=100.
      K5=1
      WRITE(3,106)
      DO 87 J=1,51
      J1=51-J
      WRITE(3,88)

```

```

88  FORMAT(9X,'I',71X,'I')
      IF((J-1)/10*10-(J-1))92,90,92
90  WRITE(3,91)  X1
91  FORMAT('+',F7.3,'--',69X,'--')
      X1=X1/10.
      IF(J.NE.1) GO TO 92
      WRITE(3,93)
93  FORMAT('+',17X,7('I',8X))
      WRITE(3,97)
97  FORMAT('+',8X,73('I'))
92  IF(K3(K5).LT.J1) GO TO 87
95  K4=K1(K5)
      WRITE(3,48)(AA(I),I=1,K4),AA(109)
      K5=K5+1
      IF(K3(K5).GE.J1) GO TO 95
87  CONTINUE
      WRITE(3,93)
      WRITE(3,97)
      WRITE(3,98)(INT(J),J=1,5)
98  FORMAT(7X,3(13,15X),14,15X,13/,1X)
      WRITE(3,177)
177 FORMAT(34X,'PLOT OF GO VERSUS THETA')
      IF(N.EQ.1) WRITE(3,178)
178  FORMAT('+',42X,'-')
      IF(N.EQ.2) WRITE(3,179)
179  FORMAT('+',42X,'/')
171 CONTINUE
170 WRITE(3,106)
      GO TO 50
52  STOP
      END

```

```

//GO.F10AF001 (D) PSNAME=EE0034,XEV1,DISP=RLD,UNIT=2314,
//          VOLTIME=SEK=SD0004,DCH=IECFM=V,ALXSI7E=1800,LECL=179A)

```

Z/01.SYSTM DD C										
DD3041037 1.4650995E+00										
0.0	0.00000	0.173A	0.2605	0.3473	0.4341	0.5209	0.6078	0.6946	0.7814	
0.8682	0.9551	1.0419	1.1287	1.2155	1.3024	1.3892	1.4760	1.5628	1.6497	
1.7365	1.8233	1.9101	1.9970	2.0838	2.1706	2.2574	2.3442	2.4311	2.5179	
2.6047	2.6915	2.7783	2.8651	2.9519	3.0387	3.1255	3.2123	3.2991	3.3859	

0.0	0.6424	0.9448	1.6772	1.9444	2.4420	2.9544	3.4448	3.9402	4.4314
4.4240	5.4164	5.9048	6.4013	6.8477	7.3481	7.8745	8.3709	8.8433	9.3557
9.8481	10.3405	10.8329	11.3253	11.8177	12.3101	12.8025	13.2949	13.7873	14.2797
14.7721	15.2645	15.7569	16.2542	16.7225	17.1474	17.5177	17.8405	18.0427	18.1704

[illegible]

/ 8

KK= 3 NP= 41 NT= 37 BK= 0.4659995E 00

RH

0.0	0.0868	0.1736	0.2605	0.3473	0.4341	0.5209	0.6078	0.6946	0.7814
0.8682	0.9551	1.0419	1.1287	1.2155	1.3024	1.3892	1.4760	1.5628	1.6497
1.7365	1.8233	1.9101	1.9970	2.0838	2.1706	2.2574	2.3442	2.4311	2.5179
2.6047	2.6837	2.6863	2.5969	2.4184	2.1570	1.8216	1.4238	0.9772	0.4971
-0.0									

ZH

0.0	0.4924	0.9848	1.4772	1.9696	2.4620	2.9544	3.4468	3.9392	4.4316
4.9240	5.4164	5.9088	6.4013	6.8937	7.3861	7.8785	8.3709	8.8633	9.3557
9.8481	10.3405	10.8329	11.3253	11.8177	12.3101	12.8025	13.2949	13.7873	14.2797
14.7721	15.2657	15.7650	16.2562	16.7225	17.1478	17.5177	17.8195	18.0427	18.1796
18.2260									

E0

0.0	0.0	0.0	0.0	0.0	0.0	0.0
0.0	0.0	0.0	0.0	0.0	0.0	0.0
0.0	0.0	0.0	0.0	0.0	0.0	0.0
0.0	0.0	0.0	0.0	0.0	0.0	0.0
0.0	0.0	0.0	0.0	0.0	0.0	0.0
0.0	0.0	0.0	0.0	0.0	0.0	0.0
0.0	0.0	0.0	0.0	0.0	0.0	0.0
0.0	0.0	0.0	0.0	0.0	0.0	0.0
0.0	0.0	0.0	0.0	0.0	0.0	0.0
0.0	0.0	0.0	0.0	0.0	0.0	0.0
0.0	-0.3380E 02	0.0	0.0	0.0	0.0	0.0
0.0	0.0	0.0	0.0	0.0	0.0	0.0
0.0	0.0	0.0	0.0	0.0	0.0	0.0

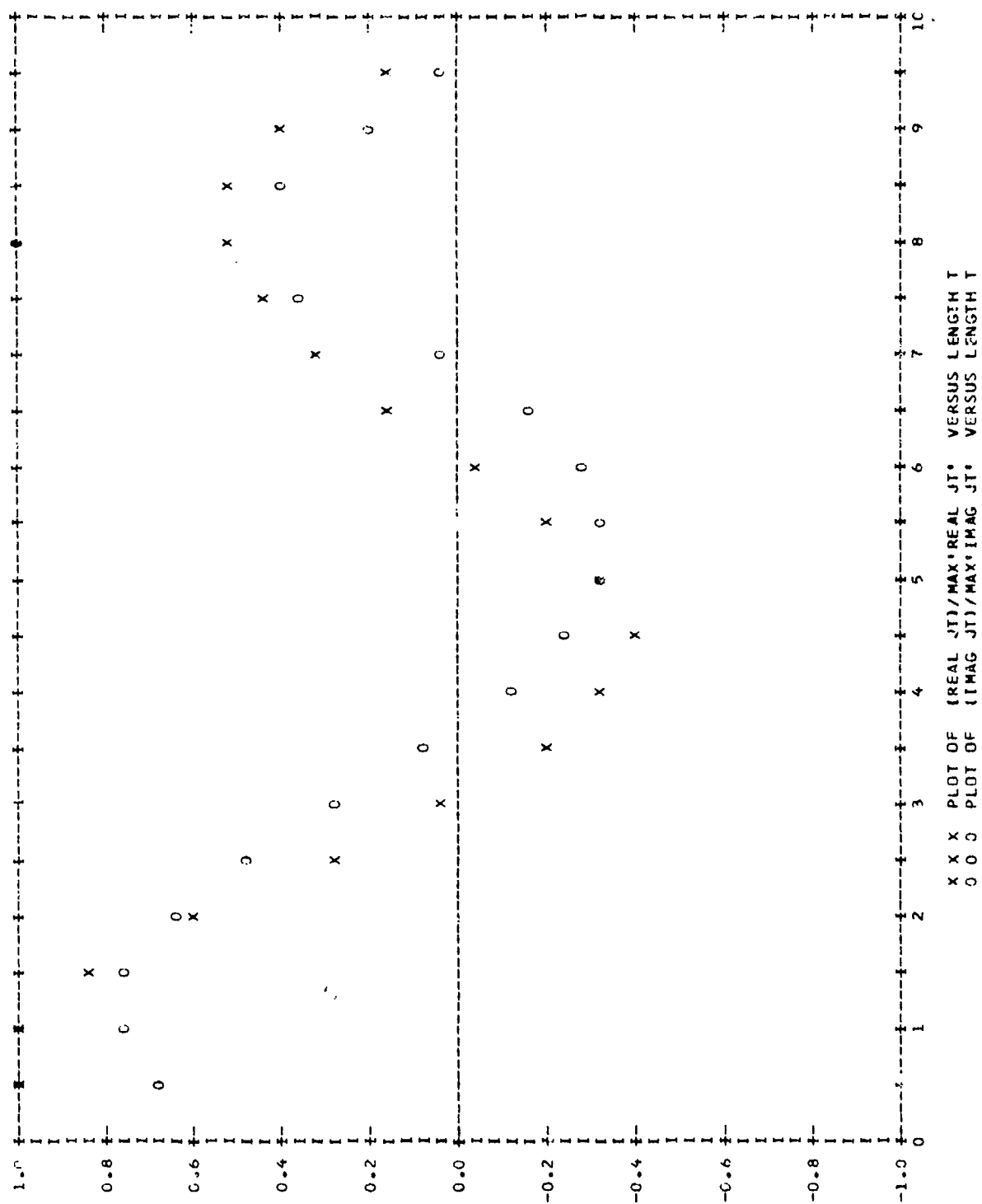
E0

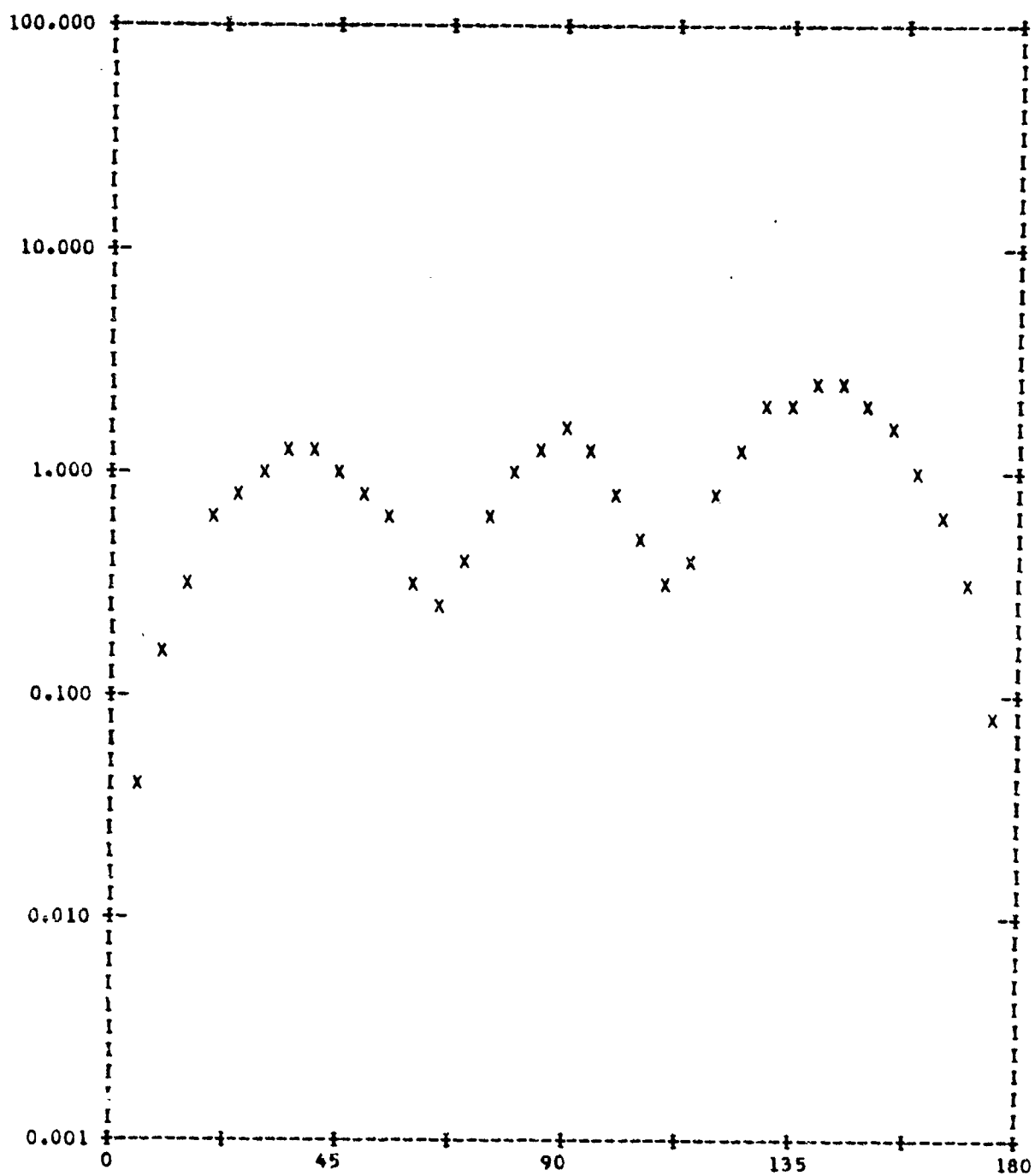
0.0	0.0	0.0	0.0	0.0	0.0	0.0
0.0	0.0	0.0	0.0	0.0	0.0	0.0
0.0	0.0	0.0	0.0	0.0	0.0	0.0
0.0	0.0	0.0	0.0	0.0	0.0	0.0
0.0	0.0	0.0	0.0	0.0	0.0	0.0
0.0	0.0	0.0	0.0	0.0	0.0	0.0
0.0	0.0	0.0	0.0	0.0	0.0	0.0
0.0	0.0	0.0	0.0	0.0	0.0	0.0
0.0	0.0	0.0	0.0	0.0	0.0	0.0
0.0	0.0	0.0	0.0	0.0	0.0	0.0
0.0	0.0	0.0	0.0	0.0	0.0	0.0
0.0	-0.3380E 02	0.0	0.0	0.0	0.0	0.0
0.0	0.0	0.0	0.0	0.0	0.0	0.0
0.0	0.0	0.0	0.0	0.0	0.0	0.0
0.0	0.0	0.0	0.0	0.0	0.0	0.0

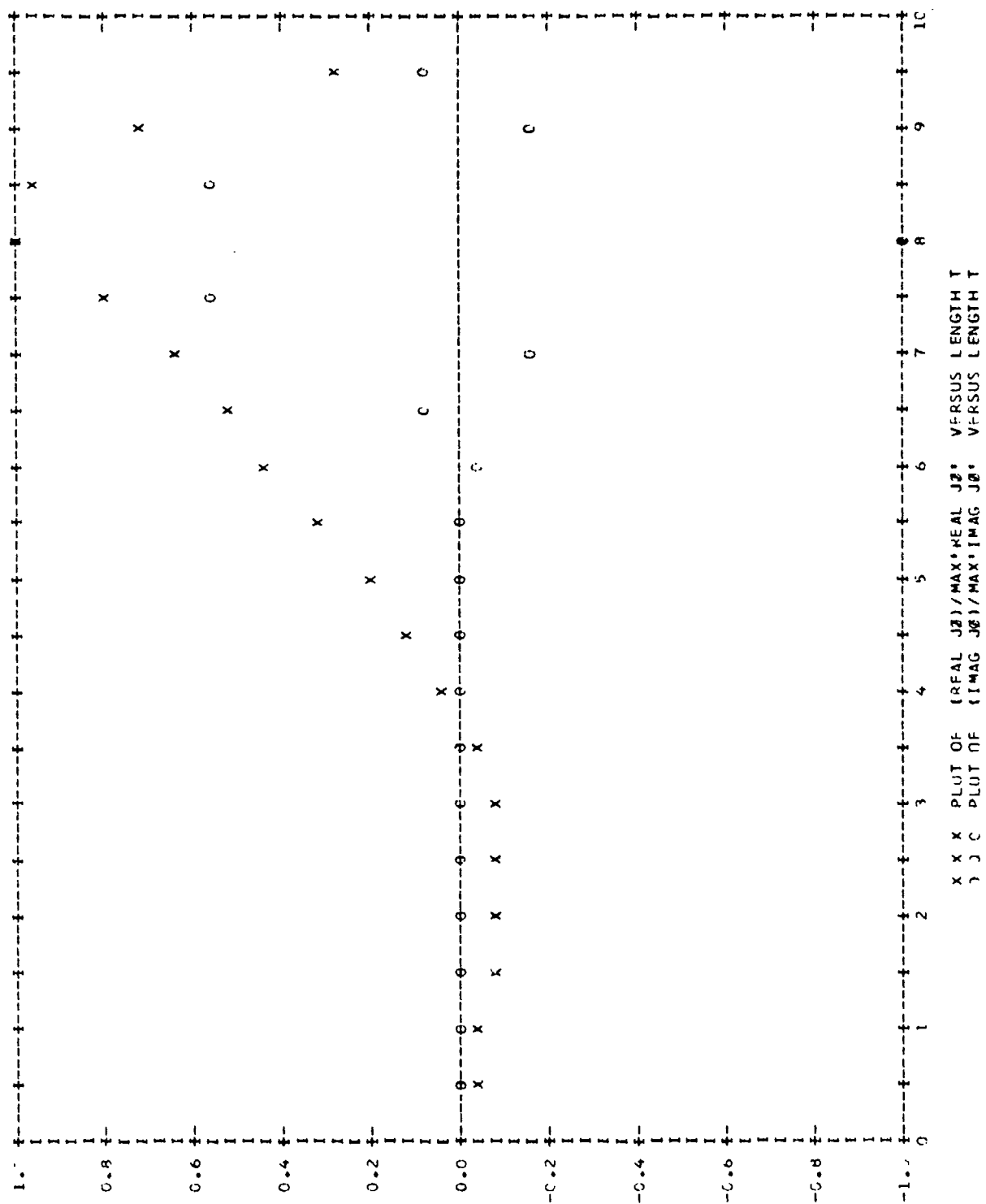
0.3961E 01 0.2006E 01 0.1536E 00

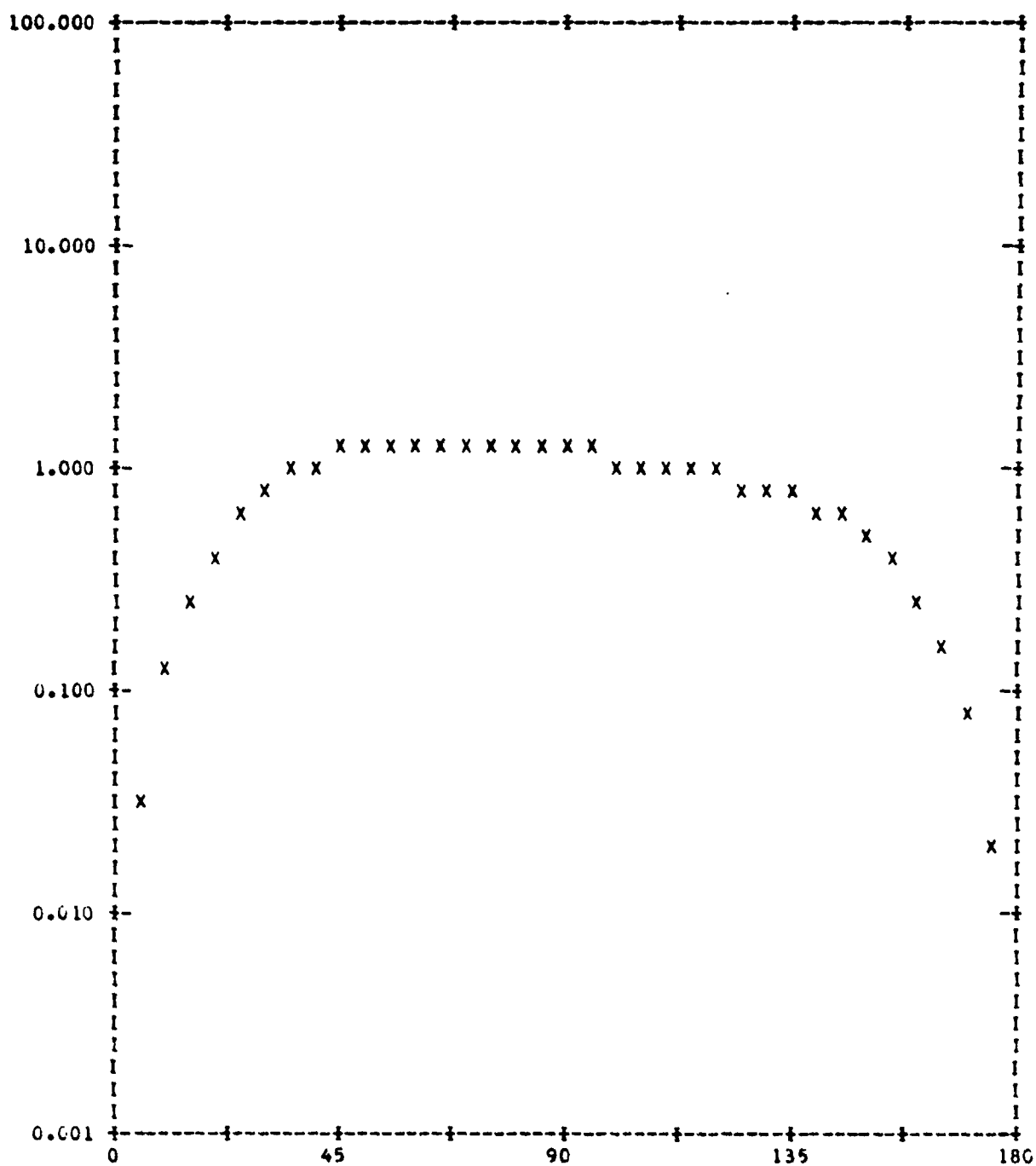
T	REAL JT	IMAG JT	REAL J0	IMAG J0
0.50	0.278E-01	0.269E-01	-0.159E-03	0.442E-03
1.00	0.278E-01	0.303E-01	-0.378E-03	0.362E-03
1.50	0.232E-01	0.291E-01	-0.554E-03	0.213E-03
2.00	0.162E-01	0.249E-01	-0.656E-03	-0.660E-04
2.50	0.828E-02	0.184E-01	-0.657E-03	-0.301E-03
3.00	0.662E-03	0.107E-01	-0.521E-03	0.775E-03
3.50	-0.550E-02	0.279E-02	-0.232E-03	0.720E-03
4.00	-0.941E-02	-0.431E-02	0.215E-03	-0.169E-02
4.50	-0.107E-01	-0.971E-02	0.807E-03	0.772E-04
5.00	-0.928E-02	-0.128E-01	0.152E-02	-0.377E-02
5.50	-0.575E-02	-0.132E-01	0.231E-02	0.631E-02
6.00	-0.845E-03	-0.109E-01	0.311E-02	-0.142E-01
6.50	0.448E-02	-0.608E-02	0.395E-02	0.394E-01
7.00	0.925E-02	0.127E-02	0.468E-02	-0.717E-01
7.50	0.126E-01	0.134E-01	0.579E-02	0.261E 00
8.00	0.144E-01	0.391E-01	0.739E-02	-0.468E 00
8.50	0.141E-01	0.163E-01	0.711E-02	0.268E 00
9.00	0.110E-01	0.718E-02	0.536E-02	-0.769E-01
9.50	0.466E-02	0.226E-02	0.202E-02	0.446E-01

0	G0	E0	ANG E0	G0	E0	ANG E0
0.0	0.000	0.000	0.0	0.000	0.000	0.0
5.0	0.040	0.199	-47.6	0.030	0.173	77.0
10.0	0.155	0.394	-51.4	0.116	0.341	72.3
15.0	0.337	0.580	-57.6	0.249	0.499	64.6
20.0	0.565	0.752	-66.3	0.416	0.645	53.9
25.0	0.811	0.900	-77.3	0.600	0.774	40.3
30.0	1.032	1.016	-90.6	0.785	0.886	23.9
35.0	1.181	1.087	-106.2	0.957	0.978	4.7
40.0	1.213	1.101	-124.2	1.105	1.051	-16.9
45.0	1.106	1.052	-145.0	1.223	1.106	-40.9
50.0	0.878	0.937	-169.3	1.308	1.144	-67.2
55.0	0.592	0.769	160.9	1.361	1.167	-95.4
60.0	0.352	0.594	120.6	1.387	1.178	-125.5
65.0	0.265	0.514	65.1	1.389	1.179	-157.2
70.0	0.389	0.623	9.0	1.374	1.172	169.7
75.0	0.698	0.835	-33.5	1.345	1.160	135.4
80.0	1.076	1.037	-67.7	1.308	1.144	100.1
85.0	1.359	1.166	-98.6	1.266	1.125	64.0
90.0	1.417	1.191	-128.5	1.219	1.104	27.4
95.0	1.217	1.103	-159.0	1.171	1.082	-9.5
100.0	0.850	0.922	167.7	1.122	1.059	-46.5
105.0	0.490	0.700	126.9	1.072	1.035	-83.4
110.0	0.312	0.559	71.1	1.024	1.012	-119.8
115.0	0.417	0.646	11.4	0.977	0.988	-155.5
120.0	0.791	0.889	-31.6	0.930	0.965	169.9
125.0	1.320	1.149	-62.6	0.883	0.940	136.7
130.0	1.848	1.360	-87.7	0.831	0.912	105.3
135.0	2.232	1.494	-109.1	0.770	0.878	76.0
140.0	2.387	1.545	-127.9	0.697	0.835	49.3
145.0	2.296	1.515	-144.4	0.608	0.780	25.2
150.0	2.000	1.414	-158.8	0.505	0.711	4.0
155.0	1.575	1.255	-171.1	0.391	0.626	-14.1
160.0	1.104	1.050	178.7	0.275	0.524	-29.1
165.0	0.661	0.813	170.7	0.167	0.408	-40.8
170.0	0.306	0.553	165.0	0.078	0.280	-49.3
175.0	0.078	0.280	161.5	0.020	0.142	-54.3
180.0	0.000	0.000	0.0	0.000	0.000	0.0



PLOT OF $G\theta$ VERSUS θ



PLOT OF $G\theta$ VERSUS θ

```

//          (0034,EE,R,2),'MAUTZ,JOE',MSGLEVEL=1
// EXEC FORTGCLG,PARM.FORT='MAP'
//FORT.SYSIN DD *
SUBROUTINE PLANE(VVR,THR,NT)
COMPLEX VVR(1),A5,A6,U
COMMON U,R(42),ZS(42),SV(42),CV(42),BK,NP,NN,T(80),TR(80)
DIMENSION BJ(126),THR(1),FK(20)
KG=NP-1
NM=KG/2-1
M2=NN+2
A5=2.*3.141593*U**(NN+1)
NV=NM*4
FK(1)=1.
DO 153 J=1,M2
J1=J+1
FK(J1)=FK(J)*J
153 CONTINUE
DO 156 L=1,NT
L1=(L-1)*NV
CS=COS(THR(L))
SN=SIN(THR(L))
RCS=BK*CS
DO 302 J=1,KG
X=R(J)*BK*SN
J1=J
I1=NN
IF(I1) 303,304,303
304 I1=I1+1
J1=J1+KG
303 DO 305 JJ=I1,M2
IF(X-1.E-5) 1,1,2
1 IF(JJ-1) 3,3,4
3 BJ(J1)=1.
GO TO 306
4 BJ(J1)=0.
GO TO 306
2 RH=X/2.
RH2=RH*RH
RH3=RH**(JJ-1)
BJ(J1)=RH3/FK(JJ)
SS=BJ(J1)
8 SST=SS*1.E-7
DO 155 K=1,20
SS=-SS*RH2/K/(K+JJ-1)
BJ(J1)=BJ(J1)+SS
IF(ABS(SS)-SST) 306,306,155
155 CONTINUE
STOP 155
306 J1=J1+KG
305 CONTINUE
302 CONTINUE
IF(NN) 307,308,307
308 DO 309 J=1,KG
J1=J+2*KG
BJ(J)=-BJ(J1)
309 CONTINUE
307 DO 300 J=1,NM
J1=J+L1
J2=J1+NM
J3=J2+NM

```

```

J4=J3+NM
VVR(J1)=0.
VVR(J2)=0.
VVR(J3)=0.
VVR(J4)=0.
DO 301 I=1,4
  I1=2*(J-1)+I
  I4=4*(J-1)+I
  I2=I1+KG
  I3=I2+KG
  A6=(COS(ZS(I1)*BCS)+U*SIN(ZS(I1)*BCS))*A5
  BJ1=(BJ(I3)+BJ(I1))*0.5
  BJ2=(BJ(I3)-BJ(I1))*0.5
  VVR(J1)=VVR(J1)+A6*(CS*SV(I1)*BJ2+SN*CV(I1)*BJ(I2)*U)*T(I4)
  VVR(J2)=VVR(J2)+A6*CS*BJ1*U*TR(I4)
  VVR(J3)=VVR(J3)-A6*SV(I1)*BJ1*U*T(I4)
  VVR(J4)=VVR(J4)+A6*BJ2*TR(I4)
301 CONTINUE
300 CONTINUE
156 CONTINUE
  RETURN
  END
  SUBROUTINE REORD(K1,K3,L)
  DIMENSION K1(1),K3(1)
  DO 81 J=1,L
    K8=K3(J)
    K6=J
    DO 82 I=J,L
      IF(K3(I)-K8) 82,82,84
    84 K8=K3(I)
    K6=I
  82 CONTINUE
    K3(K6)=K3(J)
    K3(J)=K8
    K8=K1(K6)
    K1(K6)=K1(J)
    K1(J)=K8
  81 CONTINUE
    K3(L+1)=-1
    RETURN
  END
  COMPLEX A3,Y(1600),VVR(5840),E3(40),E4(40),E1(73),E2(73),U
  COMMON U,R(42),ZS(42),SV(42),CV(42),BK,NP,NN,T(80),TR(80)
  DIMENSION RH(43),ZH(43),DH(42),TJ(20),INT(5),THR(73)
  DIMENSION AA(110),K1(73),K2(73),K3(73),K4(73)
  DATA AA(1),AA(109),AA(110)/' ','X','O'/
  DO 107 I=1,107
107 AA(I+1)=AA(I)
  U=(0.,1.)
  ETA=376.707
  PI=3.141593
  PR=180./PI
  REWIND 6
  50 READ(1,51,END=52) KK,NP,NT,BK
  51 FORMAT(3I3,E14.7)
  READ(1,53)(RH(I),I=1,NP)
  READ(1,53)(ZH(I),I=1,NP)
  53 FORMAT(10F8.4)
  76 WRITE(3,54) KK,NP,NT,BK

```



```

54 FORMAT(1X// ' KK=',I3,' NP=',I3,' NT=',I3,' RK=',E14.7)
   WRITE(3,55)
55 FORMAT(1X/ ' RH' )
   WRITE(3,46)(RH(I),I=1,NP)
46 FORMAT(1X,10F8.4)
   WRITE(3,56)
56 FORMAT(1X/ ' ZH' )
   WRITE(3,46)(ZH(I),I=1,NP)
   KL=1
126 IF((RH(1)-RH(NP)).NE.0..OR.(ZH(1)-ZH(NP)).NE.0.) GO TO 58
   KL=0
   RH(NP+1)=RH(2)
   ZH(NP+1)=ZH(2)
   RH(NP+2)=RH(3)
   ZH(NP+2)=ZH(3)
   NP=NP+2
58 DO 57 I=2,NP
   I2=I-1
   RR1=RH(I)-RH(I2)
   RR2=ZH(I)-ZH(I2)
   DH(I2)=SQRT(RR1*RR1+RR2*RR2)
   ZS(I2)=.5*(ZH(I)+ZH(I2))
   R(I2)=.5*(RH(I)+RH(I2))
   SV(I2)=RR1/DH(I2)
   CV(I2)=RR2/DH(I2)
57 CONTINUE
   DT=PI/(NT-1)
   DO 1 J=1,NT
   THR(J)=DT*(J-1)
1 CONTINUE
   BK2=BK*BK
   P1=SQRT(BK2+BK2*ETA*ETA/4./PI**3)
   NM=(NP-3)/2
   NM4=NM*4
   NM2=NM*2
   NZ=NM2*NM2
   DO 74 J=1,NM
   J2=2*(J-1)+1
   J3=J2+1
   J4=J3+1
   J5=J4+1
   J6=4*(J-1)+1
   J7=J6+1
   J8=J7+1
   J9=J8+1
   DEL1=DH(J2)+DH(J3)
   DEL2=DH(J4)+DH(J5)
   T(J6)=DH(J2)*DH(J2)/2./DEL1
   T(J7)=DH(J3)*(DH(J2)+DH(J3)/2.)/DEL1
   T(J8)=DH(J4)*(DH(J5)+DH(J4)/2.)/DEL2
   T(J9)=DH(J5)*DH(J5)/2./DEL2
74 CONTINUE
   DO 75 J=1,NM4
   TR(J)=T(J)
75 CONTINUE
115 IF(KL.EQ.0) GO TO 78
   IF(RH(1)) 77,23,77
77 DEL1=DH(1)+DH(2)
   TR(1)=DH(1)*(1.+(DH(2)+DH(1)/2.)/DEL1)
   TR(2)=DH(2)*(1.+(DH(2)+DH(1)/2.)/DEL1)

```

```

23 IF(RH(NP)) 79,78,79
79 J1=(NM-1)*4+3
   J2=J1+1
   DEL2=DH(NP-2)+DH(NP-1)
   TR(J1)=DH(NP-2)*(1.+DH(NP-2)/2./DEL2)
   TR(J2)=DH(NP-1)*(1.+(DH(NP-2)+DH(NP-1)/2.)/DEL2)
78 SS=0.
   DO 7 I=1,NM
     I1=2*(I-1)+1
     I2=I1+1
     SS=SS+DH(I1)+DH(I2)
     TJ(I)=SS
7  CONTINUE
   DEL=TJ(NM)
   IF(KL,NE,0) DEL=DEL+DH(NP-2)+DH(NP-1)
   DEL=DEL/10.
   DO 8 J=1,NM
     TJ(J)=TJ(J)/DEL
8  CONTINUE
   DO 42 J=1,NT
     E1(J)=0.
     E2(J)=0.
42  CONTINUE
   DO 40 M=1,KK
     NN=M-1
     CALL PLANE(VVR,THR,NT)
127 READ(6)(Y(I),I=1,NZ)
     WRITE(3,112)
112 FORMAT(/3X,'0',4X,'SIG 00',2X,'MAG 500',1X,'SIG 00',2X,'MAG 500')
     WRITE(3,113)
113 FORMAT('+-',8X,'--',7X,'--',5X,'//',7X,'//')
   DO 41 L=1,NT
     L1=(L-1)*NM4
     DO 2 J=1,NM2
       E3(J)=0.
       E4(J)=0.
       DO 3 I=1,NM
         J1=J+(I-1)*NM2
         J2=J1+NM*NM2
         I1=I+L1
         I2=I1+NM
         I3=I1+NM2
         I4=I3+NM
         E3(J)=E3(J)+Y(J1)*VVR(I1)-Y(J2)*VVR(I2)
         E4(J)=E4(J)-Y(J1)*VVR(I3)+Y(J2)*VVR(I4)
3  CONTINUE
2  CONTINUE
   DO 43 J=1,NM2
     J1=J+L1
     J2=J1+NM2
     E1(L)=E1(L)+E3(J)*VVR(J1)
     E2(L)=E2(L)+E4(J)*VVR(J2)
43  CONTINUE
   IF(NN) 44,45,44
45  E1(L)=.5*E1(L)
     E2(L)=.5*E2(L)
44  X1=THR(L)*P4
     X3=P1*CAHS(E1(L))
     X2=X3*X3

```

```

      X5=P1*CAHS(E2(L))
      X4=X5*X5
      WRITE(3,111) X1,X2,X3,X4,X5
111  FORMAT(1X,F5.1,4F8.3)
      41 CONTINUE
      40 CONTINUE
      WRITE(3,106)
      WRITE(3,112)
      WRITE(3,113)
      DO 80 J=1,NT
      K1(J)=THR(J)*72./PI+8.5
      K2(J)=K1(J)
      K3(J)=20.*ALOG10(P1*CAHS(E1(J)))+20.5
      K4(J)=20.*ALOG10(P1*CAHS(E2(J)))+20.5
      X1=THR(J)*PR
      X3=P1*CAHS(E1(J))
      X2=X3*X3
      X5=P1*CAHS(E2(J))
      X4=X5*X5
      WRITE(3,111) X1,X2,X3,X4,X5
      80 CONTINUE
      14 CALL REORD(K1,K3,NT)
      15 CALL REORD(K2,K4,NT)
      DO 105 J=1,5
      INT(J)=(J-1)*45
105  CONTINUE
      X1=1000.
      K5=1
      K6=1
      WRITE(3,106)
106  FORMAT('1')
      DO 87 J=1,51
      J1=51-J
      WRITE(3,88)
      88  FORMAT(9X,'1',71X,'1')
      IF((J-1)/10*10-(J-1))92,90,92
      90  WRITE(3,91) X1
      91  FORMAT('1',F7.2,'---',69X,'---')
      X1=X1/10.
      IF(J.NE.1) GO TO 92
      WRITE(3,93)
      93  FORMAT('1',17X,7('1',8X))
      WRITE(3,97)
      97  FORMAT('1',8X,73('1'))
      92  IF(K3(K5).LT.J1) GO TO 94
      95  KR=K1(K5)
      WRITE(3,48)(AA(I),I=1,KR),AA(109)
      48  FORMAT('1',110A1)
      K5=K5+1
      IF(K3(K5).GE.J1) GO TO 95
      94  IF(K4(K6).LT.J1) GO TO 87
      96  KR=K2(K6)
      WRITE(3,48)(AA(I),I=1,KR),AA(110)
      K6=K6+1
      IF(K4(K6).GE.J1) GO TO 96
      97 CONTINUE
      WRITE(3,93)
      WRITE(3,97)
      WRITE(3,98)(INT(J),J=1,5)
      98  FORMAT(7X,3(13,15X),14,15X,13/,1X)

```

88

```

WRITE(3,99)
99 FORMAT(16X,'X X X PLOT OF SIGMA 00 OVER LAMBDA SQUARED VERSUS THE
1TA')
WRITE(3,101)
101 FORMAT('+',36X,'--')
WRITE(3,100)
100 FORMAT(16X,'O O O PLOT OF SIGMA 00 OVER LAMBDA SQUARED VERSUS THE
1TA')
WRITE(3,102)
102 FORMAT('+',36X,'//')
WRITE(3,106)
GO TO 50
52 STOP
END

```

```

/*
//GO.FTO6F001 DD DSNAME=EE0034.REV1,DISP=OLD,UNIT=2314, X
// VOLUME=SER=SU0004,DCH=(RECFM=V,BLKSIZE=1800,LRECL=1796)
//GO.SYSIN DD *
005041037 0.4659995E+00
0.0 0.0868 0.1736 0.2605 0.3473 0.4341 0.5209 0.6078 0.6946 0.7814
0.8682 0.9551 1.0419 1.1287 1.2155 1.3024 1.3892 1.4760 1.5628 1.6497
1.7365 1.8233 1.9101 1.9970 2.0838 2.1706 2.2574 2.3442 2.4311 2.5179
2.6047 2.6837 2.6863 2.5969 2.4184 2.1570 1.8216 1.4238 0.9772 0.4971
-0.0000
0.0 0.4924 0.9848 1.4772 1.9696 2.4620 2.9544 3.4468 3.9392 4.4316
4.9240 5.4164 5.9088 6.4013 6.8937 7.3861 7.8785 8.3709 8.8633 9.3557
9.8481 10.3405 10.8329 11.3253 11.8177 12.3101 12.8025 13.2949 13.7873 14.2797
14.7721 15.2657 15.7650 16.2562 16.7225 17.1478 17.5177 17.8195 18.0427 18.1798
18.2260
/*

```

KK= 5 NP= 41 NT= 37 RK= 0.4659995E 00

RH

0.0	0.0868	0.1736	0.2605	0.3473	0.4341	0.5209	0.6078	0.6946	0.7814
0.8642	0.9551	1.0419	1.1287	1.2155	1.3024	1.3892	1.4760	1.5628	1.6497
1.7365	1.8233	1.9101	1.9970	2.0838	2.1706	2.2574	2.3442	2.4311	2.5179
2.6047	2.6915	2.7783	2.8651	2.9519	3.0387	3.1255	3.2123	3.2991	3.3859
-0.0									

ZH

0.0	0.4924	0.9848	1.4772	1.9696	2.4620	2.9544	3.4468	3.9392	4.4316
4.9240	5.4164	5.9088	6.4013	6.8937	7.3861	7.8785	8.3709	8.8633	9.3557
9.8481	10.3405	10.8329	11.3253	11.8177	12.3101	12.8025	13.2949	13.7873	14.2797
14.7721	15.2645	15.7569	16.2493	16.7417	17.2341	17.7265	18.2189	18.7113	19.2037
18.2260									

0	SIG 00	MAG S00	SIG 00	MAG S00
0.0	0.0	0.0	0.0	0.0
5.0	0.001	0.025	0.000	0.001
10.0	0.010	0.102	0.000	0.004
15.0	0.051	0.225	0.000	0.010
20.0	0.152	0.389	0.000	0.017
25.0	0.337	0.581	0.001	0.027
30.0	0.603	0.776	0.001	0.038
35.0	0.890	0.944	0.003	0.052
40.0	1.094	1.046	0.005	0.068
45.0	1.107	1.052	0.007	0.084
50.0	0.911	0.954	0.011	0.105
55.0	0.610	0.781	0.015	0.124
60.0	0.352	0.543	0.021	0.144
65.0	0.182	0.427	0.030	0.174
70.0	0.053	0.230	0.052	0.228
75.0	0.006	0.080	0.095	0.308
80.0	0.253	0.503	0.158	0.397
85.0	0.891	0.944	0.221	0.470
90.0	1.605	1.767	0.254	0.504
95.0	1.871	1.369	0.238	0.488
100.0	1.499	1.224	0.181	0.426
105.0	0.813	0.902	0.112	0.335
110.0	0.266	0.516	0.056	0.237
115.0	0.033	0.181	0.023	0.153
120.0	0.010	0.101	0.009	0.094
125.0	0.043	0.208	0.004	0.062
130.0	0.062	0.250	0.002	0.047
135.0	0.065	0.254	0.001	0.037
140.0	0.059	0.243	0.001	0.028
145.0	0.049	0.222	0.000	0.020
150.0	0.036	0.188	0.000	0.014
155.0	0.021	0.146	0.000	0.010
160.0	0.010	0.101	0.000	0.006
165.0	0.004	0.060	0.000	0.003
170.0	0.001	0.027	0.000	0.001
175.0	0.000	0.007	0.000	0.000
180.0	0.000	0.000	0.0	0.0

0	SIG 00	MAG S00	SIG 00	MAG S00
0.0	0.172	0.414	0.172	0.414
5.0	0.192	0.434	0.172	0.415

10.0	0.259	0.509	0.172	0.415
15.0	0.385	0.621	0.174	0.417
20.0	0.576	0.759	0.176	0.419
25.0	0.811	0.900	0.179	0.423
30.0	1.027	1.014	0.185	0.430
35.0	1.128	1.062	0.192	0.438
40.0	1.032	1.016	0.198	0.445
45.0	0.749	0.866	0.197	0.444
50.0	0.428	0.654	0.186	0.431
55.0	0.264	0.514	0.167	0.409
60.0	0.326	0.571	0.165	0.407
65.0	0.451	0.671	0.226	0.476
70.0	0.403	0.635	0.396	0.629
75.0	0.183	0.427	0.680	0.825
80.0	0.106	0.326	1.009	1.004
85.0	0.483	0.695	1.253	1.120
90.0	1.218	1.104	1.296	1.138
95.0	1.835	1.354	1.109	1.053
100.0	1.916	1.384	0.774	0.880
105.0	1.463	1.209	0.431	0.657
110.0	0.816	0.903	0.189	0.434
115.0	0.314	0.561	0.078	0.279
120.0	0.070	0.264	0.065	0.255
125.0	0.009	0.092	0.095	0.308
130.0	0.020	0.142	0.128	0.357
135.0	0.044	0.210	0.147	0.383
140.0	0.067	0.259	0.153	0.392
145.0	0.090	0.300	0.153	0.391
150.0	0.111	0.334	0.151	0.388
155.0	0.127	0.357	0.147	0.384
160.0	0.136	0.369	0.144	0.380
165.0	0.140	0.374	0.141	0.376
170.0	0.139	0.373	0.139	0.373
175.0	0.138	0.371	0.138	0.371
180.0	0.137	0.371	0.137	0.371

0	SIG 00	MAG 500	SIG 00	MAG 500
0.0	0.172	0.414	0.172	0.414
5.0	0.192	0.438	0.171	0.414
10.0	0.256	0.506	0.170	0.412
15.0	0.377	0.614	0.168	0.410
20.0	0.559	0.748	0.165	0.407
25.0	0.784	0.886	0.163	0.404
30.0	0.995	0.998	0.162	0.403
35.0	1.105	1.051	0.162	0.403
40.0	1.037	1.018	0.160	0.400
45.0	0.796	0.892	0.151	0.389
50.0	0.500	0.707	0.132	0.364
55.0	0.316	0.562	0.107	0.327
60.0	0.311	0.557	0.095	0.308
65.0	0.365	0.604	0.133	0.364
70.0	0.294	0.543	0.256	0.506
75.0	0.106	0.326	0.470	0.685
80.0	0.065	0.255	0.716	0.846
85.0	0.421	0.649	0.896	0.947
90.0	1.072	1.036	0.920	0.959
95.0	1.596	1.263	0.770	0.878
100.0	1.638	1.280	0.515	0.718
105.0	1.224	1.106	0.263	0.513
110.0	0.663	0.814	0.093	0.306
115.0	0.243	0.492	0.027	0.164

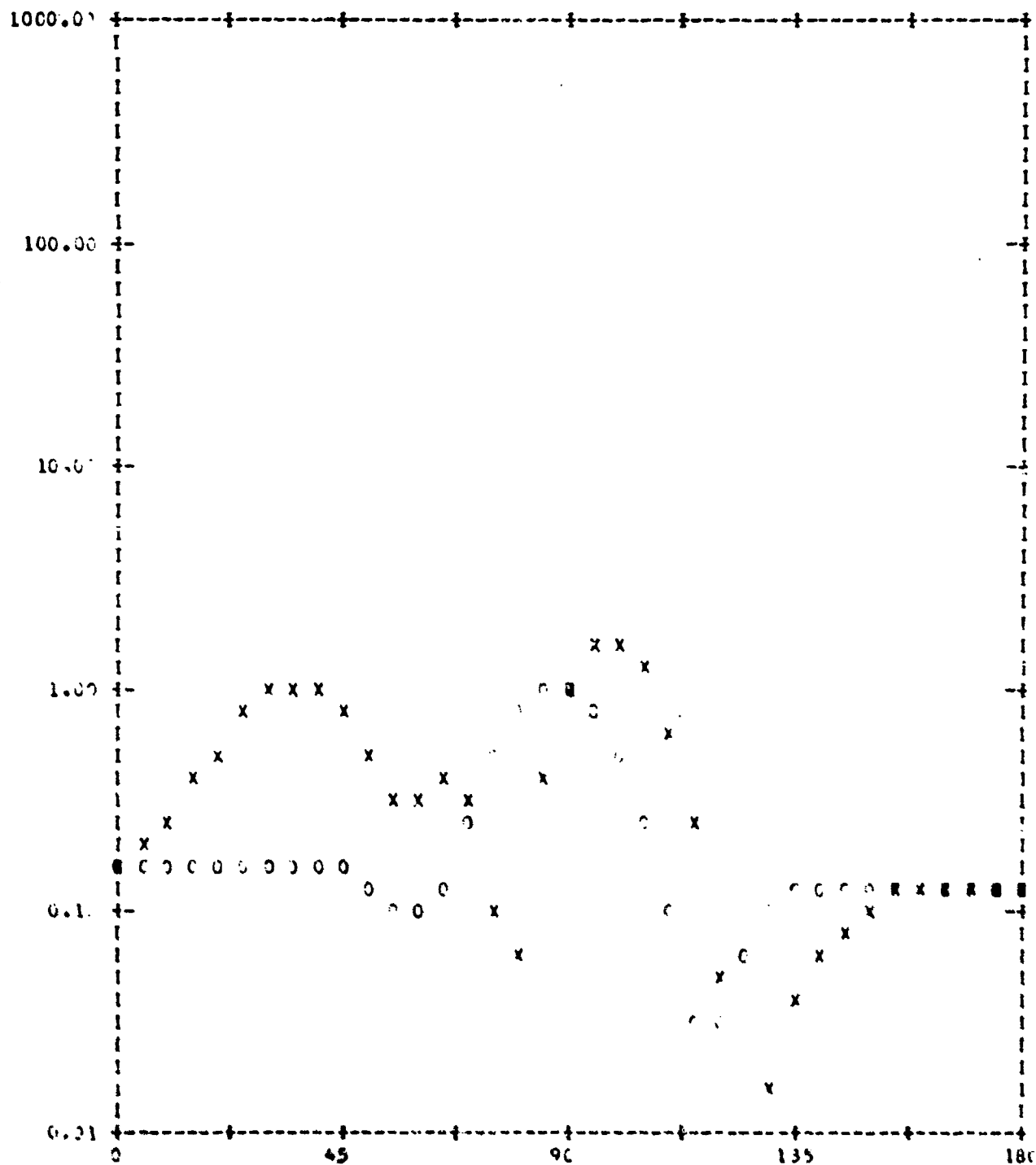
120.0	0.046	0.213	0.033	0.181
125.0	0.001	0.030	0.068	0.260
130.0	0.014	0.120	0.101	0.317
135.0	0.037	0.193	0.121	0.349
140.0	0.060	0.244	0.131	0.362
145.0	0.082	0.286	0.135	0.368
150.0	0.103	0.322	0.137	0.370
155.0	0.120	0.347	0.137	0.371
160.0	0.131	0.362	0.138	0.371
165.0	0.136	0.369	0.138	0.371
170.0	0.138	0.371	0.138	0.371
175.0	0.138	0.371	0.137	0.371
180.0	0.137	0.371	0.137	0.371

0	SIG 60	MAG 506	SIG 72	MAG 522
0.0	0.172	0.414	0.172	0.414
5.0	0.192	0.438	0.171	0.414
10.0	0.256	0.506	0.170	0.412
15.0	0.377	0.614	0.168	0.410
20.0	0.560	0.748	0.165	0.407
25.0	0.785	0.886	0.164	0.405
30.0	0.996	0.998	0.163	0.404
35.0	1.105	1.051	0.163	0.403
40.0	1.037	1.018	0.161	0.401
45.0	0.795	0.891	0.153	0.351
50.0	0.497	0.705	0.134	0.306
55.0	0.313	0.560	0.109	0.331
60.0	0.311	0.557	0.098	0.312
65.0	0.368	0.607	0.136	0.360
70.0	0.300	0.548	0.262	0.511
75.0	0.110	0.332	0.478	0.691
80.0	0.067	0.259	0.728	0.853
85.0	0.424	0.651	0.912	0.955
90.0	1.081	1.140	0.937	0.965
95.0	1.611	1.267	0.786	0.887
100.0	1.655	1.286	0.527	0.726
105.0	1.237	1.112	0.270	0.520
110.0	0.670	0.819	0.097	0.312
115.0	0.245	0.495	0.029	0.169
120.0	0.046	0.213	0.034	0.184
125.0	0.001	0.030	0.068	0.260
130.0	0.014	0.121	0.101	0.317
135.0	0.038	0.194	0.122	0.349
140.0	0.060	0.244	0.132	0.361
145.0	0.082	0.287	0.135	0.368
150.0	0.104	0.322	0.137	0.370
155.0	0.120	0.347	0.137	0.371
160.0	0.131	0.362	0.138	0.371
165.0	0.136	0.369	0.138	0.371
170.0	0.138	0.371	0.138	0.371
175.0	0.138	0.371	0.137	0.371
180.0	0.137	0.371	0.137	0.371

0	SIG 60	MAG 506	SIG 72	MAG 522
0.0	0.172	0.414	0.172	0.414
5.0	0.192	0.438	0.171	0.414
10.0	0.256	0.506	0.170	0.412
15.0	0.377	0.614	0.168	0.410
20.0	0.560	0.748	0.165	0.407
25.0	0.785	0.886	0.164	0.405
30.0	0.996	0.998	0.163	0.404

35.0	1.105	1.051	0.163	0.403
40.0	1.037	1.018	0.161	0.401
45.0	0.795	0.891	0.153	0.391
50.0	0.497	0.705	0.134	0.366
55.0	0.313	0.560	0.109	0.331
60.0	0.311	0.557	0.097	0.312
65.0	0.368	0.607	0.136	0.369
70.0	0.300	0.548	0.261	0.511
75.0	0.110	0.332	0.478	0.691
80.0	0.067	0.258	0.728	0.853
85.0	0.424	0.651	0.911	0.955
90.0	1.081	1.040	0.936	0.968
95.0	1.610	1.269	0.785	0.886
100.0	1.655	1.286	0.527	0.726
105.0	1.237	1.112	0.270	0.519
110.0	0.670	0.819	0.097	0.312
115.0	0.245	0.495	0.029	0.169
120.0	0.046	0.215	0.034	0.184
125.0	0.001	0.033	0.068	0.262
130.0	0.015	0.121	0.101	0.319
135.0	0.038	0.194	0.122	0.349
140.0	0.060	0.244	0.132	0.363
145.0	0.082	0.287	0.135	0.368
150.0	0.104	0.322	0.137	0.370
155.0	0.120	0.347	0.137	0.371
160.0	0.131	0.362	0.138	0.371
165.0	0.136	0.369	0.138	0.371
170.0	0.138	0.371	0.138	0.371
175.0	0.138	0.371	0.137	0.371
180.0	0.137	0.371	0.137	0.371

θ	SIG θ	MAG S θ	SIG 2θ	MAG S 2θ
0.0	0.172	0.414	0.172	0.414
5.0	0.192	0.438	0.171	0.414
10.0	0.256	0.506	0.170	0.412
15.0	0.377	0.614	0.168	0.410
20.0	0.560	0.748	0.165	0.407
25.0	0.785	0.886	0.164	0.405
30.0	0.996	0.999	0.163	0.404
35.0	1.175	1.051	0.163	0.403
40.0	1.037	1.018	0.161	0.401
45.0	0.795	0.891	0.153	0.391
50.0	0.497	0.705	0.134	0.366
55.0	0.313	0.560	0.109	0.331
60.0	0.311	0.557	0.097	0.312
65.0	0.368	0.607	0.136	0.360
70.0	0.300	0.548	0.261	0.511
75.0	0.110	0.332	0.478	0.691
80.0	0.067	0.258	0.728	0.853
85.0	0.424	0.651	0.911	0.955
90.0	1.081	1.040	0.936	0.968
95.0	1.610	1.269	0.785	0.886
100.0	1.655	1.285	0.527	0.726
105.0	1.237	1.112	0.270	0.510
110.0	0.670	0.819	0.097	0.312
115.0	0.245	0.495	0.029	0.169
120.0	0.046	0.215	0.034	0.184
125.0	0.001	0.033	0.068	0.262
130.0	0.015	0.121	0.101	0.319
135.0	0.038	0.194	0.122	0.340
140.0	0.060	0.244	0.132	0.363
145.0	0.082	0.287	0.135	0.368
150.0	0.104	0.322	0.137	0.371
155.0	0.120	0.347	0.137	0.371
160.0	0.131	0.362	0.138	0.371
165.0	0.136	0.369	0.138	0.371
170.0	0.138	0.371	0.138	0.371
175.0	0.138	0.371	0.137	0.371
180.0	0.137	0.371	0.137	0.371



X X X PLOT OF SIGMA 98 OVER LAMBDA SQUARED VERSUS THETA
 O O O PLOT OF SIGMA 96 OVER LAMBDA SQUARED VERSUS THETA

Security Classification

DOCUMENT CONTROL DATA - R & D		
(Security classification of title, body of abstract and indexing annotation must be entered when the overall report is classified)		
1. ORIGINATING ACTIVITY (Corporate author) Syracuse University Department of Electrical Engineering Syracuse, New York 13210		2a. REPORT SECURITY CLASSIFICATION Unclassified
3. REPORT TITLE RADIATION AND SCATTERING FROM BODIES OF REVOLUTION		2b. GROUP
4. DESCRIPTIVE NOTES (Type of report and inclusive dates) Scientific Final 1 June 1967 to 31 July 1969		Approved 11 Aug. 1969
5. AUTHOR(S) (First name, middle initial, last name) Roger F. Harrington Joseph R. Mautz		
6. PUBLICATION DATE July, 1969	7a. TOTAL NO. OF PAGES 96	7b. NO. OF REFS 13
8a. CONTRACT OR GRANT NO. F-19628-67-C-0233	8b. ORIGINATOR'S REPORT NUMBER(S)	
9. PROJECT, TASK, AND WORK UNIT NO. 8683-02-01		
c. JOD ELEMENT 6240539F	9b. OTHER REPORT NO(S) (Any other numbers that may be assigned this report)	
d. JOD SUBELEMENT 681000	AFCRL-69-0305	
10. DISTRIBUTION STATEMENT 2. This document is subject to special export controls and each transmittal to foreign governments or foreign nationals may be made only with the prior approval of AFMRL (CRDG), L.G. Hanscom Field, Bedford, Massachusetts 01730.		
11. SUPPLEMENTARY NOTES TECH, OTHER	12. SPONSORING MILITARY ACTIVITY Air Force Cambridge Research Laboratories (CRD) L.G. Hanscom Field Bedford, Massachusetts 01730	
13. ABSTRACT The problem of electromagnetic radiation and scattering from conducting bodies of revolution, both loaded and unloaded, is considered. The solution is obtained by the method of moments applied to the integro-differential equation, and is expressed in terms of generalized network parameters. Computer programs are given for plane-wave scattering and for radiation from apertures. The programs are valid for solid bodies, zero thickness conductors, and bodies with points and edges. The solution for planar bodies is also a solution for diffraction through apertures in a conducting plane, according to Babinet's principle. Representative computations are given for scattering and radiation from disk washers, toroids, hemispheres, and cone-spheres.		

14 KEY WORDS	LINK A		LINK B		LINK C	
	ROLE	WT	ROLE	WT	ROLE	WT
Aperture antennas Bodies of revolution Computer programs Computer solutions Conducting disks Conducting washers Conducting toroids Conducting hemispheres Cone-spheres Generalized impedances Generalized network parameters Loaded antennas Loaded scatterers Method of moments Plane-wave scattering Radar cross sections						